AFFDL-TR-65-107
PART II

CALCULATION OF LAMINAR SEPARATION WITH FREE INTERACTION BY THE METHOD OF INTEGRAL RELATIONS

PART II — TWO-DIMENSIONAL SUPERSONIC NONADIABATIC FLOW AND AXISYMMETRIC SUPERSONIC ADIABATIC AND NONADIABATIC FLOWS

JACK N. NIELSEN
LARRY L. LYNES
FREDERICK K. GOODWIN

FOREWORD

This report[1] represents the second report in an investigation entitled "Calculation of Laminar Separation with Free Interaction by the Method of Integral Relations" being performed under Contract AF 33(615)-1591, Project No. 8219, Task No. 821902, for the Flight Control Division of the Air Force Flight Dynamics Laboratory. The first report bearing the subtitle "Part I - Two-Dimensional Supersonic Adiabatic Flow" was issued by the Air Force Flight Dynamics Laboratory as Technical Report AFFDL-TR-65-107.

The authors are indebted to Wright-Patterson Air Force Base for many of the calculations which are presented in this report. They would like to acknowledge the contributions of Mr. Eugene Fleeman for technical assistance in the machine computations and for supersonic data on laminar separation used in checking the theory. The data were taken in Tunnel D at Arnold Engineering Development Center.

The manuscript was released by the authors in October 1965 as an AFFDL Technical Report.

This technical report has been reviewed and is approved.

C. B. Westbrook
Chief, Control Criteria Branch
Flight Control Division
Air Force Flight Dynamics Laboratory

[1]This is Vidya Report No. 203.

ABSTRACT

A calculative method is presented for determining separated, laminar, boundary-layer characteristics from in front of the separation point to the reattachment point under the influence of "free interaction" between the main flow and the boundary layer. The analysis herein covers supersonic flow over two-dimensional and axisymmetric configurations with adiabatic or nonadiabatic wall conditions. For nonadiabatic wall conditions, theories based on first-order coupling and second-order coupling between velocity and total temperature profiles have been presented. The theory based on first-order coupling has been included in a machine calculation program with options for two-dimensional or axisymmetric flow and adiabatic or nonadiabatic wall conditions. Extensive systematic calculations have been made to determine the range of possible separated flows over a two-dimensional configuration as a function of separation point location and wall temperatures. Comparison between experiment and theory for separation pressure distributions on two-dimensional or axisymmetric adiabatic configurations shows generally good agreement. Good comparison between experiment and theory is indicated for a moderately-cooled axisymmetric configuration. For a highly-cooled axisymmetric configuration, the prediction of the machine program based on first-order coupling is inadequate, indicating the necessity for a higher-order coupling theory.

TABLE OF CONTENTS

ILLUSTRATIONS

LIST OF SYMBOLS

a	local speed of sound
a_o	speed of sound at outer edge of boundary layer at x_o
a_1	speed of sound at outer edge of boundary layer for any value of x
b_o	first-order temperature profile coefficient of the outer flow, Equation (69)
b_1, b_2, b_3	coefficients specifying the temperature profile of the inner flow, Equation (82)
c_o, c_1, c_2, c_3	coefficients specifying the velocity profile of the outer flow, Equation (67)
$\dot{c}_o, \dot{c}_1, \dot{c}_2, \dot{c}_3$	derivatives of velocity profile coefficients with respect to ξ
c_p	specific heat of gas at constant pressure
C	numerical constant in viscosity relationship, $\mu/\mu_o = CT/T_o$
C_f	skin-friction coefficient, $\tau/(1/2)\rho_1 u_1^2$
d_n	defined by Equations (I-11)
$\dot{d}_n$	defined by Equations (I-11)
${}_nD_m$	matrix coefficients for up to fourth-order coupling, Appendix I
E_o, E_1, E_2, E_3	coefficients specifying the temperature profile of the outer flow, Equation (69)
$\dot{E}_o, \dot{E}_1, \dot{E}_2, \dot{E}_3$	derivatives of temperature profile coefficients with respect to ξ
f'	$df/d\bar{u}$
f''	$d^2f/d\bar{u}^2$
$f_n(\bar{u})$	family of smoothing functions, $(1 - \bar{u})^n$
$\bar{f}_n$	defined by Equations (I-11)
$\bar{f}^n$	defined by Equations (I-11)
f_s	value of f on $u = 0$ line
f_s'	$df/d\bar{u}$ at $\eta = \eta_s$
f_w	value of f at wall
f_w'	$df/d\bar{u}$ at $\eta = 0$

g	acceleration of gravity, 32.2 ft/sec^2
$\dot{g}_n$	dg_n/dc_3
$g_n(c_3)$	family of definite integrals given by Equations (I-11)
H_n	defined by Equations (I-11)
$\bar{H}_n$	defined by Equations (I-11)
$\bar{I}_n$	defined by Equations (I-11)
J	mechanical equivalent of heat, 778 ft-lbs/Btu
J_n	defined by Equations (I-11)
k	thermal conductivity of gas
k_o, k_1, k_2, k_3	Dorodnitsyn coefficients for a Blasius velocity profile defined by Equation (30)
ℓ	reference length, taken equal to x_o, herein
L	reference length in axisymmetric plane, taken equal to x_o', herein
L_b	distance from leading edge to end of wedge
L_b'	distance from stagnation point to end of flare, see Figure 11
L_{b_E}'	distance from leading edge of cylinder to end of flare in the equivalent plane, see Figure 11
L_c	length of flat plate up to compression corner
L_c'	distance from stagnation point to beginning of compression corner; see Figure 11
L_{c_E}'	distance from leading edge of cylinder to end of flare in the equivalent plane, see Figure 11
L_E	equivalent run length in axisymmetric plane
m_o	$\left(\frac{\gamma - 1}{2}\right) \frac{u_o^2}{a_o^2}$
m_1	$\left(\frac{\gamma - 1}{2}\right) \frac{u_1^2}{a_1^2}$
M	local Mach number
M'	local Mach number in axisymmetric plane

M_o	Mach number parallel to x-axis at edge of boundary layer at x_o
M_o'	Mach number parallel to x'-axis at edge of boundary layer in axisymmetric plane at x_o'
M_1	Mach number parallel to x-axis at edge of boundary layer for any value of x
M_1'	Mach number parallel to x'-axis at edge of boundary layer in axisymmetric plane for any value of x'
M_∞	free-stream Mach number
n	index
$\bar{N}_n$	defined by Equations (I-11)
p	local static pressure
p_o	static pressure at x_o
p_t	local stagnation pressure
p_1	static pressure at edge of boundary layer for any value of x
$\bar{P}_n$	defined by Equations (I-11)
$\tilde{P}_n$	defined by Equations (I-11)
Pr	Prandtl number
$\bar{Q}_n$	defined by Equations (I-11)
$\tilde{Q}_n$	defined by Equations (I-11)
$Q_n(c_o,c_1,c_2)$	family of definite integrals defined by Equations (I-11)
r_o	radius of the cylinder prior to the compression corner
r(x')	local body radius in the axisymmetric plane
R	radius of compression corner
$_nR$	right-hand side of the nonhomogeneous equations for up to fourth-order coupling, Appendix I
R_o	Reynolds number, $U_o \ell/\nu_o$
R_∞	Reynolds number, $u_\infty \delta_o/\nu_\infty$
s(x)	y-coordinate of u = 0 line between separation and reattachment
S	temperature parameter, $S = \frac{T_t}{T_{t_o}} - 1$

S_s	value of S along the $\bar{u} = 0$ line
S_w	value of S at the wall, $S_w = \frac{T_w}{T_{t_o}} - 1$
S_1	symbol for S for first-order coupling
S_2	symbol for S for second-order coupling
T	local absolute temperature
T_o	temperature at edge of boundary layer at $x = x_o$
T_t	local stagnation temperature
T_{t_o}	stagnation temperature at edge of boundary layer at x_o
T_w	temperature of the wall
T_1	temperature at edge of boundary layer at any value of x
u	axial velocity in x,y plane
u'	axial velocity in the axisymmetric plane
$u_i(y)$	initial velocity profile at x_o
$u_i'(y')$	initial velocity profile in axisymmetric plane at x_o'
u_o	value of u at edge of boundary layer at x_o
u_o'	value of u' at edge of boundary layer in axisymmetric plane at x_o'
$u_1(x)$	value of u at edge of boundary layer for any value of x
$u_1'(x')$	value of u' in axisymmetric plane at edge of boundary layer for any value of x'
u_∞	free-stream velocity
$\bar{u}$	U/U_1
$\bar{u}_i(\eta)$	value of $\bar{u}$ at ξ_o
$\bar{u}_s$	symbol used to represent u component of velocity at the boundary between the inner and outer flow regions; it is always zero, but the symbol is used for clarity
U	axial velocity in X,Y plane, ua_o/u_1
$U_i(Y)$	initial velocity profile at X_o in the Stewartson plane
U_o	value of U at edge of boundary layer at X_o
U_1	value of U at edge of boundary layer for any X

$\dot{U}_1$	$dU_1/d\xi$
v	normal velocity in x,y plane
v'	radial velocity in the axisymmetric plane
v_s	value of v at $s(x)$
v_1	value of v at the edge of boundary layer for any x
$\bar{v}$	normal velocity in ξ,η plane, $\frac{V}{U_1}\sqrt{\frac{U_o \ell}{\nu_o}}$
$\bar{v}_s$	value of $\bar{v}$ at η_s
V	normal velocity in X,Y plane
V_s	value of V at Y_s
$w(x)$	y-coordinate of solid surface
$\bar{w}$	$\bar{v} + \bar{u}\eta \frac{\dot{U}_1}{U_1}$
$\bar{w}_s$	value of $\bar{w}$ at η_s
x_c	value of x where compression ramp begins
x_c'	value of x' where the compression flare begins
x_o	value of x where interaction begins
x_o'	value of x' where interaction begins
x_p	value of x at the peak value of the plateau pressure
x_R	value of x at the reattachment point
x_R'	value of x' at the reattachment point
x_s	value of x at the separation point
x_s'	value of x' at the separation point
x,y	coordinates of two-dimensional flow under consideration
x',y'	coordinates of physical flow in the axisymmetric plane; x' lies along centerline of body (see Fig. 1)
X_o	value of X corresponding to x_o
X_s	value of X at the separation point
X,Y	coordinates after Stewartson transformation; $X = \int_o^x \frac{p_1 a_1}{p_o a_o} dx$; $Y = \int_{w(x)}^{y} \frac{\rho_1 a_1}{\rho_o a_o} \frac{\rho}{\rho_1} dy$

Y_s value of Y corresponding to $s(x)$

α_s value of $\partial\bar{u}/\partial\eta$ at η_s

α_w value of $\partial\bar{u}/\partial\eta$ at wall

$\dot{\alpha}_w$ value of $\partial^2 u/\partial\eta\,\partial\xi$ at the wall

β flare angle, see Figure 11, or wedge angle

β_D slope of the dividing streamline at separation

β_R slope of the dividing streamline at reattachment

β_u slope of $u = 0$ line at the separation point

γ ratio of specific heats

δ boundary-layer thickness

δ' boundary-layer thickness in the axisymmetric plane

δ^* displacement thickness in physical plane,
$$\int_0^\infty \left(1 - \frac{\rho u}{\rho_1 u_1}\right) dy$$

δ^{**} momentum thickness in physical plane

$\delta^{*'}$ displacement thickness in axisymmetric physical plane, defined by Equation (20)

δ_i^* displacement thickness of inner flow

$\delta_{i_A}^*$ displacement thickness of the inner flow for an adiabatic wall

$\delta_{i_N}^*$ displacement thickness of the inner flow for a nonadiabatic wall

δ_o' value of δ at the start of interaction in the axisymmetric plane

δ_o^* displacement thickness of outer flow

δ_S^* displacement thickness in the Stewartson plane,
$$\int_0^\infty \left(1 - \frac{U}{U_1}\right) dY$$

δ_S^{**} momentum thickness in the Stewartson plane,
$$\int_0^\infty \frac{U}{U_1}\left(1 - \frac{U}{U_1}\right) dY$$

$\eta_s(\xi)$	η-coordinate of the $u = 0$ line between separation and reattachment
$\dot{\eta}_s$	derivative of η_s with respect to ξ
λ_1, λ_2	constants defined by Equation (32)
μ	absolute viscosity
μ_o	absolute viscosity at outer edge of boundary layer at x_o
ν	kinematic viscosity, μ/ρ
ν_o	kinematic viscosity at outer edge of boundary layer at x_o, μ_o/ρ_o
ν_1	value of ν at edge of boundary layer for any x
ν_∞	kinematic viscosity in free stream
ξ_o	value of ξ corresponding to x_o
ξ_s	value of ξ at the separation point
ξ, η	coordinates in Dorodnitsyn plane, $\xi = \int_o^X \frac{U_1}{U_o} \frac{dX}{\ell}$, $\eta = \frac{U_1}{U_o \ell} \sqrt{\frac{U_o \ell}{\nu_o}}\, Y$
ρ	local mass density
ρ'	local mass density in axisymmetric plane
ρ_o	value of ρ at edge of boundary layer at x_o
ρ_1	value of ρ at edge of boundary layer for any x
ρ_1'	value of ρ' at edge of boundary layer for any x'
ρ_∞	value of ρ in free stream
τ	shear stress at the wall
ϕ	slope of streamline outside of boundary layer
ϕ'	slope of streamline outside of boundary layer in axisymmetric plane
ϕ_o	value of ϕ at $x = x_o$
ϕ_o'	value of ϕ' at $x' = x_o'$
ϕ_1	value of ϕ at edge of boundary layer for any x

CALCULATION OF LAMINAR SEPARATION WITH FREE INTERACTION BY THE METHOD OF INTEGRAL RELATIONS

PART II - TWO-DIMENSIONAL SUPERSONIC NONADIABATIC FLOW AND AXISYMMETRIC SUPERSONIC ADIABATIC AND NONADIABATIC FLOWS

1. INTRODUCTION

This paper is the second one describing the calculation of laminar separation with free interaction by the method of integral relations. In the first paper, Reference 1, a method was developed for calculating laminar separated flow fields up to the reattachment point for supersonic adiabatic flow over a two-dimensional surface. The general method is also applicable to the calculation of the laminar boundary layer subject to prescribed pressure distribution for any Mach number. A computer program for the case of a flat plate and a plane ramp was developed and was delivered to the sponsor. This program is capable of simple extension to ramps of fairly general shape.

It is the purpose of this report to describe the extension of the work to the cases of nonadiabatic laminar flow and to axisymmetric flow. A computer program is developed on the basis of the present analysis which contains an option of two-dimensional or axisymmetric flow and an option for adiabatic flow (with the surface at recovery temperature) or for nonadiabatic flow.

A basic objective of the current investigation has been to avoid a priori specification of velocity and temperature profiles, and to present a method whereby these profiles can be calculated with greater precision as the order of approximation of the calculative technique is increased. In this context, several degrees of approximation are considered in determining the effect of the nonadiabatic temperature profiles on the velocity profiles. Another assumption made in the analysis is that of "free interaction" between the boundary layer and the outer flow. Free interaction will be handled by increasing the normal coordinates of the surface contour by the boundary-layer displacement thickness when using inviscid supersonic flow theory to calculate the pressure distribution acting on the boundary layer.

The analysis will be presented in the order of axisymmetric adiabatic flow, two-dimensional nonadiabatic flow, and axisymmetric nonadiabatic flow. Illustrative calculative examples will be presented for each case, and the corresponding calculative program will be described.

2. AXISYMMETRIC ADIABATIC FLOW

2.1 Boundary Value Problem in Axisymmetric Plane

Consider a body of revolution as shown in Figure 1 consisting of a cylindrical section on which separation is induced by a flare. Let x', y' be the coordinates in the axisymmetric plane as shown and let $r(x')$ be the equation of the flare. For a compressible laminar boundary layer, the boundary-layer equations as given in Reference 2, page 384, will be utilized on the basis of the following assumptions:

(1) Perfect gas with constant specific heats.
(2) Boundary-layer thickness small compared to the body radius.
(3) The ramp slopes dr/dx' are small compared to unity.

$$\left.\begin{aligned} \rho u' \frac{\partial u'}{\partial x'} + \rho v' \frac{\partial u'}{\partial y'} &= -\frac{\partial p}{\partial x'} + \frac{\partial}{\partial y'}\left(\mu \frac{\partial u'}{\partial y'}\right) \\ \frac{\partial}{\partial x'}(\rho u' r) + \frac{\partial}{\partial y'}(\rho v' r) &= 0 \end{aligned}\right\} \qquad (1)$$

Following the two-dimensional analysis of Reference 1, we define a domain with the following boundaries:

Boundary A:

$$\left.\begin{aligned} y' &= r_o(x') && x_o' \le x' \le x_c' \\ y' &= r(x'), \text{ a given function} && x_c' \le x' \le x_R' \end{aligned}\right\} \qquad (2)$$

Boundary B:

$$x' = x_o' \qquad r_o \le y' \le \infty \qquad (3)$$

Boundary C:

$$y' = \infty \qquad x_o' \le x' \le x_R' \qquad (4)$$

Boundary D:

$$x' = x_R' \qquad r(x_R') \le y' \le \infty \qquad (5)$$

Boundary conditions for the velocity components are

Boundary A:

$$u' = 0, \quad v' = 0 \qquad (6)$$

Boundary B:

$$\left.\begin{aligned} u' &= u_i'(y') \\ u' = u_o' \qquad \frac{\partial u'}{\partial y'} &= 0 \quad \text{at} \quad y' = \infty \end{aligned}\right\} \tag{7}$$

Boundary C:

(a) Prescribed pressure distribution

$$\left.\begin{aligned} u' = u_1'(x') \qquad x_o' \le x' \le x_R' \quad &\text{at} \quad y = \infty \\ u' = u_o' \quad &\text{at} \quad x' = x_o' \end{aligned}\right\} \tag{8}$$

(b) Free interaction

$$u_1' = u_o' \quad \text{at} \quad x' = x_o' \tag{9}$$

u_1' is to be determined for $x_o' < x' \le x_R'$

The boundary-layer assumption is made that the static pressure is constant across the boundary layer at any given axial location. Note that this assumption in the region of the flare is not the same as the constancy of the pressure in planes normal to the flare. The difference is allowable provided the slopes of the flare are sufficiently small.

With regard to pressure boundary conditions, the pressure at the edge of the layer, if prescribed, yields the value of u_1' along Boundary C with an initial value of u_o'. For free interaction the initial value of the pressure at x_o' is p_o, and the subsequent pressures are calculated.

Assuming a Prandtl number of one, the total temperature is constant; that is,

$$T_t = T\left(1 + \frac{\gamma - 1}{2} M^2\right) = T_{t_o} \tag{10}$$

2.2 Transformation to Two-Dimensional Plane

We will utilize the Mangler transformation to reduce the axisymmetric problem to an equivalent two-dimensional one for which the solution and computer program have already been developed. The coordinate transformations are

$$x = \int_o^{x'} r^2(x')\, dx' \qquad y = \int_{r(x')}^{y'} r(x')\, dy' \tag{11}$$

Under this transformation the equations become

$$\left.\begin{aligned} \frac{\partial}{\partial x}(\rho u) + \frac{\partial}{\partial y}(\rho v) &= 0 \\ \rho u \frac{\partial u}{\partial x} + \rho v \frac{\partial u}{\partial y} &= -\frac{\partial P}{\partial x} + \frac{\partial}{\partial y}\left(\mu \frac{\partial u}{\partial y}\right) \end{aligned}\right\} \qquad (12)$$

where u and v are given by

$$\left.\begin{aligned} u &= u' \\ v &= \frac{v'}{r} + \frac{u'(y' - 2r)}{r^2}\frac{dr}{dx'} \end{aligned}\right\} \qquad (13)$$

The density, temperature, and viscosity are the same at corresponding points. It is noted that the axisymmetric boundary-layer equations have been reduced to the two-dimensional ones by means of nonlinear transformations of the x and y axes. The axial velocity field remains untransformed, but the radial velocity field has undergone a nonlinear transformation. The transformed problem in the two-dimensional plane is similar to that shown in Figure 2 except that the ramp angle is zero.

The question of the boundary conditions under the transformation is now considered.

Boundary A:

$$u = v = 0 \quad \text{at} \quad y = 0 \qquad (14)$$

Boundary B:

$$\left.\begin{aligned} u = u_i(y) = u_i'(y') \quad &\text{at} \quad x = x_o \\ u = u_o \qquad \frac{\partial u}{\partial y} = 0 \quad &\text{at} \quad y = \infty \end{aligned}\right\} \qquad (15)$$

Boundary C:

(a) Prescribed pressure distribution

$$\left.\begin{aligned} u = u_1(x) = u_1'; \quad x_o \le x \le x_R \\ u = u_o = u_o' \quad \text{at} \quad x = x_o \end{aligned}\right\} \qquad (16)$$

(b) Free interaction

$$u_1 = u_o \quad \text{at} \quad x = x_o \qquad (17)$$

u_1 to be calculated for $x_o < x < x_R$

It is noted that by use of the Mangler transformation we have reduced the axisymmetric problem given by the differential equations, Equations (1), and the boundary conditions given by Equations (6) to (9) to an equivalent two-dimensional problem given by Equations (12), with boundary conditions given by Equations (14) to (17). Furthermore, the Boundary A has been transformed into a flat plate for both its cylindrical part and its flared part. By analogy with Reference 1, we thus have the original boundary value problem of that paper as given by differential equations in Equations (1) and (2) of that report and boundary conditions given by Equations (4) to (7). The domain in the present case coincides with that of Reference 1 with $w(x)$ taken as zero. The only difference that occurs is in the free-interaction equation, which is not the same in each case. Also, in obtaining the solution in the axisymmetric plane, a new set of transformations for coordinates and velocities has now been added.

In the solution of the problem the transformations of Stewartson and Dorodnitsyn are used just as in Reference 1. The boundaries in the Stewartson and Dorodnitsyn planes are shown in Figure 3.

2.3 Free-Interaction Equation

In the axisymmetric case, it is assumed that the normal coordinates of the contour of the body are increased by the amount of the displacement thickness of the boundary layer for the purposes of calculating the pressure of the flow external to the boundary layer by inviscid-flow theory. Furthermore, the pressure external to the boundary layer will be computed in the axisymmetric case by the use of the Prandtl-Meyer relationship.

Let the primed quantities refer to the axisymmetric plane. We then have for the equation of free interaction

$$\tan \phi' = \frac{d\delta^{*\prime}}{dx'} + \frac{dr}{dx'} \tag{18}$$

with the turning angle ϕ' of the outer flow being related to the local Mach number at the edge of the boundary layer by

$$\phi' = -\sqrt{\frac{\gamma+1}{\gamma-1}} \arctan\sqrt{\frac{\gamma-1}{\gamma+1}\left(M_1'^2 - 1\right)} + \arctan\sqrt{M_1'^2 - 1} + C \tag{19}$$

where C is the constant of integration. We desire to write Equation (18) in terms of $d\delta^*/dx$. From the following relationships

$$\left.\begin{aligned} \delta^{*\prime} &= \int_{r(x')}^{\delta'+r} \left(1 - \frac{\rho}{\rho_1}\,\frac{u'}{u_1'}\right) dy' \\ \delta^{*} &= \int_{0}^{\delta} \left(1 - \frac{\rho u}{\rho_1 u_1}\right) dy \end{aligned}\right\} \qquad (20)$$

we find that

$$\delta^{*\prime} = \frac{\delta^*}{r} \qquad (21)$$

Differentiating, we find that

$$\frac{d\delta^{*\prime}}{dx'} = \frac{1}{r(x')}\,\frac{d\delta^*}{dx'} - \frac{\delta^*}{r^2}\,\frac{dr}{dx'}$$

and

$$\frac{d\delta^*}{dx'} = \frac{d\delta^*}{dx} \cdot \frac{dx}{dx'} = r^2\,\frac{d\delta^*}{dx}$$

Substituting into Equation (18),

$$\tan\phi' = r\,\frac{d\delta^*}{dx} - \frac{\delta^*}{r^2}\,\frac{dr}{dx'} + \frac{dr}{dx'}$$

$$\frac{d\delta^*}{dx} = \frac{\left(\tan\phi' - \frac{dr}{dx'}\right)}{r} + \frac{\delta^*\,\frac{dr}{dx'}}{r^3} \qquad (22)$$

We need an initial value of ϕ' to determine C in Equation (19). The function dr/dx' is a known one for a specified flare shape. Comparing Equation (22) with that for two-dimensional flow,

$$\frac{d\delta^*}{dx} = \tan\phi - \frac{dw}{dx} \qquad (23)$$

we can readily see the difference in the right-hand term for two-dimensional and axisymmetric flares. Consider Equation (22) in the form used in the two-dimensional analysis of Reference 1,

$$\frac{R_o^{1/2}}{1+m_o}\left(\frac{d\delta_o^*}{dx} + \frac{d\delta_i^*}{dx}\right) = \frac{R_o^{1/2}}{(1+m_o)r}\left(\tan\phi' - \frac{dr}{dx'}\right) + \frac{R_o^{1/2}\,\frac{dr}{dx'}}{(1+m_o)r^3}\,(\delta_o^* + \delta_i^*) \qquad (24)$$

Also we find that

$$R_o = \frac{u_o \ell}{\nu_o} = \frac{u_o r_o^2 L}{\nu_o} \tag{25}$$

since

$$\ell = \int_o^L r^2(x')\, dx' = r_o^2 L \tag{26}$$

where L is the reference length in the axisymmetric plane.

2.4 Initial Conditions

For the initial conditions, we note that the coefficients in the initial velocity profile are given in the Dorodnitsyn plane in Reference 1 as

$$\left.\begin{aligned} c_o &= k_o\sqrt{\xi} \\ c_1 &= k_1\sqrt{\xi} \\ c_2 &= k_2\sqrt{\xi} \\ c_3 &= k_3 \end{aligned}\right\} \tag{27}$$

Since interaction starts on a cylinder of radius r_o at a distance L, we must transform through the following transformations:

Mangler:

$$x = \int_o^{x'} r_o^2\, dx'$$

Stewartson:

$$X = \int_o^x \frac{p_1 a_1}{p_o a_o}\, dx$$

Dorodnitsyn:

$$\xi = \int_o^X \frac{u_1}{u_o}\, \frac{dX}{\ell}$$

For constant pressure, we find

$$\left.\begin{aligned} x &= r_o^2 x' \\ X &= x \\ \xi &= \frac{X}{\ell} \\ \xi &= \frac{r_o^2 x'}{\ell} = \frac{x'}{L} \end{aligned}\right\} \qquad (28)$$

Since we start interaction at $x' = L$, we find that the initial value of ξ is

$$\xi_o = \frac{r_o^2 L}{\ell} = 1.0 \qquad (29)$$

where

ℓ reference length in x,y-plane

L reference length in x',y'-plane

so that the present program based on starting interaction at ξ_o of unity can be used unmodified provided L is the distance to the beginning of interaction. The initial values of the c's are

$$\left.\begin{aligned} c_o &= k_o \sqrt{\frac{x'}{L}} \\ c_1 &= k_1 \sqrt{\frac{x'}{L}} \\ c_2 &= k_2 \sqrt{\frac{x'}{L}} \\ c_3 &= k_3 \end{aligned}\right\} \qquad (30)$$

With regard to the initial values of ϕ_o', we have

$$\left.\begin{aligned} \tan \phi_o' &= \left(\frac{d\delta^{*\prime}}{dx'}\right)_o \\ \tan \phi_o &= \left(\frac{d\delta^*}{dx}\right)_o \\ \tan \phi_o' &= \frac{\tan \phi_o \left(\frac{d\delta^{*\prime}}{dx'}\right)}{\frac{d\delta^*}{dx}} = r_o \tan \phi_o \end{aligned}\right\} \qquad (31)$$

Since $\tan \phi_o$ is known from Reference 1, we can write

$$\tan \phi_o = \sqrt{\frac{\ell}{x_o}} \frac{1}{\sqrt{R_o}} \left[\frac{\lambda_1}{2} + m_o \left(\frac{\lambda_1 + \lambda_2}{2}\right)\right] \tag{32}$$

$$\lambda_1 = 1.73$$

$$\lambda_2 = 0.664$$

Since

$$\frac{x_o'}{L} = \frac{x_o}{\ell} \qquad u_o = u_o' \qquad M_o = M_o'$$

we have

$$\tan \phi_o' = r_o \sqrt{\frac{L}{x_o'}} \frac{1}{\sqrt{\frac{u_o r_o^2 L}{\nu_o}}} \left[\frac{\lambda_1}{2} + m_o \left(\frac{\lambda_1 + \lambda_2}{2}\right)\right] \tag{33}$$

2.5 Transformations to Axisymmetric Plane

Values of x, y, u, and v in the two-dimensional plane will be available from the present computer program. It is necessary to obtain values of the quantities in the axisymmetric plane. The direct transforms for x',y' to x,y are given by Equation (11). The inverse transforms are given below.

$$\left.\begin{aligned} x' &= \frac{x}{r_o^2} && 0 \le x \le r_o^2 x_c' \\ x' &= x_c' + \int_{r_o^2 x_c'}^{x} \frac{dx}{r^2} && r_o^2 x_c' \le x \end{aligned}\right\} \tag{34}$$

$$\left.\begin{aligned} y' &= r_o + \frac{y}{r_o} && 0 \le x \le r_o^2 x_c' \\ y' &= r + \frac{y}{r} && r_o^2 x_c' \le x \end{aligned}\right\} \tag{35}$$

The direct transforms of the velocities u',v' into u,v are given by Equation (13). The inverse transformation to obtain v' for u and v is now derived. Since

$$v' = rv - \frac{u'}{r}\frac{dr}{dx'}(y' - 2r)$$

and

$$y' = r + \frac{y}{r} \qquad u' = u$$

we have

$$\begin{aligned} v' &= rv - \frac{u}{r}\frac{dr}{dx'}\left(\frac{y}{r} - r\right) && r_o^2 x_c' < x \\ v' &= r_o v && 0 \le x \le r_o^2 x_c' \end{aligned} \tag{36}$$

2.6 Programing

We are given a body shape consisting of a cylinder of radius r_o with a flare given by $r(x')$ in functional form. The function dr/dx' is also known. The interaction is assumed to start at $x' = L$ with initial values of u_1', M_1', etc. A transformation of x' to x and y' to y is accomplished analytically by means of Equation (11) so that $r(x')$ is now known in the form $r(x)$. The initial values of u_1', M_1', etc., are also transformed to the x,y-plane as follows:

$$u_1 = u_1'$$

$$M_1 = M_1'$$

$$\ell = r_o^2 L$$

We now have a two-dimensional problem for which the existing program can be used. We must, however, modify the free-interaction equation to that given by Equation (24). The term $\tan \phi_o'$ is evaluated from Equation (33). The initial values of c_o, c_1, c_2, and c_3 are obtained from Equation (30). In calculating values of x', y', and v' for any purpose, a special subroutine based on Equations (34) to (36) must be written.

2.7 Sample Calculated Results

Several exploratory runs have been made with the computer program for axisymmetric flow to check out the program and to see how variations in the configuration flare angle and body radius affect the separation pressure distribution for a fixed position of the separation point. The effect of flare angle is shown in Figure 4. This configuration and the separation point for

a wedge angle of 10° are the same as those shown in Figure 12. The flow is two-dimensional up to the intersection of the cylinder and the flare. The computer runs show that the reattachment point moves forward and the dividing streamline moves outward as the flare angle is increased for fixed position of the separation point. Actually, we would anticipate an upstream motion of the separation point as the flare angle increases for a real flow.

Another series of runs for variable body radius is shown in Figure 5 for fixed flare angle and fixed position of the separation point. For large body radii the flow is nearly two dimensional, but for small body radii the flow is definitely three dimensional. The ratio of the flare radius at reattachment to that of the cylinder is taken as a measure of the three dimensionality of the separated flow. For large values of this parameter, there are large changes in body circumference which tend to thin the boundary layer. However, the increase in skin friction area tends to thicken the boundary layer. The net result of these two compensating three-dimensional effects delays the onset of the reattachment pressure rise but causes steeper pressure gradients as the flow becomes more three dimensional. At the same time, there is an increase in reattachment pressure and a movement of the reattachment point downstream.

3. TWO-DIMENSIONAL NONADIABATIC FLOW

In Reference 1 a method was developed for calculating the flow field over a two-dimensional surface with a compression wedge causing separation of a supersonic laminar boundary layer. The surface was taken to be at recovery temperature, and the entire boundary layer total temperature was assumed to be uniform since the Prandtl number was taken as unity. In this analysis we will take the surface temperature at a uniform value which may be different from the recovery temperature. The surface temperature is taken uniform to simplify the analysis, but a nonuniform surface temperature distribution can readily be handled within the framework of the method.

In the ensuing analysis we will develop the Dorodnitsyn integral relationships for both momentum and energy, and then use these relations to obtain the ordinary differential equations governing the velocity and temperature profiles. The relationship will be developed for both first-order and second-order coupling between temperature and velocity profiles.

3.1 Differential Equations and Boundary Conditions

The configuration of the present problem is illustrated by Figure 2 and is the same as that treated in Reference 1 except that the wall is either hot or cold. The differential equations governing the flow as taken from Reference 2, pp. 379-381, are:

Momentum:

$$\rho \left(u \frac{\partial u}{\partial x} + v \frac{\partial u}{\partial y} \right) = \rho_1 u_1 \frac{\partial u_1}{\partial x} + \frac{\partial}{\partial y} \left(\mu \frac{\partial u}{\partial y} \right) \tag{37}$$

Continuity:

$$\frac{\partial}{\partial x} (\rho u) + \frac{\partial}{\partial y} (\rho v) = 0 \tag{38}$$

Energy:

$$\rho C_p \left(u \frac{\partial T}{\partial x} + v \frac{\partial T}{\partial y} \right) + \rho_1 u u_1 \frac{\partial u_1}{\partial x} = \frac{\partial}{\partial y} \left(k \frac{\partial T}{\partial y} \right) + \mu \left(\frac{\partial u}{\partial y} \right)^2 \tag{39}$$

Assuming that the Prandtl number and the specific heat at constant pressure are constant and using Equation (37), we can write the energy equation as

$$\rho u \frac{\partial T_t}{\partial x} + \rho v \frac{\partial T_t}{\partial y} = \frac{1}{Pr} \frac{\partial}{\partial y} \left(\mu \frac{\partial T_t}{\partial y} \right) + \left(1 - \frac{1}{Pr} \right) \frac{\partial}{\partial y} \left[\mu \frac{\partial}{\partial y} \left(\frac{u^2}{2C_p} \right) \right] \tag{40}$$

where the total temperature T_t is defined as

$$T_t = T + \frac{u^2}{2C_p} \tag{41}$$

A temperature parameter S will be defined and used in the subsequent analysis

$$S = \frac{T_t}{T_{t_o}} - 1 \tag{42}$$

where T_{t_o} is the total temperature at the edge of the boundary layer.

In terms of S and with a Prandtl number of unity, the energy equation becomes

$$\rho u \frac{\partial S}{\partial x} + \rho v \frac{\partial S}{\partial y} = \frac{\partial}{\partial y}\left(\mu \frac{\partial S}{\partial y}\right) \tag{43}$$

with the boundary conditions

$$y = 0 \qquad S = S_w = \frac{T_w}{T_{t_o}} - 1 \tag{44}$$

$$y = \infty \qquad S = 0 \tag{45}$$

At the beginning of interaction at $x = x_o$ the distribution of S across the boundary layer is an initial condition to be specified. For the adiabatic case the distribution was $S = 0$. For the nonadiabatic case, the initial distribution will be taken as that given by the present solution for a flat plate with no pressure gradient.

With regard to velocity, the boundary conditions on A, B, and C, of Figure 2, are the same as those specified by Equations (14), (15), (16), and (17). On Boundary B, the initial velocity profile in the Dorodnitsyn plane is the Blasius profile for the adiabatic case. For the cooled case with no pressure gradient, we still have a Blasius profile but the boundary-layer displacement thickness is different from that for the adiabatic case for the same value of x_o.

3.2 Transformation to Dorodnitsyn Plane

The compressible flow problem is first reduced to an equivalent incompressible flow problem by means of the Stewartson transformation. For this purpose an additional assumption between the temperature and viscosity is made in accordance with the following equation:

$$\frac{\mu}{\mu_o} = C \frac{T}{T_o} \tag{46}$$

We will let C equal unity. The spatial coordinates undergo a nonlinear scaling,

$$X = \int_o^x \frac{p_1 a_1}{p_o a_o}\, dx \qquad Y = \int_{w(x)}^{y} \frac{\rho_1 a_1}{\rho_o a_o} \left(\frac{\rho}{\rho_1}\right) dy \tag{47}$$

New velocity components U and V are defined by

$$\left.\begin{aligned} u &= \frac{a_1}{a_o} U \\ v &= \frac{\rho_o}{\rho} \frac{p_1}{p_o} \frac{a_1}{a_o} V - \frac{\rho_o}{\rho} U \frac{\partial Y}{\partial x} \end{aligned}\right\} \tag{48}$$

The equations under this transformation become

Momentum:

$$U \frac{\partial U}{\partial X} + V \frac{\partial U}{\partial Y} = (S + 1) U_1 \frac{\partial U_1}{\partial X} + \nu_o \frac{\partial^2 U}{\partial Y^2} \tag{49}$$

Continuity:

$$\frac{\partial U}{\partial X} + \frac{\partial V}{\partial Y} = 0 \tag{50}$$

Energy:

$$U \frac{\partial S}{\partial X} + V \frac{\partial S}{\partial Y} = \nu_o \frac{\partial^2 S}{\partial Y^2} \tag{51}$$

The boundary conditions are transformed as follows:

Boundary A:

The surface $y = w(x)$ transforms to the flat plate $Y = 0$. Thus, for

$$Y = 0; \quad U = 0, \; V = 0, \; S = S_w = \frac{T_w}{T_{t_o}} - 1 \tag{52}$$

Boundary B:

The initial velocity and temperature profiles will be specified in the Dorodnitsyn plane; their shape here is not required.

Boundary C:

$$\left.\begin{aligned} Y = \infty: \quad U &= U_1(X) = \frac{a_o}{a_1}\, u_1(x) \\ V &= \frac{\rho}{\rho_o}\,\frac{a_o}{a_1}\,\frac{p_o}{p_1}\, v_1(x) + \frac{p_o}{p_1}\left(\frac{a_o}{a_1}\right)^2 u_1(x)\,\frac{\partial Y}{\partial x} \\ S &= 0 \end{aligned}\right\} \qquad (53)$$

The next step is to introduce the Dorodnitsyn transformation to eliminate the viscosity explicitly and to normalize the axial velocity component. We introduce new coordinates and velocity components

$$\left.\begin{aligned} \xi &= \int_o^X \frac{U_1}{U_o}\,\frac{dX}{\ell} & \eta &= \frac{U_1}{U_o \ell}\sqrt{\frac{U_o \ell}{\nu_o}}\, Y \\ \bar{u} &= \frac{U}{U_1} & \bar{v} &= \frac{V}{U_1}\sqrt{\frac{U_o \ell}{\nu_o}} \\ \bar{w} &\equiv \bar{v} + \bar{u}\eta\,\frac{\dot{U}_1}{U_1} \end{aligned}\right\} \qquad (54)$$

Under these transformations the differential equations become

Momentum:

$$\bar{u}\,\frac{\partial \bar{u}}{\partial \xi} + \bar{w}\,\frac{\partial \bar{u}}{\partial \eta} = \left[(S+1) - \bar{u}^2\right]\frac{\dot{U}_1}{U_1} + \frac{\partial^2 \bar{u}}{\partial \eta^2} \qquad (55)$$

Continuity:

$$\frac{\partial \bar{u}}{\partial \xi} + \frac{\partial \bar{w}}{\partial \eta} = 0 \qquad (56)$$

Energy:

$$\bar{u}\,\frac{\partial S}{\partial \xi} + \bar{w}\,\frac{\partial S}{\partial \eta} = \frac{\partial^2 S}{\partial \eta^2} \qquad (57)$$

The boundary conditions are now considered

Boundary A:

$$\eta = 0, \quad \bar{u} = 0, \quad \bar{v} = 0, \quad \bar{w} = 0, \quad S = S_w$$

Boundary B:

On this boundary the initial velocity and temperature profiles are taken to be those on a flat plate with no pressure gradient.

Boundary C:

$$\eta = \infty, \quad \bar{u} = 1, \quad S = 0$$

3.3 Integral Relations for Momentum and Energy

We will develop the integral relationship for momentum in a manner similar to that for the adiabatic analysis of Reference 1. To obtain this relationship we introduce the family of smoothing functions

$$f_n(\bar{u}) = (1 - \bar{u})^n \tag{58}$$

so chosen that they approach zero as η approaches ∞ and 1 as η approaches zero. The integral relationship is formed by multiplying the continuity equation by $f(\bar{u})$, the momentum equation by $f'(\bar{u})$, adding, and integrating across the boundary layer. The limits in front of separation are the wall and infinity, and the limits downstream of separation are the η_s line and infinity. The subscript "s" is used to denote the lower limit for both cases. With the assumption that $\partial\bar{u}/\partial\eta$ is function only of $\bar{u}$, we obtain

$$\frac{d}{d\xi}\int_{\bar{u}_s}^{1} \frac{f\bar{u}\, d\bar{u}}{\frac{\partial\bar{u}}{\partial\eta}} - (f\bar{v})_s = \frac{\dot{U}_1}{U_1}\int_{\bar{u}_s}^{1} \frac{f'(S + 1 - \bar{u}^2)}{\frac{\partial\bar{u}}{\partial\eta}}\, d\bar{u} - \left(f' \frac{\partial\bar{u}}{\partial\eta}\right)_s - \int_{\bar{u}_s}^{1} f'' \frac{\partial\bar{u}}{\partial\eta}\, d\bar{u} \tag{59}$$

Note that this equation is precisely the same as Equation (33) of Reference 1 except for the addition of the S term. It could have been written by inspection.

Another momentum integral relation exists for the inner flow by carrying the integration between the surface and the η_s line

$$\frac{d}{d\xi}\int_0^{\bar{u}_s}\frac{f\bar{u}\,d\bar{u}}{\left(\frac{\partial\bar{u}}{\partial\eta}\right)}+(f\bar{v})_s=\frac{\dot{U}_1}{U_1}\int_0^{\bar{u}_s}\frac{f'(S+1-\bar{u}^2)}{\left(\frac{\partial\bar{u}}{\partial\eta}\right)}\,d\bar{u}+\left(f'\frac{\partial\bar{u}}{\partial\eta}\right)_s$$

$$-\left(f'\frac{\partial\bar{u}}{\partial\eta}\right)_w-\int_0^{\bar{u}_s}f''\frac{\partial\bar{u}}{\partial\eta}\,d\bar{u} \qquad (60)$$

The subscript s denotes quantities evaluated at the η_s line, and the symbol $\bar{u}_s$ is retained for clarity even though $\bar{u}_s$ is zero.

Using the first four smoothing functions and forming linear combinations of the four equations resulting from Equation (59), we find for the outer flow

$$\left.\begin{aligned}
&\frac{d}{d\xi}\int_{\bar{u}_s}^1\frac{(1-\bar{u})\bar{u}\,d\bar{u}}{\frac{\partial\bar{u}}{\partial\eta}}=\bar{v}_s-\frac{\dot{U}_1}{U_1}\int_{\bar{u}_s}^1\frac{(S+1-\bar{u}^2)}{\frac{\partial\bar{u}}{\partial\eta}}\,d\bar{u}+\left.\frac{\partial\bar{u}}{\partial\eta}\right|_s\\
&-\frac{d}{d\xi}\int_{\bar{u}_s}^1\frac{(1-\bar{u})\bar{u}^2d\bar{u}}{\frac{\partial\bar{u}}{\partial\eta}}=-\frac{\dot{U}_1}{U_1}\int_{\bar{u}_s}^1\frac{(S+1-\bar{u}^2)(1-2\bar{u})d\bar{u}}{\frac{\partial\bar{u}}{\partial\eta}}+\left.\frac{\partial\bar{u}}{\partial\eta}\right|_s-2\int_{\bar{u}_s}^1\frac{\partial\bar{u}}{\partial\eta}\,d\bar{u}\\
&\frac{d}{d\xi}\int_{\bar{u}_s}^1\frac{(1-\bar{u})\bar{u}^3d\bar{u}}{\frac{\partial\bar{u}}{\partial\eta}}=\frac{\dot{U}_1}{U_1}\int_{\bar{u}_s}^1\frac{(S+1-\bar{u}^2)(2-3\bar{u})\bar{u}\,d\bar{u}}{\frac{\partial\bar{u}}{\partial\eta}}-2\int_{\bar{u}_s}^1(1-3\bar{u})\frac{\partial\bar{u}}{\partial\eta}\,d\bar{u}\\
&-\frac{d}{d\xi}\int_{\bar{u}_s}^1\frac{(1-\bar{u})\bar{u}^4d\bar{u}}{\frac{\partial\bar{u}}{\partial\eta}}=-\frac{\dot{U}_1}{U_1}\int_{\bar{u}_s}^1\frac{(S+1-\bar{u}^2)(3-4\bar{u})\bar{u}^2d\bar{u}}{\frac{\partial\bar{u}}{\partial\eta}}+6\int_{\bar{u}_s}^1(1-2\bar{u})\bar{u}\frac{\partial\bar{u}}{\partial\eta}\,d\bar{u}
\end{aligned}\right\} \qquad (61)$$

These equations can also be obtained directly from Equation (59) by using the following four smoothing functions successively for the four equations:

$$(1-\bar{u}) \qquad -\bar{u}(1-\bar{u}) \qquad \bar{u}^2(1-\bar{u}) \qquad -\bar{u}^3(1-\bar{u})$$

Treating Equation (60) for the inner flow with the same smoothing functions, we find for the inner flow

$$\left.\begin{aligned}
&\frac{d}{d\xi}\int_0^{\bar{u}_s}\frac{(1-\bar{u})\bar{u}\,d\bar{u}}{\frac{\partial\bar{u}}{\partial\eta}} = -\bar{v}_s - \frac{\dot{U}_1}{U_1}\int_0^{\bar{u}_s}\frac{(S+1-\bar{u}^2)}{\frac{\partial\bar{u}}{\partial\eta}}\,d\bar{u} - \left.\frac{\partial\bar{u}}{\partial\eta}\right|_w^s \\
&-\frac{d}{d\xi}\int_0^{\bar{u}_s}\frac{(1-\bar{u})\bar{u}^2 d\bar{u}}{\frac{\partial\bar{u}}{\partial\eta}} = -\frac{\dot{U}_1}{U_1}\int_0^{\bar{u}_s}\frac{(S+1-\bar{u}^2)(1-2\bar{u})d\bar{u}}{\frac{\partial\bar{u}}{\partial\eta}} - \left.\frac{\partial\bar{u}}{\partial\eta}\right|_w^s - 2\int_0^{\bar{u}_s}\frac{\partial\bar{u}}{\partial\eta}\,d\bar{u} \\
&\frac{d}{d\xi}\int_0^{\bar{u}_s}\frac{(1-\bar{u})\bar{u}^3 d\bar{u}}{\frac{\partial\bar{u}}{\partial\eta}} = +\frac{\dot{U}_1}{U_1}\int_0^{\bar{u}_s}\frac{(S+1-\bar{u}^2)(2-3\bar{u})\bar{u}\,d\bar{u}}{\frac{\partial\bar{u}}{\partial\eta}} - 2\int_0^{\bar{u}_s}(1-3\bar{u})\frac{\partial\bar{u}}{\partial\eta}\,d\bar{u} \\
&-\frac{d}{d\xi}\int_0^{\bar{u}_s}\frac{(1-\bar{u})\bar{u}^4 d\bar{u}}{\frac{\partial\bar{u}}{\partial\eta}} = -\frac{\dot{U}_1}{U_1}\int_0^{\bar{u}_s}\frac{(S+1-\bar{u}^2)(3-4\bar{u})\bar{u}^2 d\bar{u}}{\frac{\partial\bar{u}}{\partial\eta}} + 6\int_0^{\bar{u}_s}(1-2\bar{u})\bar{u}\frac{\partial\bar{u}}{\partial\eta}\,d\bar{u}
\end{aligned}\right\} \qquad (62)$$

In Equations (61) the value of $\bar{v}_s$ is zero in front of separation. It is noted that S enters linearly in one integral of each equation. If S is taken proportional to $(1-\bar{u})$ the pole due to $\partial\bar{u}/\partial\eta$ at $\bar{u}=1$ will be overcome by a zero in the numerator and the integrals will be convergent for all finite S. Downstream of separation v_s can be evaluated by the continuity relationship for a specified velocity profile.

The energy integral velocities are obtained by multiplying the momentum equation by Sf', the continuity equation by Sf, the energy equation by f, adding, and integrating between the same limits as before. The outer energy equation is

$$\begin{aligned}
\frac{d}{d\xi}\int_{\bar{u}_s}^{1}\frac{Sf\bar{u}\,d\bar{u}}{\frac{\partial\bar{u}}{\partial\eta}} - (Sf\bar{v})_s &= \frac{\dot{U}_1}{U_1}\int_{\bar{u}_s}^{1}\frac{Sf'(S+1-\bar{u}^2)d\bar{u}}{\frac{\partial\bar{u}}{\partial\eta}} - \left(Sf'\frac{\partial\bar{u}}{\partial\eta}\right)_s \\
&- \int_{\bar{u}_s}^{1}\frac{\partial(Sf')}{\partial\bar{u}}\left(\frac{\partial\bar{u}}{\partial\eta}\right)d\bar{u} - \left(f\frac{\partial S}{\partial\eta}\right)_s \\
&- \int_{\bar{u}_s}^{1} f'\frac{\partial S}{\partial\bar{u}}\frac{\partial\bar{u}}{\partial\eta}\,d\bar{u}
\end{aligned} \qquad (63)$$

Here the subscript "s" refers to the inner boundary which is the wall in front of separation and the η_s line downstream of separation. It is noted that if S is constant, this equation reduces to Equation (59).

For the inner flow between the wall and the η_s line, the energy integral relation is

$$\frac{d}{d\xi}\int_0^{\bar{u}_s} \frac{Sf\bar{u}\,d\bar{u}}{\frac{\partial\bar{u}}{\partial\eta}} + (Sf\bar{v})_s = \frac{\dot{U}_1}{U_1}\int_0^{\bar{u}_s} \frac{Sf'(S+1-\bar{u}^2)d\bar{u}}{\frac{\partial\bar{u}}{\partial\eta}}$$

$$+ \left(Sf'\frac{\partial\bar{u}}{\partial\eta}\right)_s - \left(Sf'\frac{\partial\bar{u}}{\partial\eta}\right)_w - \int_0^{\bar{u}_s} \frac{\partial(Sf')}{\partial\bar{u}}\frac{\partial\bar{u}}{\partial\eta}\,d\bar{u}$$

$$+ \left(f\frac{\partial S}{\partial\eta}\right)_s - \left(f\frac{\partial S}{\partial\eta}\right)_w - \int_0^{\bar{u}_s} f'\frac{\partial S}{\partial\bar{u}}\frac{\partial\bar{u}}{\partial\eta}\,d\bar{u} \qquad (64)$$

Equations (63) and (64) can be simplified somewhat by observing that

$$\left.\begin{aligned} f_s &= f_w = 1 \\ f_s' &= f_w' = -n \end{aligned}\right\} \qquad (65)$$

The equations for $n = 1$ are then

$$\frac{d}{d\xi}\int_{\bar{u}_s}^{1} \frac{S(1-\bar{u})\bar{u}\,d\bar{u}}{\frac{\partial\bar{u}}{\partial\eta}} - (S\bar{v})_s = -\frac{\dot{U}_1}{U_1}\int_{\bar{u}_s}^{1} \frac{S(S+1-\bar{u}^2)d\bar{u}}{\frac{\partial\bar{u}}{\partial\eta}}$$

$$+ \left(S\frac{\partial\bar{u}}{\partial\eta}\right)_s - \left(\frac{\partial S}{\partial\eta}\right)_s + 2\int_{\bar{u}_s}^{1} \frac{\partial S}{\partial\bar{u}}\frac{\partial\bar{u}}{\partial\eta}\,d\bar{u}$$

for the outer layer and

$$\frac{d}{d\xi}\int_0^{\bar{u}_s} \frac{S(1-\bar{u})\bar{u}\,d\bar{u}}{\frac{\partial \bar{u}}{\partial \eta}} + (S\bar{v})_s = -\frac{\dot{U}_1}{U_1}\int_0^{\bar{u}_s} \frac{S(S+1-\bar{u}^2)d\bar{u}}{\frac{\partial \bar{u}}{\partial \eta}} - S\left.\frac{\partial \bar{u}}{\partial \eta}\right|_w^s$$

$$+ \left.\frac{\partial S}{\partial \eta}\right|_w^s + 2\int_0^{\bar{u}_s} \frac{\partial S}{\partial \bar{u}}\,\frac{\partial \bar{u}}{\partial \eta}\,d\bar{u} \qquad (66)$$

for the inner layer.

3.4 Choice of Temperature Profile

An examination of Equations (59) and (63) for the outer flow shows the integrals will be functions only of $\bar{u}$ if $\partial\bar{u}/\partial\eta$ and S are expanded as functions of $\bar{u}$. In the present work the velocity profiles will be represented by the following form

$$\frac{\partial \bar{u}}{\partial \eta} = \frac{(1-\bar{u})\sqrt{\bar{u}+c_3}}{c_0 + c_1\bar{u} + c_2\bar{u}^2 + \cdots} \qquad (67)$$

so that $\partial\bar{u}/\partial\eta = 0$ when $\bar{u} = 1$. At separation we have

$$\bar{u} = 0 \qquad c_3 = 0 \qquad \frac{\partial \bar{u}}{\partial \eta} = 0$$

With regard to the total temperature profiles, we have defined S so that it has the following properties:

$$\eta = 0 \qquad S = \frac{T_w}{T_{t_o}} - 1 = S_w$$

$$\eta = \infty \qquad S = 0$$

The condition at infinity can be met by making $(1-\bar{u})$ a multiplication factor in the expression for S. However, let us examine the value of $\partial S/\partial\eta$ at separation

$$\frac{\partial S}{\partial \eta} = \frac{\partial S}{\partial \bar{u}} \cdot \frac{\partial \bar{u}}{\partial \eta} \qquad (68)$$

Since $\partial\bar{u}/\partial\eta$ is zero at separation, we must have $\partial S/\partial\bar{u}$ is infinite at separation if the heat-transfer rate is not zero there. This can be achieved

by having a term of the type $\sqrt{\bar{u} + c_3}$ in the expansion for S. We therefore try the following expansion:

$$S(\bar{u}) = -E_o(1 - \bar{u})\sqrt{\bar{u} + c_3} + (1 - \bar{u})\left(b_o + E_1\bar{u} + E_2\bar{u}^2 + E_3\bar{u}^3 + \cdots\right) \quad (69)$$

Since $\bar{u} = 0$ at the wall

$$S_w = -E_o\sqrt{c_3} + b_o$$

Thus, the expansion becomes

$$S(\bar{u}) = -E_o(1 - \bar{u})\sqrt{\bar{u} + c_3} + (1 - \bar{u})\left(S_w + E_o\sqrt{c_3} + E_1\bar{u} + E_2\bar{u}^2 + E_3\bar{u}^3 + \cdots\right) \quad (70)$$

Note here that E_o is proportional to the heat-transfer rate at the separation point.

It will be noted that if

$$E_o = E_1 = E_2 = E_3 = \cdots = 0 \quad (71)$$

we have

$$S_1(\bar{u}) = S_w(1 - \bar{u}) \quad (72)$$

which is just the Crocco relationship valid for no pressure gradients. Consider now the momentum integral given by Equation (59). If S is small or if no pressure gradients occur, the velocity field for the nonadiabatic case can be well calculated using the Crocco integral without the necessity of calculating the temperature profiles explicitly. We shall call this type of coupling between temperature and velocity fields <u>first-order coupling</u>. We note that E_o is zero so that the heat-transfer rate at the separation point is zero.

In second-order coupling, we take the next higher order term in $S(\bar{u})$,

$$S_2(\bar{u}) = S_w(1 - \bar{u}) + E_o(1 - \bar{u})\left(\sqrt{c_3} - \sqrt{\bar{u} + c_3}\right) \quad (73)$$

In this equation we have the unknown E_o for which an additional differential equation is required. This is obtained by taking one moment of the energy equation.

3.5 Differential Equations of Outer Layer

From the integral equations for momentum and energy and the assumed velocity and temperature profiles, we can derive the ordinary differential equations which are to be solved by numerical methods. Consider first the outer layer, and consider second-order coupling described by Equation (73). Under these circumstances, the set of equations, Equations (61), yields the following for momentum equations for the outer layer

$$g_1\dot{c}_o + g_2\dot{c}_1 + g_3\dot{c}_2 + (c_o\dot{g}_1 + c_1\dot{g}_2 + c_2\dot{g}_3)\dot{c}_3 + \left[(c_o g_o + c_1 g_1 + c_2 g_2)\left(1 + E_o\sqrt{c_3} + S_w\right) + (c_o g_1 + c_1 g_2 + c_2 g_3) - E_o\left(c_o + \frac{c_1}{2} + \frac{c_2}{3}\right)\right]\frac{\dot{U}_1}{U_1} = \frac{\sqrt{c_3}}{c_o} + v_s \tag{74}$$

$$g_2\dot{c}_o + g_3\dot{c}_1 + g_4\dot{c}_2 + (c_o\dot{g}_2 + c_1\dot{g}_3 + c_2\dot{g}_4)\dot{c}_3 - \left[(c_o g_o + c_1 g_1 + c_2 g_2)\left(1 + E_o\sqrt{c_3} + S_w\right) - (c_o g_1 + c_1 g_2 + c_2 g_3)\left(1 + 2E_o\sqrt{c_3} + 2S_w\right) - 2(c_o g_2 + c_1 g_3 + c_2 g_4) + E_o\left(\frac{c_1}{6} + \frac{c_2}{6}\right)\right]\frac{\dot{U}_1}{U_1} = 2(P_o - P_1) - \frac{\sqrt{c_3}}{c_o} \tag{75}$$

$$g_3\dot{c}_o + g_4\dot{c}_1 + g_5\dot{c}_2 + (c_o\dot{g}_3 + c_1\dot{g}_4 + c_2\dot{g}_5)\dot{c}_3 - \left[2(c_o g_1 + c_1 g_2 + c_2 g_3)\left(1 + E_o\sqrt{c_3} + S_w\right) - (c_o g_2 + c_1 g_3 + c_2 g_4)\left(1 + 3E_o\sqrt{c_3} + 3S_w\right) - 3(c_o g_3 + c_1 g_4 + c_2 g_5) + E_o\left(\frac{c_1}{12} + \frac{c_2}{10}\right)\right]\frac{\dot{U}_1}{U_1} = -2P_o + 8P_1 - 6P_2 \tag{76}$$

$$g_4\dot{c}_o + g_5\dot{c}_1 + g_6\dot{c}_2 + (c_o\dot{g}_4 + c_1\dot{g}_5 + c_2\dot{g}_6)\dot{c}_3 - \left[3(c_o g_2 + c_1 g_3 + c_2 g_4)\left(1 + E_o\sqrt{c_3} + S_w\right) - (c_o g_3 + c_1 g_4 + c_2 g_5)\left(1 + 4E_o\sqrt{c_3} + 4S_w\right) - 4(c_o g_4 + c_1 g_5 + c_2 g_6) + E_o\left(\frac{c_1}{20} + \frac{c_2}{15}\right)\right]\frac{\dot{U}_1}{U_1} = -6P_1 + 18P_2 - 12P_3 \tag{77}$$

It is to be noted that for first-order coupling, the quantity S_w, which has been taken as a constant, enters in a very simple way into the above equations, and they can be solved independently of the temperature equations. In case E_o is not taken to be zero, an additional differential equation based on Equation (66) must be used.

A complete derivation of the momentum and energy differential equations for fourth-order coupling has been made, and the results are presented in Appendix I. From these results the energy equation for second-order coupling was obtained on the assumption that E_1, E_2, and E_3 equal zero. The resulting equation was simplified using the first two momentum equations to obtain

$$-E_o\left(\frac{\dot{c}_o}{6}+\frac{\dot{c}_1}{12}+\frac{\dot{c}_2}{20}\right)+\frac{E_o}{2\sqrt{c_3}}(\bar{f}_2-\bar{f}_3)\dot{c}_3+\left[\sqrt{c_3}(\bar{f}_2-\bar{f}_3)-\left(\frac{c_o}{6}+\frac{c_1}{12}+\frac{c_2}{20}\right)\right]\dot{E}_o$$

$$-\left[\left(E_o\sqrt{c_3}+S_w\right)^2(\bar{f}_1-\bar{f}_2)+\left(E_o\sqrt{c_3}+S_w\right)(\bar{f}_1-\bar{f}_3)\right.$$

$$\left.-E_o^{\,2}(\bar{f}_2-\bar{f}_3+c_3\bar{f}_1-c_3\bar{f}_2)+E_o\left(\frac{2c_o}{3}+\frac{c_1}{4}+\frac{2c_2}{15}\right)\right]\frac{\dot{U}_1}{U_1}$$

$$=E_o\left[-\frac{2c_3}{c_o}+\frac{1}{2c_o}+(2c_3-1)(Q_o-Q_1)+3(Q_1-Q_2)\right] \tag{78}$$

where

$$\bar{f}_n=c_o g_{n-1}+c_1 g_n+c_2 g_{n+1} \tag{79}$$

The structure of this equation can readily be seen. If $\dot{U}_1/U_1$ is zero so that there are no pressure gradients, and if the initial value of E_o is zero as for the Crocco relationship, the solution to the equation is that E_o remains zero. This result is in accord with the known result that the Crocco integral is a solution to the energy equation if there are no pressure gradients. Equation (78) must be included in the set together with Equations (74) through (77) for second-order coupling.

3.6 Momentum and Energy Relations for Inner Layer

In Reference 1 it was shown that the continuity of the first and second derivatives at the $\bar{u}=0$ line specified a quadratic profile for the inner layer and also determined the distance of the $\bar{u}=0$ line from the wall. To

this degree of approximation, any additional momentum equations for the inner layer were superfluous. However, the use of a cubic profile, which has been built into the calculative program, requires an additional relationship. Rather than use the first equation of the set given by Equation (62) as the additional relationship, it was decided to use a relationship obtained by applying the momentum equation at the wall. At the wall, this relationship becomes

$$(S_w + 1)\frac{\dot{U}_1}{U_1} = \frac{2\left(2\alpha_w + \frac{\sqrt{c_s}}{c_o}\right)}{\eta_s} \tag{80}$$

We have assumed that the wall temperature throughout the separated flow region is equal to S_w, its value in front of separation.

With regard to the energy relationship within the inner layer, certain assumptions will be made depending on whether first-order coupling or second-order coupling is considered. In the inner layer, the calculated flows in the past have been seen to be subsonic so that little static temperature variation occurs because of velocity variations. The principal effect of cooling (or heating) insofar as the outer flow is concerned is associated with changes in density of the inner layer which affect the momentum thickness. Accordingly, for first-order coupling we will assume that the inner layer is at a uniform value of S equal to S_w. This assumption gives no information concerning the variation of S within the inner layer and in particular does not yield the sign of the heat transfer at the wall. Accordingly, it avoids the difficulty, previously encountered in applying the Crocco relationship to the inner layer, that the heat transfer to the wall changes sign going through the separation point.

Along the $\bar{u} = 0$ line, the temperature gradient is given by

$$\frac{\partial T}{\partial \eta} = -S_w T_{t_o} \frac{\partial \bar{u}}{\partial \eta}, \quad \bar{u} = 0 \tag{81}$$

The net heat conduction for a cool wall, S_w being negative, is thus into the inner layer. This is physically in the correct direction. The heat transferred across the $\bar{u} = 0$ line by convection is zero since the flow is circulating and both enters and leaves the inner region at T_w. Accordingly, evaluation of the heat conduction along the $\bar{u} = 0$ line yields the net cooling of the outer flow by the inner region. No information concerning the distribution of the heat transfer at the wall in the separated region is given.

In second-order coupling the inner region will no longer be considered at uniform stagnation temperature, nor will the $\bar{u} = 0$ line be uniformly at S_w. Let the S profile be expanded in a power series in the inner region

$$S = S_w + b_1\eta + b_2\eta^2 + b_3\eta^3 + \cdots \tag{82}$$

It is interesting to note that the differential equation for S, Equation (57), yields the result that $\partial^2 S/\partial\eta^2$ is zero at the wall. Accordingly, the coefficient b_2 is zero. We thus have the result that second-order coupling corresponds to a linear gradient of S in the inner layer.

Let the value of S on the $\bar{u} = 0$ line be S_s. Therefore, in Equation (73), S_w should be replaced by S_s. It is clear that S_s and E_o are both functions of ξ in second-order coupling. They are not independent, since the relationship between them can be obtained from Equation (82) by matching $\partial S/\partial\eta$ between the inner and outer flows at the $\bar{u} = 0$ line. From Equation (73) we find that the derivative is given by

$$\left.\frac{\partial S_2}{\partial \eta}\right|_{\bar{u}=o} = \frac{\partial S_2}{\partial \bar{u}} \left.\frac{\partial \bar{u}}{\partial \eta}\right|_{\bar{u}=o} = -\frac{\sqrt{c_3}}{c_o}\left(S_s + \frac{E_o}{2\sqrt{c_3}}\right) \tag{83}$$

Matching this derivative with the corresponding derivatives given by Equation (82) at η_s yields

$$S_s = \frac{S_w - \eta_s\left(\frac{E_o}{2c_o}\right)}{1 + \eta_s\frac{\sqrt{c_3}}{c_o}} \tag{84}$$

An additional equation for determining E_o can be obtained by substituting the temperature profile of the outer layer

$$S = S_s(1 - \bar{u}) + E_o(1 - \bar{u})\left(\sqrt{c_3} - \sqrt{\bar{u} + c_3}\right) \tag{85}$$

into Equation (66). It must also be remembered that S_s is a function of ξ. The derivation is not carried out here since second-order coupling downstream of the separation point will not be calculated herein.

3.7 Free-Interaction Equation

When the boundary layer is cooled, the density of the fluid near the wall is increased. Cooling thus tends to reduce the boundary-layer displacement thickness, and heating tends to increase it. The free-interaction assumption used in the analysis is that the pressure distribution acting on a body in a viscous flow can be calculated by inviscid flow theory provided the body dimensions are expanded by the amount of the boundary-layer displacement thickness. In supersonic flow this assumption combined with Prandtl-Meyer theory forms a basis for calculating the pressure distribution. The derivation for nonadiabatic supersonic flow is given in Appendix II for both the preseparation region and the post-separation region. The analysis for the pre-separation region has been made for second-order coupling, but that for the post-separation region has been made only for first-order coupling.

3.8 Initial Conditions

To start the integration, a point is selected as the beginning of interaction, and it is assumed that the velocity profile of the boundary layer is that corresponding to flow over a flat plate with no pressure gradients at uniform wall temperature S_w up to the beginning of interaction. It is also assumed that the initial value of ϕ to be used in the free-interaction equation also corresponds to this condition. Further integration would continue to develop a Blasius-type solution. To start the separation solution, a small pressure disturbance is applied to the boundary layer as part of the initial conditions.

To obtain the initial velocity profile, we noted that the boundary-layer equation in the Stewartson plane, Equations (49) and (50), represent the laminar incompressible flow of a fluid of uniform viscosity ν_o. We thus have a Blasius profile in the Stewartson plane. Also, the profile is independent of S_w. If interaction starts at X_o in the Stewartson plane, it will start at ξ_o in the Dorodnitsyn plane where the integrations are actually carried out.

$$\xi_o = \frac{X_o}{\ell} \tag{86}$$

It was shown in Reference 1 that the values of c_o, c_1, c_2, and c_3 which describe the initial velocity profile are then given by

$$c_0 = 3.157\sqrt{\xi_0}$$
$$c_1 = -1.923\sqrt{\xi_0}$$
$$c_2 = -0.3133\sqrt{\xi_0} \qquad (87)$$
$$c_3 = 1.100$$

These values apply also to the nonadiabatic case since the Blasius velocity profile in the Stewartson plane is independent of S_w for no pressure gradients.

The initial value of ϕ does depend on S_w, since the displacement thickness of the boundary layer will depend on S. In the Stewartson plane, the Blasius expressions for the displacement thickness and momentum thickness are

$$\delta_S^* = \lambda_1\sqrt{\frac{\nu_0 X}{U_0}} = \int_0^\infty \left(1 - \frac{U}{U_1}\right) dY$$
$$\qquad (88)$$
$$\delta_S^{**} = \lambda_2\sqrt{\frac{\nu_0 X}{U_0}} = \int_0^\infty \frac{U}{U_1}\left(1 - \frac{U}{U_1}\right) dY$$

The displacement thickness of the original flow expressed in the variables of the Stewartson flow is

$$\delta^* = \frac{\rho_0 a_0}{\rho_1 a_1}\left[(1 + m_1)\int_0^\infty S\, dY + (1 + m_1)\int_0^\infty \left(1 - \frac{U}{U_1}\right) dY + m_1\int_0^\infty \frac{U}{U_1}\left(1 - \frac{U}{U_1}\right) dY\right] \qquad (89)$$

The integral containing S becomes for first-order coupling or no pressure gradients

$$\int_0^\infty S\, dY = S_w\int_0^\infty (1 - \bar{u})\, dY = S_w\delta_S^* \qquad (90)$$

The displacement thickness is now

$$\delta^* = \frac{\rho_0 a_0}{\rho_1 a_1}\left[(1 + m_1)(1 + S_w)\delta_S^* + m_1\delta_S^{**}\right] \qquad (91)$$

For zero pressure gradient

$$\rho_1 = \rho_o \qquad a_1 = a_o \qquad X = x$$

$$\delta^* = (1 + m_o)(1 + S_w)\lambda_1\sqrt{\frac{\nu_o X}{U_o}} + m_o\lambda_2\sqrt{\frac{\nu_o X}{U_o}} \tag{92}$$

$$\left.\frac{d\delta^*}{dx}\right|_{x_o} = \tan\phi_o = \sqrt{\frac{\nu_o}{u_o x}}\left[(1 + m_o)(1 + S_w)\frac{\lambda_1}{2} + m_o\frac{\lambda_2}{2}\right] \tag{93}$$

We have thus established the initial value of ϕ_o before a pressure wave is applied to the boundary layer.

The free-interaction solution is started by introducing a discontinuous pressure jump at the beginning of interaction of 0.1 percent of the absolute pressure. This jump causes a small change in ϕ_o. This calculation is based on Prandtl-Meyer flow at the outer edge of the boundary layer. It is unaffected by the cooling or heating of the boundary layer, and for this case is exactly as presented in Reference 1.

3.9 Calculative Examples

It is usually easy to obtain an accurate position of the separation point, x_s, from experimental pressure data since it falls nearly halfway between p_o and p_s. It is not easy to obtain an experimental value of the distance to the beginning of interaction, x_o. As a result, a systematic series of calculations has been made to show how x_s/x_o varies with R_o and M_o. The results of these calculations are shown in Figure 13. Figure 13 presents the ratio of the distance to separation to the distance to the start of interaction as a function of M_o for various Reynolds numbers. It is seen from Figure 13 that the effect of Reynolds number upon x_s/x_o is substantial. For low Reynolds numbers, x_s/x_o decreases with increasing M_o but, for large Reynolds numbers, the trend changes sign.

In order to obtain some insight into the effect of cooling on the separated flow pattern, a series of runs was made on an IBM 7094 computing machine for a flat plate with a 10^o wedge. The basic parameters of the outer flow are

$$M_o = 2.55$$

$$R_o/\ell = 8.5\times10^5 \text{ per ft}$$

$$S_w = 0,\ -0.2,\ -0.4,\ -0.6$$

A list of the runs made is given in Table I together with some calculated quantities.

In Figure 6 a plot is shown of the effect of wall cooling on separation pressure distribution for a fixed location of the beginning of interaction. We see that the effect of cooling shortens the distance from the beginning of interaction to the separation point, but does not cause much change in separation pressure or plateau pressure. Accordingly, the pressure gradients are increased by cooling. The pressure gradients in front of the reattachment point are also increased. This is the same result found previously in the investigation described in Reference 3.

In the particular case shown in Figure 6, the beginning of interaction is taken fairly close to the start of the wedge so that no extensive plateau regions can develop. It is noted that the pressure ratio for T_w/T_{t_o} of 0.4 exhibits a falling pressure downstream of separation. There is a possibility that the first-order coupling solution, on which this figure is based, is reaching its limit of accuracy for such large amounts of cooling as represented by a value of T_w/T_{t_o} of 0.4. Since no second-order coupling calculations have been made in this report, we do not know the accuracy of the first-order coupling solution for low values of T_w/T_{t_o}. It is important to extend the results of the calculative program to second-order coupling to investigate this point. Some light will subsequently be shed on this question through comparison between experiment and theory.

What is of interest is whether the extent of separation increases or decreases due to wall cooling. A proven reattachment criterion is required to pick out the correct location of separation for a given value of S_w before a firm answer to this question can be given. However, some insight into this question is given in Figure 7. Here we have shown the distance from the beginning of interaction to separation as a function of the location of the beginning of interaction for various values of T_w/T_{t_o}. As x_o is decreased, the distance to separation reduces. The extension of the curves should tend toward the origin as might be expected. As shown previously, we can move the point x_o forward until the dividing streamline curve is tangent to the compression wedge. At this point β_R is zero and a more forward location of x_o will not be accompanied by reattachment of the boundary layer. The reattachment angles are given as a function of the reattachment point location in Figure 8. The point at which the angle β_R is zero moves down the ramp as the wall is cooled. This means that a lesser extent of separation is possible with a cooled wall than without. If the reattachment criterion is that $\beta_R = 0$, then the extent of separation is reduced by wall cooling.

In Figure 7, another boundary is shown for which the separation point would fall right at the juncture of the plate and wedge. The flow would separate and then immediately reattach on the wedge. Accordingly, the boundary for which separation is at the corner represents the limiting line for separated flow. The curves of reattachment point location are plotted versus separation position in Figure 9 to see if cooling has much influence on the location of reattachment for fixed separation point. It is seen that there is only a weak effect of cooling. What this result implies is that the shape of the dividing streamline emanating from a given separation point is not sensitive to cooling. Another point of interest is that all curves seem to tend to a point for which x_s and x_R are equal to the value of x at the corner of the wedge and plate.

Returning now to Figure 7, we see that if the plate is cooled below a critical value of T_w/T_{t_o} no separated flow is possible. While this highly-cooled condition is probably beyond the range of accuracy of first-order coupling, it is nevertheless of interest because the qualitative results are probably unchanged by second-order coupling.

In order to illustrate the changes in separation pressure distribution as the plate is cooled towards its critical value of T_w/T_{t_o}, the systematic set of curves shown in Figure 10 has been prepared. As the value of T_w/T_{t_o} decreases, the separation pressure distributions tend toward a limiting distribution. As T_w/T_{t_o} is decreased below a critical value between 0.133 and 0.132, there is a discontinuous change in the solution from that for a separated layer to that for an attached layer. This interesting result can be explained on mathematical grounds and a condition for its occurrence derived.

In order to explain the above phenomenon on mathematical grounds, let us consider the Equations (74), (75), (76), (77), and Equation (II-10) of Appendix II. We will assume first-order coupling so that E_o is zero. This assumption is justified by examining the set of equations just below the critical temperature ratio for which the pressure ratio p_1/p_o is nearly constant. For initial conditions, let ξ_o be unity and assume a Blasius profile so that $c_o = 3.157$, $c_1 = -1.923$, $c_2 = 0.3133$, $c_3 = 1.100$.

Consider now the coefficient matrix of the five simultaneous equations (see pg. 31) for the conditions of a Blasius-type solution for which c_o, c_1, and c_2 vary as $\xi^{1/2}$ and c_3 is constant. The functions f_{ij} for which no parameters are specified depend only on the initial values of c_o, c_1, c_2, and c_3. The function f_{55} warrants special mention since the Reynolds number falls out of this term through the use of Equation (92).

Equation	$\dot{c}_0$	$\dot{c}_1$	$\dot{c}_2$	$\dot{c}_3$	$\dot{U}_1/U_1$	Right-Hand Term
(74)	f_{10}	f_{11}	f_{12}	$\xi^{1/2} f_{13}$	$\xi^{1/2}\ f_{14}(S_w)$	$\frac{f_{15}}{\xi^{1/2}}$
(75)	f_{20}	f_{21}	f_{22}	$\xi^{1/2} f_{23}$	$\xi^{1/2}\ f_{24}(S_w)$	$\frac{f_{25}}{\xi^{1/2}}$
(76)	f_{30}	f_{31}	f_{32}	$\xi^{1/2} f_{33}$	$\xi^{1/2} f_{34}(S_w)$	$\frac{f_{35}}{\xi^{1/2}}$
(77)	f_{40}	f_{41}	f_{42}	$\xi^{1/2} f_{43}$	$\xi^{1/2}\ f_{44}(S_w)$	$\frac{f_{45}}{\xi^{1/2}}$
(II-10)	$f_{50}(S_w,M_1)$	$f_{51}(S_w,M_1)$	$f_{52}(S_w,M_1)$	$\xi^{1/2} f_{53}(S_w,M_1)$	$\xi^{1/2} f_{54}(S_w,M_1,\gamma)$	$\frac{f_{55}(S_w,M_1)}{\xi^{1/2}}$

Let us first consider the first four equations with the additional condition that $\dot{U}_1$ is zero. It is clear that the solution with c_o, c_1, and c_2 proportional to $\xi^{1/2}$ and with c_3 constant is the similarity solution to these equations provided that the initial values of c_o, c_1, c_2, and c_3 correspond to the Blasius velocity profile. In fact if the initial conditions do not correspond precisely to a Blasius profile, the equations will generate the Blasius profile asymptotically.

Let us now consider the case for which the determinant of the coefficent matrix is zero. In this case one of the equations of the set is redundant, say Equation (II-10). Note that if it is redundant for one value of ξ, it is redundant for all values of ξ. Accordingly, if the initial value of $\dot{U}_1$ is zero and the other initial conditions are as previously specified, then the complete set will still develop the Blasius similarity solution. If the initial value of $\dot{U}_1$ is not zero, the set will still develop the Blasius solution asymptotically with $\dot{U}_1$ decaying proportional to ξ^{-1}. The boundary layer thus damps out any pressure disturbance which tends to separate it. For very large disturbances which propagate their effects upstream and destroy the free interaction, this result will not apply.

It is apparent that the vanishing of the determinant yields a relationship between Mach number and critical temperature ratio. For wall temperatures less than this temperature ratio, the laminar boundary layer cannot be separated by free interaction between the boundary layer and the outer flow. It is interesting that this relationship is independent of Reynolds number. The calculated variation of the critical value of T_w/T_{t_o} with Mach number is listed below for a Prandtl number of unity and for γ of 1.4.

M_o	1.2	2	3	5	8	12	20
T_w/T_{t_o}	0.026	0.091	0.160	0.231	0.267	0.281	0.289

An experiment to test the theory is clearly needed. Also the dependence of the Prandtl number, ratio of specific heats, and the viscosity relationship on the critical value of T_w/T_{t_o} should be calculated.

4. AXISYMMETRIC NONADIABATIC FLOW

For axisymmetric nonadiabatic flow, the analysis combines elements of both previous sections. We will generally not repeat the previous analysis, but will indicate how the previous results are modified for this case.

4.1 Differential Equations and Boundary Conditions

With regard to the coordinate system described in Figure 1, the differential equations for momentum and continuity taken from Reference 2, page 389, are

$$\left.\begin{aligned} \rho u' \frac{\partial u'}{\partial x'} + \rho v' \frac{\partial u'}{\partial y'} &= -\frac{\partial p}{\partial x'} + \frac{\partial}{\partial y'}\left(\mu \frac{\partial u'}{\partial y'}\right) \\ \frac{\partial}{\partial x'}(\rho r u') + \frac{\partial}{\partial y'}(\rho r v') &= 0 \end{aligned}\right\} \tag{94}$$

The continuity equation applies to a boundary layer for which the boundary-layer thickness is small compared to the radius. It is noted that ρ and p are not primed since only transformations of coordinates and velocity components will be used. For a Prandtl number of unity, the energy equation has the form

$$\rho u' \frac{\partial S}{\partial x'} + \rho v' \frac{\partial S}{\partial y'} = \frac{\partial}{\partial y'}\left(\mu \frac{\partial S}{\partial y'}\right) \tag{95}$$

Note that two of these equations, momentum and energy, have the same form as the corresponding two-dimensional equations.

In the physical plane, the boundary conditions are the same as those given by Equations (7) to (9) for the velocity components. For the temperature boundary conditions, we have

$$\left.\begin{aligned} y' = 0 \qquad S &= S_w = \frac{T_w}{T_{t_o}} - 1 \\ y' = \infty \qquad S &= 0 \end{aligned}\right\} \tag{96}$$

We also use the condition that S_w is uniform. At the onset of interaction it is assumed that the initial velocity profile is the same as that for the adiabatic case. The initial temperature profile will be subsequently discussed.

We now apply the same transformation as used previously to transform the differential equations of the axisymmetric plane to the two-dimensional plane.

$$x = \int_0^{x'} r^2(x')dx' \qquad y = \int_{r(x')}^{y'} r(x')dy' = r(x')\left[y' - r(x')\right] \tag{97}$$

If the transformation of the velocity components is given by the following equations

$$\left.\begin{aligned} u &= u' \\ v &= \frac{v'}{r} + \frac{u'}{r^2}(y' - 2r)\frac{dr}{dx'} \end{aligned}\right\} \tag{98}$$

then the differential equations of continuity, momentum, and energy are of the form:

Continuity:

$$\frac{\partial}{\partial x}(\rho u) + \frac{\partial}{\partial y}(\rho v) = 0 \tag{99}$$

Momentum:

$$\rho u \frac{\partial u}{\partial x} + \rho v \frac{\partial u}{\partial y} = \rho_1 u_1 \frac{du_1}{dx} + \frac{\partial}{\partial y}\left(\mu \frac{\partial u}{\partial y}\right) \tag{100}$$

Energy:

$$\rho u \frac{\partial S}{\partial x} + \rho v \frac{\partial S}{\partial y} = \frac{\partial}{\partial y}\left(\mu \frac{\partial S}{\partial y}\right) \tag{101}$$

The boundary conditions for the velocity components are the same as for the adiabatic axisymmetrical case as given by Equations (14) to (17). The temperature boundary conditions are that S is zero at the outer edge of the boundary layer, and that S equals S_w uniformly at the wall. The values of density, pressure, and temperature are the same at corresponding points (x,y) and (x',y') under the transformation.

Since the Equations (99), (100), and (101) are identical in form to Equations (37), (38), and (43) with identical boundary conditions, the transformations to the Stewartson and Dorodnitsyn planes are identical to those for the two-dimensional nonadiabatic case. It is noted that the shape of the flare in the two-dimensional plane is not the same as in the axisymmetric plane, but is, in fact, a flat plate. One difference that occurs is that the free-interaction equation is not the same as that for two-dimensional flow when transformed to the two-dimensional plane.

4.2 Free-Interaction Equation

Let $\delta^{*\prime}$ be the boundary-layer displacement thickness in the axisymmetric plane. For thin boundary layers, that is, for $\delta^{*\prime}/r$ much less than unity, we can write

$$\delta^{*\prime} = \int_{r}^{r+\delta^{\prime}} \left(1 - \frac{\rho u^{\prime}}{\rho_1 u_1^{\prime}}\right) dy^{\prime}$$

$$= \int_{0}^{\delta} \left(1 - \frac{\rho u}{\rho_1 u_1}\right) \frac{dy}{r} = \frac{\delta^*}{r} \tag{102}$$

In the axisymmetric plane we will use shock-expansion theory to evaluate the pressure distribution assuming that the displacement thickness in that plane is added to the body contour. The turning angle of the outer flow $\phi^{\prime}$ is thus given by

$$\tan \phi^{\prime} = \frac{dr}{dx^{\prime}} + \frac{d\delta^{*\prime}}{dx^{\prime}} \tag{103}$$

or

$$\tan \phi^{\prime} + \left(\frac{\delta^*}{r^2} - 1\right) \frac{dr}{dx^{\prime}} = r \frac{d\delta^*}{dx} \tag{104}$$

This equation can be written in the form

$$\frac{R_o^{1/2}}{(1 + m_o)r} \left(\tan \phi^{\prime} - \frac{dr}{dx^{\prime}}\right) + \frac{R_o^{1/2}}{(1 + m_o)r^3} \delta^* \frac{dr}{dx^{\prime}} = \frac{R_o^{1/2}}{(1 + m_o)} \frac{d\delta^*}{dx} \tag{105}$$

analogous to that given by Equation (24) for adiabatic axisymmetric flow. The expression for $d\delta^*/dx$ is that pertaining to two-dimensional nonadiabatic flow as already derived in Appendix II.

The right-hand term of Equation (105) is given by the sum of the right-hand sides of Equations (II-10) and (II-16) of Appendix II of this report and Equation (II-15) of Appendix II of Reference 1. The difference between the free-interaction equation above for axisymmetric flow and that for two-dimensional flow occurs only on the left-hand side of the equation as can be seen by comparison with Equation (II-11) of Appendix II.

It is assumed that the Prandtl-Meyer relationship for two-dimensional flow is valid for three-dimensional shapes utilizing $\phi^{\prime}$ as the turning angle, as given by Equation (19). The initial value of $\phi_o^{\prime}$ must, however, be derived since it is not the same as for adiabatic axisymmetric flow.

4.3 Initial Conditions

The initial conditions are taken as those on a cylinder or a flat plate with zero pressure gradient for the external flow at uniform Mach number M_o, uniform wall temperature given by S_w, with interaction starting at $x' = L$ at a Reynolds number R_o. Under these circumstances, the velocity profile in the Stewartson plane at a distance x_o is that of Blasius based on viscosity ν_o, and the velocity profile is independent of S_w. This point is discussed in Section 3.8. If interaction starts at a value of $x' = L$ on the cylindrical part of the axisymmetric body, then

$$x_o = \int_o^L r_o^2 \, dx' = r_o^2 L \tag{106}$$

For constant pressure at the edge of the boundary layer

$$X_o = x_o \tag{107}$$

$$\xi_o = \frac{X_o}{\ell} = \frac{r_o^2 L}{\ell} = \frac{x_o}{\ell} = 1 \tag{108}$$

since we are taking the reference length ℓ equal to x_o. The coefficients in the initial velocity profile are thus given by Equation (87) with $\xi_o = 1$. In the region in front of the beginning of interaction, the temperature profile is given by Equation (72).

Now with regard to the initial value of ϕ' in the axisymmetric plane, we can write

$$\tan \phi' = \frac{d\delta^{*'}}{dx'} \tag{109}$$

Since in front of the beginning of interaction

$$\delta^{*'} = \frac{\delta^*}{r_o} \qquad x = r_o^2 x' \tag{110}$$

we have

$$\tan \phi_o' = r_o \frac{d\delta^*}{dx} = r_o \tan \phi_o \tag{111}$$

where $\tan \phi_o$ is given by Equation (93) and depends on S_w. We have thus established all required initial quantities for the axisymmetric nonadiabatic case.

4.4 Geometrical Relationships Used in Computational Program

In determining the initial conditions it has been assumed that the boundary layer up to the beginning of interaction corresponds to that on a flat plate at uniform pressure. This condition could be met approximately if the cylindrical part of the body were hollow with a sharp leading edge. In most cases we are faced with a blunt nose affixed to the cylindrical section. The method for applying the calculative program to this case is now discussed. We will consider an axially symmetric body of the type shown in Figure 11(a) wherein is shown a blunt nose of any shape attached to the cylindrical portion of the body. At the beginning of interaction, the boundary layer is assumed to have the same initial condition as if it has undergone a laminar run of length L_E with conditions at the edge of the boundary layer uniform and equal to those existing at the beginning of interaction. This statement thus specifies the equivalent hollow symmetrical body to which the computer program applies.

Several points need clarification in connection with the equivalence. First, in the case of the blunt body, the velocity profile at the beginning of interaction may not correspond to any flat plate profile as a result of the pressure distribution on the nose and the cylindrical section up to the beginning of interaction. This point is not a shortcoming of the calculative method since any initial profile can be used in the computer program. The assumption of a flat plate initial profile has been made merely as a convenience since the precise velocity profiles are not known. The assumption is probably a fairly good one so long as very large pressure gradients do not exist at the beginning of interaction. In fact, the assumption is equivalent to that of local similarity sometimes used in calculating heat transfer and skin friction in boundary layers with pressure gradients. A second point arises in what quantity should be matched at the beginning of interaction between the blunt body and the equivalent body. It seems best to match displacement thickness since the free-interaction equation governing the pressure distribution depends on variations in displacement thickness. It is possible to obtain approximate expressions for the equivalent length of laminar run L_E corresponding to the state of the boundary layer at the beginning of interaction. Such an approximate expression was developed in Reference 3, Appendix III, for a hemispherical nose on the basis of equal momentum thicknesses.

In the computer program, it is assumed that the cylinder and flare of the blunt body are faired into each other by a fillet of radius R. The equations for the slope of the body are then

$$r(x') = r_o \qquad L \le x' \le L'_c \tag{112}$$

$$r(x') = r_o + R - \sqrt{R^2 - (x' - L'_c)^2} \qquad L'_c \le x' \le L'_c + R \sin\beta \tag{113}$$

$$r(x') = r_o - \frac{R(1 - \cos\beta)}{\cos\beta} + (x' - L'_c)\tan\beta \qquad L'_c + R \sin\beta \le x' \le L'_b \tag{114}$$

5. COMPARISONS BETWEEN EXPERIMENT AND THEORY

Several comparisons between experiment and theory showing good agreement have been made for two-dimensional adiabatic flow in Reference 1. There are also available some adiabatic and nonadiabatic axisymmetric data which can be used for comparison. First, the adiabatic axisymmetric data of Kuehn, Reference 4, will be considered.

5.1 Adiabatic Axisymmetric Configuration of Kuehn

The pressure data chosen for comparison with the present theory are those presented by Kuehn in Figure 6 of Reference 4. The configuration and pressure distributions are shown in Figure 12. The data are presented in Reference 4 in terms of distance measured from the junction of the flare and cylinder made nondimensional by the boundary-layer thickness near the beginning of interaction. The boundary-layer thickness δ_o for this particular case is not given in the report but was reported by the author to be 0.019 inches in response to an inquiry. The experimental pressure data were replotted against true axial distance calculated using the above value of boundary-layer thickness.

In applying the calculative program to the present configuration, we must specify the location of the beginning of interaction for both the axisymmetric and the equivalent axisymmetric planes shown in Figure 11, the initial Mach number, and the initial Reynolds number. The Reynolds number per unit length near the beginning of interaction is found by calculation. We know from the data in Reference 4

$$M_\infty = 2.94$$

$$\frac{R_\infty}{\delta_o} = 6.6\times10^3$$

$$\frac{p_o}{p_\infty} = 0.9$$

If the boundary-layer air is assumed to undergo a normal shock at $M_\infty = 2.94$ and then expand isentropically to p_o, we find that

$$R_o/ft = 2.0\times10^6$$

$$M_o = 2.34$$

The distance to the beginning of interaction in both planes was taken as 0.07 feet for the calculation shown in Figure 12. These values of L and L_E will place the theoretical separation point at the experimental position and will approximately match the experimental pressure gradient at separation.

It would be desirable to use an experimentally measured boundary-layer displacement thickness at the beginning of interaction to obtain the value of R_o. Unfortunately only boundary-layer thickness is known. The boundary-layer thickness is obtained in Reference 4 by a very special approximate method described therein. The method can be expected to yield a boundary-layer thickness which is less than the theoretical value corresponding to a velocity of 99.9 percent of the value in the free stream. The following values are obtained:

Experiment:

$$\delta_o = 0.00158 \text{ ft}$$

Theory:

$$\frac{u}{u_\infty} = 0.950 \qquad y = 0.001215$$

$$\frac{u}{u_\infty} = 0.999 \qquad y = 0.001718$$

The experimental value as determined can reasonably be expected to fall between the two values shown, and no disagreement between the calculated and experimental values of δ_o exist within the accuracy of the experimental value. This particular case points up the desirability of matching displacement thicknesses so that ambiguities in the definitions of boundary-layer thickness are avoided.

The comparison between experiment and theory shown in Figure 12 is seen to be good.

5.2 Axisymmetric Configuration Tested at AEDC

An axisymmetric configuration capable of adiabatic or cooled operation has been tested in Tunnel D at Arnold Engineering Development Center. These unpublished data have been supplied to Vidya by Mr. Eugene Fleeman of the Flight Control Division of AFFDL, Wright-Patterson Air Force Base, as an aid in evaluating the theory reported herein. The model is described in detail in Reference 3. The data cover the following conditions:

$M_\infty = 3.0$, adiabatic model

$M_\infty = 5.0$, adiabatic model

$M_\infty = 3.0$, highly cooled model

$M_\infty = 5.0$, moderately cooled model

The comparison between experiment and theory is shown in Figure 14.

The data in Figure 14(a) for the $M_\infty = 3$ adiabatic case show good comparison between experiment and theory. There are substantial pressure gradients in front of the beginning of interaction. The beginning of interaction and the initial Reynolds number were obtained by means similar to those described in the previous section. A similar comparison at $M_\infty = 5.0$ in Figure 14(b) also shows good correlation except that the reattachment pressure rise occurs slightly early. Larger gradients are present in front of the beginning of interaction in the $M_\infty = 5.0$ case than for the $M_\infty = 3.0$ case. Some data points appear to be in error.

Figures 14(c) and (d) show the comparison between experiment and theory for the nonadiabatic cases. For the moderately cooled case at $M_\infty = 5.0$, good agreement between experiment and theory is shown although, as for the $M_\infty = 5$ adiabatic case, the reattachment pressure rise occurs slightly early. With regard to the highly cooled $M_\infty = 3$ case, the theory shows a decreasing pressure after separation not manifest in the data. We believe that this result is the consequence of applying the nonadiabatic theory based on first-order coupling beyond its limit. Only an application of second-order coupling theory to this case can answer this point conclusively. On the basis of these results, we recommend that the application of the first-order theory to temperature ratios T_w/T_{t_o} lower than 0.5 be avoided until further work to clarify the question has been carried out.

The physical explanation of the limitation of first-order theory to moderately-cooled walls is based on the displacement thickness of the inner flow beneath the $\bar{u} = 0$ line. For highly cooled walls the temperature of the $\bar{u} = 0$ line appears to be much higher than that of the wall. Accordingly, the average density of the inner flow is less than that at the wall as assumed in first-order coupling. The greater displacement of the inner flow would tend to increase the gradient of δ^* and counteract any tendency to falling pressures as shown in Figure14(c).

6. CONCLUDING REMARKS

The present paper presents a method for calculating the laminar compressible separated flow over a two-dimensional or axisymmetric compression surface of fairly arbitrary shape at uniform temperature. The only limitation on the shape is that the streamwise slopes of the surface be small.

(1) A calculative program based on the theory has been developed for a flat plate with a ramp connected by means of an arc for either adiabatic or nonadiabatic flow.

(2) The calculative program contains as an option, the axisymmetric analog of the two-dimensional problem.

(3) A number of comparisons between experiment and theory for adiabatic two-dimensional and axisymmetric configurations show reasonably good agreement.

(4) In the analysis for nonadiabatic flows, a method is derived which provides within its framework means for obtaining higher approximations to the total temperature profiles. In the first approximation, involving first-order coupling between total temperature and velocity profiles, the separated region under the $\bar{u} = 0$ line is assumed to be at a uniform total temperature, and no local heat-transfer coefficients in the separated flow are calculated. In second-order coupling total temperature gradients are allowed under the $\bar{u} = 0$ line, and local heat-transfer coefficients in the separated flow can be calculated.

(5) The present computer program based on first-order coupling yields calculated results in good agreement with experiment for moderate cooling. For the highly cooled case, it appears that higher-order coupling must be used.

(6) A systematic series of calculations to investigate the possible range of the separation point on a two-dimensional plate-wedge configuration showed that the most downstream location of the separation point occurred at the plate-wedge corner followed by immediate reattachment. The most upstream position of the separation point accompanies the most downstream position of the reattachment point, and this condition occurs when the dividing streamline comes in tangent to the wedge.

(7) As the two-dimensional configuration is cooled, the range within which the separation point must fall decreases if reattachment is to occur. At a certain critical wall temperature separation disappears altogether.

(8) The general method of solving separated flow problems developed in the present investigation is capable of extension to higher approximations within the framework of the method.

7. RECOMMENDATIONS FOR FUTURE WORK

As a result of the present investigation, certain potentially fruitful areas of further research have emerged. First let us consider possible improvements in the present theory. It has been pointed out that higher-order coupling in the nonadiabatic solution seems necessary if accurate solutions are to be obtained for highly cooled walls. While the theory for second-order coupling has been carried out in this report, no corresponding computer program has been written. It seems desirable to write such a program, and to compare the results for first-order and second-order coupling in order to assess the limits of accuracy of the first-order coupling theory.

It also seems worthwhile to obtain higher approximations to the velocity profiles in order to assess the accuracy of the velocity profiles now being used in the program. Increasing the degree of the inner flow velocity profile from cubic to quartic would seem to be a logical first step in this area. We believe that the use of the momentum equation at the wall and three smoothing functions, rather than the use of four smoothing functions is to be preferred in any future changes to the present program. If this is done, the Oswatitsch relationship at the separation point will be precisely fulfilled.

One of the assumptions of the present method is that it applies to ramps having small slopes with respect to the axial direction. This assumption follows from the assumption of constant pressure in flows normal to the axial direction rather than normal to the wall. If the y-axis had been taken normal to the wall, ambiguities immediately arise in passing from the plate to the wedge because of the discontinuity in the wall slope. This ambiguity could be eliminated and the general method could be applied to larger ramp angles if the coordinate system were set up parallel and perpendicular to the δ^* line. It appears feasible to carry out this suggestion within the framework of the present method.

There are many important problems to which the present method can be applied. It is possible to determine the least possible wedge angle for which a reattached separated flow can be found for specified initial conditions. In this way the boundaries for incipient laminar separation should be calculable. Applications to blowing or sucking in the separated flow area, particularly as it affects aerodynamic control, is a potentially interesting application. Possible extension of the method to turbulent boundary layers is another challenging problem. In the application of the method to blunt hypersonic bodies, it has been found difficult to determine good initial

conditions because of blast-wave effect and pressure gradient induced by the boundary layer itself. It would be worthwhile writing a program starting at the stagnation point and solving the equations for a prescribed pressure gradient up to some point where free interaction is to begin. In this way the proper initial conditions for the separated flow regime would be established. Alternately, for a simple configuration, such as a flat plate, it would be of interest to solve the laminar boundary-layer problem including free interaction starting at the leading-edge singularity. At the other end it would be useful to continue the present calculative program downstream of reattachment.

At low Reynolds numbers, very thick boundary layers can occur on axisymmetric bodies. This state of affairs prevailed in the data of Reference 3. Extension of the method to include axisymmetric boundary layers thick in comparison to the radius seems a worthwhile line of investigation.

There is a need for experimental data to check theory, especially in the reattachment region. While the present method permits the calculation of a number of separated flows for a given configuration, there exists no experimentally-verified criterion for choosing the correct solution from this continuum of solutions. While pressure distributions are helpful in checking theory, other types of data are also needed, such as:

(1) Velocity profiles in the separated region.

(2) Measurements of locations of separation and reattachment.

(3) Measurements of the angle of dividing streamline at reattachment.

(4) Static pressure surveys to check the adequacy of the boundary-layer approximation.

REFERENCES

1. Nielsen, J. N., Lynes, L. L., and Goodwin, F. K.: Calculation of Laminar Separation with Free Interaction by the Method of Integral Relations, Part I - Two-Dimensional Supersonic Adiabatic Flow. AFFDL-TR-65-107, June 1965.

2. Howarth, L.: Modern Developments in Fluid Dynamics. High Speed Flow, vol. 1, Oxford, 1956.

3. Abbott, D. E., Holt, M., and Nielsen, J. N.: Investigation of Hypersonic Flow Separation and its Effects on Aerodynamic Control Characteristics. ASD-TDR-62-963, Nov. 1962.

4. Kuehn, D. M.: Laminar Boundary-Layer Separation Induced by Flares on Cylinders at Zero Angle of Attack. NASA Tech. Rep. R-146, 1962.

TABLE I

QUANTITIES OBTAINED IN SYSTEMATIC SET OF CALCULATIONS TO INVESTIGATE TWO-DIMENSIONAL ADIABATIC SEPARATED FLOWS

$R_o/x_o = 0.85\times10^6$ per foot, $M_o = 2.55$, $\gamma = 1.4$, $(p_1/p_o)_{x_o} = 1.001$

$\beta = 10^o$, $L_c = 0.1855$ ft, $L_b = 0.35$ ft

T_w/T_{t_o}	R_o	x_o (ft)	x_s (ft)	x_p (ft)	x_R (ft)	$(\delta^*)_{x_o}$ (ft)	$(\delta^*)_{x_s}$ (ft)	$(\delta^*)_{x_p}$ (ft)	$(\delta^{**})_{x_o}$ (ft)	$(\delta^{**})_{x_s}$ (ft)	$(\delta^{**})_{x_p}$ (ft)	$\left(\frac{p_1}{p_o}\right)_{x_s}$	$\left(\frac{p_1}{p_o}\right)_{x_p}$	$\left(\frac{p_1}{p_o}\right)_{x_R}$	$(c_f)_{x_o}$	$\left(\frac{dp_1/p_o}{dx}\right)_{x_s}$ (1/ft)	$\frac{x_s}{x_o}$	$\frac{x_s - x_o}{(\delta^*)_{x_o}}$	$\frac{\left(\frac{p_1}{p_o} - 1\right)_{x_s}}{\left(\frac{p_1}{p_o} - 1\right)_{x_R}}$	β_R (deg)
0.1500	0.1275^a	0.1500	0.1527	0.1577	NR	0.6128^{-3}	0.6384^{-3}	0.8377^{-3}	$-.2796^{-3}$	0.2751^{-3}	0.2716^{-3}	1.097	1.178	NR	0.1861^{-2}	55.83	1.018	4.406	0.5424	--
	$.1360^b$	.1600	.1628	.1679	0.1972	$.6329^{-3}$	$.6593^{-3}$	$.8551^{-3}$	$.2887^{-3}$	$.2841^{-3}$	$.2806^{-3}$	1.096	1.175	1.690	$.1802^{-2}$	52.57	1.018	4.424	.5460	--
	$.1445^c$	.1700	.1730	.1780	.1922	$.6523^{-3}$	$.6797^{-3}$	$.8711^{-3}$	$.2976^{-3}$	$.2929^{-3}$	$.2893^{-3}$	1.095	1.172	1.495	$.1748^{-2}$	49.32	1.018	4.599	.5497	--
	$.1530^d$	.1800	.1831	NP	.1877	$.6713^{-3}$	$.6994^{-3}$	NP	$.3063^{-3}$	$.3014^{-3}$	NP	1.094	NP	1.239	$.1699^{-2}$	46.68	1.017	4.618	--	--
.2000	$.1105^a$	.1300	.1357	.1407	NR	$.6478^{-3}$	$.6979^{-3}$	$.9163^{-3}$	$.2603^{-3}$	$.2589^{-3}$	$.2564^{-3}$	1.113	1.201	NR	$.1999^{-2}$	45.66	1.044	8.799	.5600	--
	$.1148^b$	.1350	.1409	.1459	NR	$.6602^{-3}$	$.7107^{-3}$	$.9269^{-3}$	$.2652^{-3}$	$.2638^{-3}$	$.2613^{-3}$	1.112	1.199	NR	$.1962^{-2}$	43.83	1.044	8.937	.5606	--
	$.1190^c$	.1400	.1461	.1511	NR	$.6723^{-3}$	$.7242^{-3}$	$.9376^{-3}$	$.2701^{-3}$	$.2687^{-3}$	$.2661^{-3}$	1.111	1.197	NR	$.1927^{-2}$	42.60	1.044	9.073	.5612	--
	$.1233^d$	.1450	.1512	.1562	NR	$.6842^{-3}$	$.7372^{-3}$	$.9479^{-3}$	$.2749^{-3}$	$.2734^{-3}$	$.2708^{-3}$	1.110	1.195	NR	$.1893^{-2}$	40.93	1.043	9.062	.5619	--
	$.1275^e$	.1500	.1564	.1614	.2022	$.6959^{-3}$	$.7493^{-3}$	$.9585^{-3}$	$.2796^{-3}$	$.2781^{-3}$	$.2755^{-3}$	1.110	1.193	1.717	$.1861^{-2}$	39.82	1.043	9.197	.5677	--
	$.1445^f$	.1700	.1771	NP	.1905	$.7408^{-3}$	$.7974^{-3}$	NP	$.2976^{-3}$	$.2961^{-3}$	NP	1.107	NP	1.363	$.1748^{-2}$	35.38	1.042	9.584	--	--
.4000	$.0935^a$	.1100	.1270	.1421	NR	$.8807^{-3}$	$.1079^{-2}$	$.1916^{-2}$	$.2394^{-3}$	$.2513^{-3}$	$.2545^{-3}$	1.143	1.246	NR	$.2174^{-2}$	21.16	1.155	19.30	.5796	--
	$.09775^b$	.1150	.1326	.1476	NR	$.9005^{-3}$	$.1102^{-2}$	$.1926^{-2}$	$.2448^{-3}$	$.2569^{-3}$	$.2599^{-3}$	1.141	1.243	NR	$.2126^{-2}$	20.26	1.153	19.54	.5785	--
	$.1003^c$	.1180	.1359	.1510	.2268	$.9121^{-3}$	$.1116^{-2}$	$.1938^{-2}$	$.2480^{-3}$	$.2601^{-3}$	$.2632^{-3}$	1.141	1.242	1.800	$.2099^{-2}$	19.92	1.152	19.63	.5809	3.695
	$.1012^d$	.1190	.1370	.1521	.2256	$.9160^{-3}$	$.1120^{-2}$	$.1939^{-2}$	$.2490^{-3}$	$.2612^{-3}$	$.2643^{-3}$	1.140	1.241	1.789	$.2090^{-2}$	19.72	1.151	19.65	.5792	4.969
	$.1020^e$	.1200	.1381	.1532	.2250	$.9198^{-3}$	$.1124^{-2}$	$.1937^{-2}$	$.2501^{-3}$	$.2623^{-3}$	$.2653^{-3}$	1.140	1.241	1.737	$.2081^{-2}$	19.59	1.151	19.68	.5792	--
	$.1105^f$	.1300	.1493	.1643	.2109	$.9574^{-3}$	$.1169^{-2}$	$.1963^{-2}$	$.2603^{-3}$	$.2728^{-3}$	$.2757^{-3}$	1.138	1.236	1.609	$.1999^{-2}$	18.23	1.148	20.16	.5830	14.461
	$.1190^g$	.1400	.1604	.1805	.2011	$.9935^{-3}$	$.1211^{-2}$	$.2280^{-2}$	$.2701^{-3}$	$.2829^{-3}$	$.2863^{-3}$	1.135	1.232	1.469	$.1927^{-2}$	17.06	1.146	20.53	.5801	--
	$.1360^h$	.1600	.1826	NP	.1876	$.1062^{-2}$	$.1292^{-2}$	NP	$.2887^{-3}$	$.3020^{-3}$	NP	1.132	NP	1.194	$.1802^{-2}$	15.15	1.141	21.28	--	--
.6000	$.0765^a$	.0900	.1156	.1459	NR	$.1054^{-2}$	$.1440^{-2}$	$.3359^{-2}$	$.2166^{-3}$	$.2417^{-3}$	$.2518^{-3}$	1.157	1.268	NR	$.2403^{-2}$	13.91	1.284	24.29	.5843	--
	$.07905^b$	.0930	.1192	.1496	.2479	$.1072^{-2}$	$.1463^{-2}$	$.3367^{-2}$	$.2201^{-3}$	$.2455^{-3}$	$.2557^{-3}$	1.156	1.266	1.782	$.2364^{-2}$	13.51	1.282	24.44	.5849	4.068
	$.07990^c$	.0940	.1204	.1456	.2461	$.1077^{-2}$	$.1469^{-2}$	$.3010^{-2}$	$.2213^{-3}$	$.2468^{-3}$	$.2563^{-3}$	1.155	1.266	1.771	$.2351^{-2}$	13.40	1.281	24.51	.5811	4.515
	$.08075^d$	.0950	.1216	.1518	.2447	$.1083^{-2}$	$.1477^{-2}$	$.3351^{-2}$	$.2225^{-3}$	$.2480^{-3}$	$.2581^{-3}$	1.155	1.265	1.763	$.2339^{-2}$	13.26	1.280	24.56	.5833	4.922
	$.08500^e$	.1000	.1277	.1582	.2341	$.1111^{-2}$	$.1513^{-2}$	$.3384^{-2}$	$.2283^{-3}$	$.2542^{-3}$	$.2643^{-3}$	1.153	1.262	1.683	$.2280^{-2}$	12.69	1.277	24.93	.5824	7.953
	$.08925^f$	.1050	.1337	.1640	.2262	$.1139^{-2}$	$.1548^{-2}$	$.3376^{-2}$	$.2339^{-3}$	$.2602^{-3}$	$.2702^{-3}$	1.152	1.259	1.620	$.2225^{-2}$	12.15	1.273	25.20	.5853	10.995
	$.1020^g$	.1200	.1518	.1819	.2075	$.1217^{-2}$	$.1648^{-2}$	$.3395^{-2}$	$.2501^{-3}$	$.2773^{-3}$	$.2873^{-3}$	1.147	1.251	1.453	$.2081^{-2}$	10.80	1.265	26.13	.5840	17.452
	$.1148^h$	.1350	.1697	NP	.1937	$.1291^{-2}$	$.1743^{-2}$	NP	$.2652^{-3}$	$.2934^{-3}$	NP	1.144	NP	1.299	$.1962^{-2}$	9.706	1.257	26.88	--	--
	$.1241^i$	.1460	.1828	NP	.1874	$.1343^{-2}$	$.1807^{-2}$	NP	$.2758^{-3}$	$.3046^{-3}$	NP	1.141	NP	1.178	$.1887^{-2}$	9.072	1.252	27.40	--	--
.8000	$.05950^a$	.0700	.1008	.1362	NR	$.1157^{-2}$	$.1743^{-2}$	$.4157^{-2}$	$.1910^{-3}$	$.2276^{-3}$	$.2441^{-3}$	1.167	1.287	NR	$.2725^{-2}$	11.07	1.440	26.62	.5804	--
	$.06205^b$	.0730	.1048	.1454	.2713	$.1181^{-2}$	$.1777^{-2}$	$.4547^{-2}$	$.1950^{-3}$	$.2321^{-3}$	$.2492^{-3}$	1.165	1.284	1.772	$.2668^{-2}$	10.67	1.436	26.93	.5795	3.705
	$.06290^c$	.0740	.1061	.1413	.2671	$.1189^{-2}$	$.1789^{-2}$	$.4150^{-2}$	$.1964^{-3}$	$.2336^{-3}$	$.2500^{-3}$	1.165	1.283	1.751	$.2650^{-2}$	10.56	1.434	27.00	.5816	4.413
	$.06375^d$	.0750	.1074	.1482	.2623	$.1197^{-2}$	$.1799^{-2}$	$.4558^{-2}$	$.1977^{-3}$	$.2350^{-3}$	$.2522^{-3}$	1.164	1.282	1.726	$.2632^{-2}$	10.42	1.432	27.07	.5801	5.521
	$.06800^e$	.0800	.1140	.1546	.2512	$.1237^{-2}$	$.1854^{-2}$	$.4545^{-2}$	$.2042^{-3}$	$.2422^{-3}$	$.2593^{-3}$	1.162	1.278	1.672	$.2549^{-2}$	9.860	1.425	27.49	.5812	6.885
	$.08500^f$	.1000	.1403	.1857	.2170	$.1383^{-2}$	$.2054^{-2}$	$.4907^{-2}$	$.2283^{-3}$	$.2688^{-3}$	$.2864^{-3}$	1.155	1.264	1.465	$.2280^{-2}$	8.101	1.403	29.14	.5856	14.530
	$.1020^g$	.1200	.1662	NP	.1952	$.1515^{-2}$	$.2235^{-2}$	NP	$.2501^{-3}$	$.2928^{-3}$	NP	1.149	NP	1.287	$.2081^{-2}$	6.901	1.385	30.50	--	18.726
	$.1122^h$	.1320	.1816	NP	.1878	$.1589^{-2}$	$.2334^{-2}$	NP	$.2623^{-3}$	$.3062^{-3}$	NP	1.146	NP	1.181	$.1984^{-2}$	6.355	1.376	31.21	--	--
1.0	$.04463^a$	.0525	.0854	.1307	NR	$.1199^{-2}$	$.1978^{-2}$	$.5365^{-2}$	$.1654^{-3}$	$.2112^{-3}$	$.2348^{-3}$	1.175	1.303	NR	$.3146^{-2}$	9.893	1.627	27.44	.5762	--
	$.04505^b$	.0530	.0814	.1315	.3209	$.1204^{-2}$	$.1986^{-2}$	$.5369^{-2}$	$.1662^{-3}$	$.2121^{-3}$	$.2358^{-3}$	1.175	1.303	1.830	$.3131^{-2}$	9.803	1.536	23.59	.5762	--
	$.04548^c$	.0535	.08687	.1378	NR	$.1210^{-2}$	$.1995^{-2}$	$.5818^{-2}$	$.1670^{-3}$	$.2130^{-3}$	$.2374^{-3}$	1.174	1.302	NR	$.3117^{-2}$	9.734	1.624	27.58	.5748	--
	$.04590^d$	.0540	.08761	.1329	.3079	$.1216^{-2}$	$.2004^{-2}$	$.5366^{-2}$	$.1677^{-3}$	$.2139^{-3}$	$.2376^{-3}$	1.174	1.301	1.791	$.3102^{-2}$	9.647	1.622	27.64	.5767	2.178
	$.04633^e$	.0545	.08834	.1391	.3040	$.1221^{-2}$	$.2011^{-2}$	$.5805^{-2}$	$.1685^{-3}$	$.2148^{-3}$	$.2392^{-3}$	1.174	1.301	1.779	$.3088^{-2}$	9.579	1.621	27.71	.5767	2.568
	$.04675^f$	.0550	.08908	.1398	.3029	$.1227^{-2}$	$.2020^{-2}$	$.5799^{-2}$	$.1693^{-3}$	$.2157^{-3}$	$.2401^{-3}$	1.173	1.300	1.777	$.3074^{-2}$	9.494	1.620	27.78	.5753	2.622
	$.04888^g$	.0575	.09274	.1431	.2926	$.1254^{-2}$	$.2061^{-2}$	$.5765^{-2}$	$.1731^{-3}$	$.2201^{-3}$	$.2445^{-3}$	1.172	1.297	1.746	$.3006^{-2}$	9.140	1.613	28.10	.5777	3.727
	$.05100^h$	.0600	.09639	.1470	.2822	$.1281^{-2}$	$.2101^{-2}$	$.5773^{-2}$	$.1768^{-3}$	$.2245^{-3}$	$.2488^{-3}$	1.170	1.295	1.710	$.2943^{-2}$	8.807	1.607	28.41	.5748	4.906
	$.05312^i$	.0625	.1000	.1506	.2733	$.1308^{-2}$	$.2141^{-2}$	$.5772^{-2}$	$.1805^{-3}$	$.2287^{-3}$	$.2530^{-3}$	1.169	1.292	1.677	$.2884^{-2}$	8.493	1.600	28.67	.5773	6.115
	$.05950^j$	.0700	.1109	.1664	.2519	$.1384^{-2}$	$.2253^{-2}$	$.6136^{-2}$	$.1910^{-3}$	$.2408^{-3}$	$.2658^{-3}$	1.165	1.285	1.589	$.2725^{-2}$	8.216	1.584	29.55	.5775	--
	$.07650^k$	.0900	.1394	NP	.2160	$.1569^{-2}$	$.2523^{-2}$	NP	$.2166^{-3}$	$.2702^{-3}$	NP	1.157	NP	1.411	$.2403^{-2}$	6.192	1.549	31.49	--	14.795
	$.09350^l$	.1100	.1674	NP	.1939	$.1735^{-2}$	$.2766^{-2}$	NP	$.2394^{-3}$	$.2962^{-3}$	NP	1.151	NP	1.254	$.2174^{-2}$	5.190	1.522	33.08	--	18.324
	$.1020^m$	.1200	.1812	NP	--	$.1812^{-2}$	$.2876^{-2}$	NP	$.2501^{-3}$	$.3083^{-3}$	NP	1.148	NP	--	$.2081^{-2}$	4.815	1.510	33.77	--	--
2.0	$.02550^a$	.0300	.07971	.1865	.3050	$.1650^{-2}$	$.3783^{-2}$	$.1342^{-1}$	$.1250^{-3}$	$.2113^{-3}$	$.2741^{-3}$	1.172	1.302	1.502	$.4162^{-2}$	4.664	2.657	30.13	.5681	--
	$.03400^b$	.0400	.1020	NP	.2553	$.1905^{-2}$	$.4281^{-2}$	NP	$.1444^{-3}$	$.2390^{-3}$	NP	1.164	NP	1.409	$.3604^{-2}$	3.658	2.550	32.55	--	--
	$.04675^c$	.0550	.1341	NP	.2149	$.2233^{-2}$	$.4904^{-2}$	NP	$.1693^{-3}$	$.2740^{-3}$	NP	1.156	NP	1.296	$.3074^{-2}$	2.799	2.438	35.42	--	--

NP - No plateau.

NR - No reattachment.

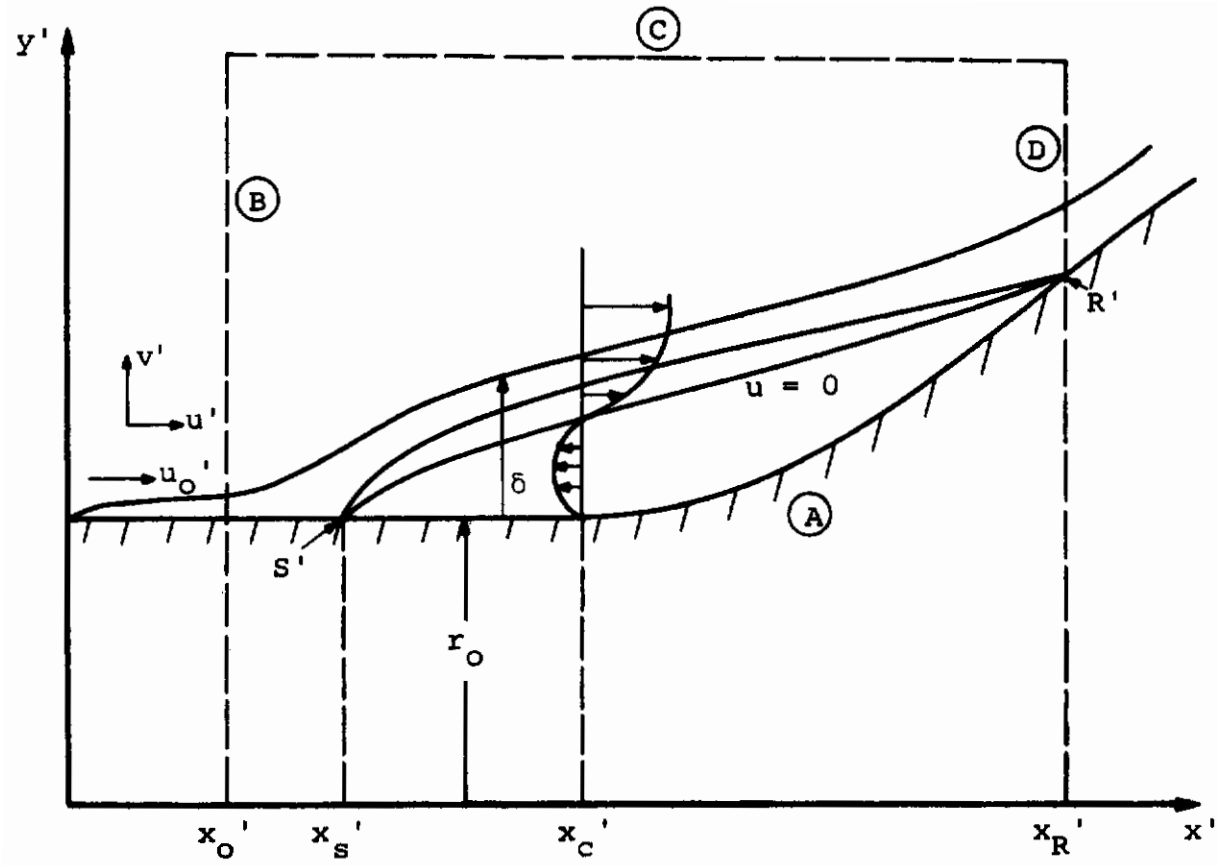

Figure 1.- Laminar separated flow over axisymmetric body.

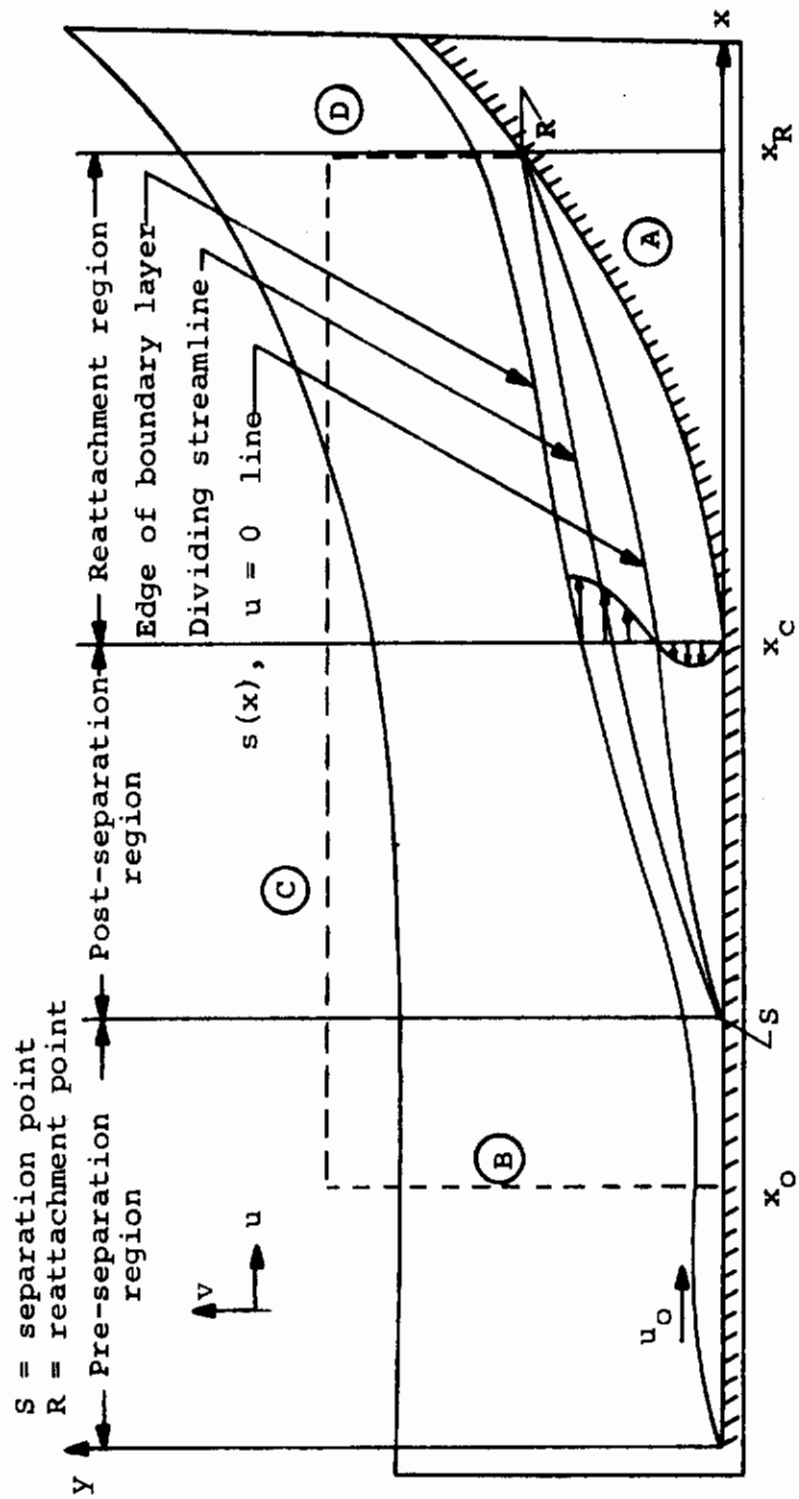

Figure 2.- Separated laminar supersonic flow over a flat plate with a ramp.

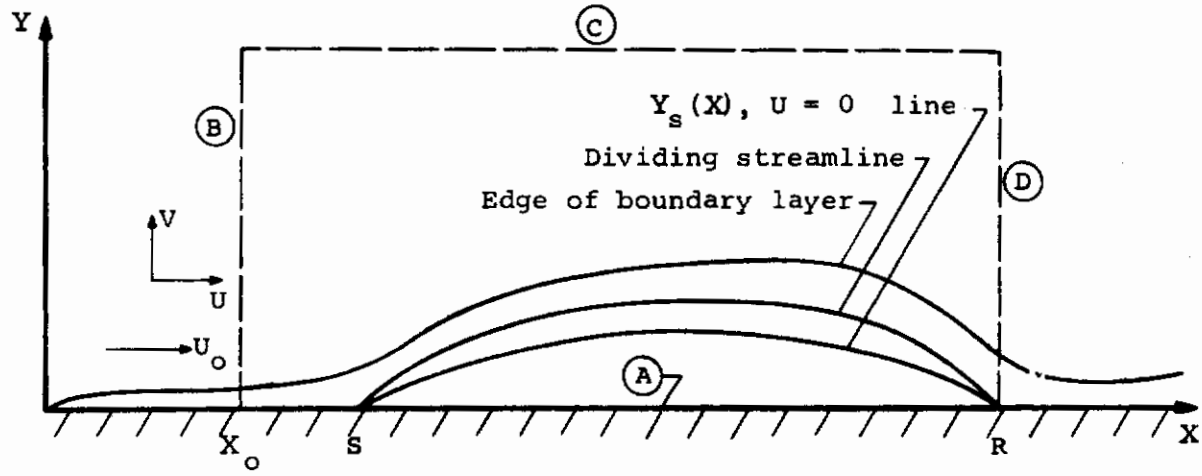

Stewartson plane

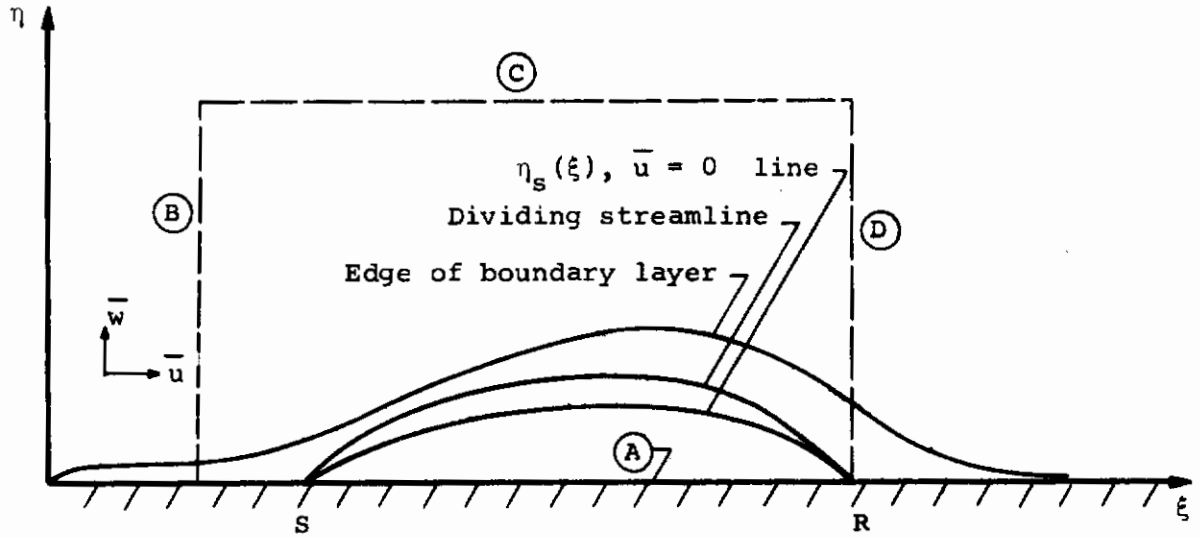

Dorodnitsyn plane

Figure 3.- Boundaries and domains in the Stewartson and Dorodnitsyn planes.

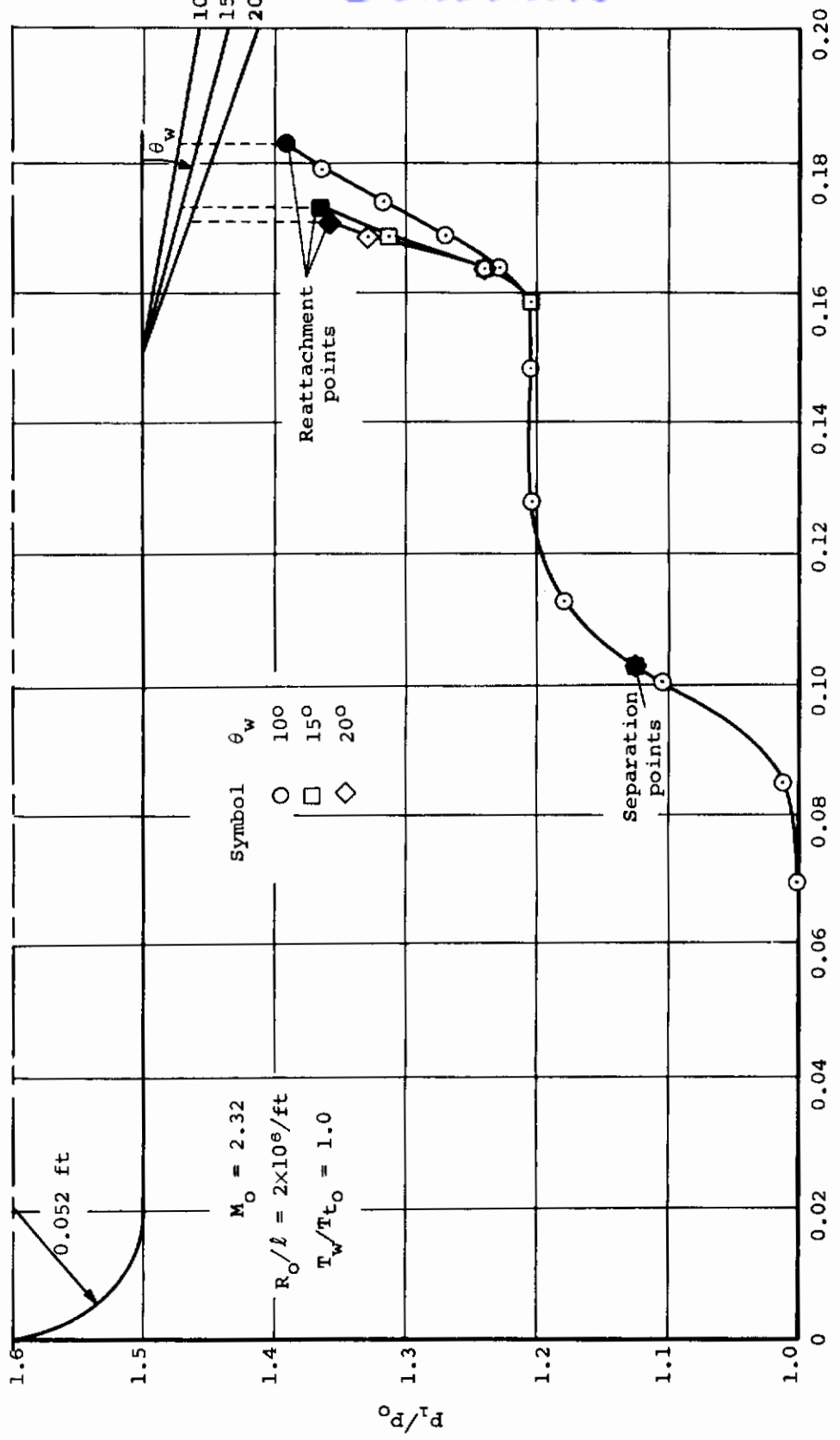

Figure 4.- Calculated effect of flare angle on separation pressure distribution.

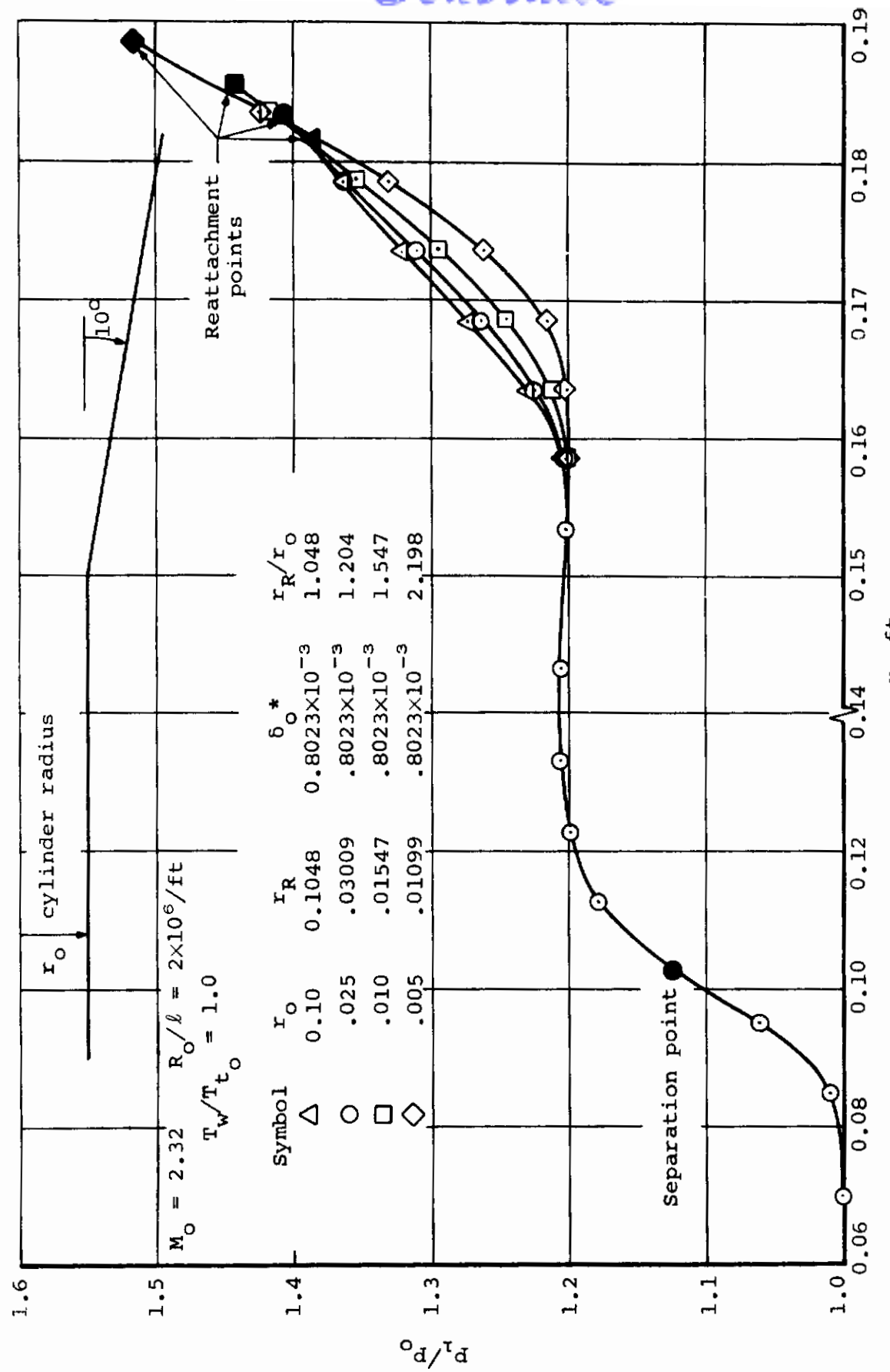

Figure 5.- Calculated effect of body radius on separation pressure distribution for fixed flare angle.

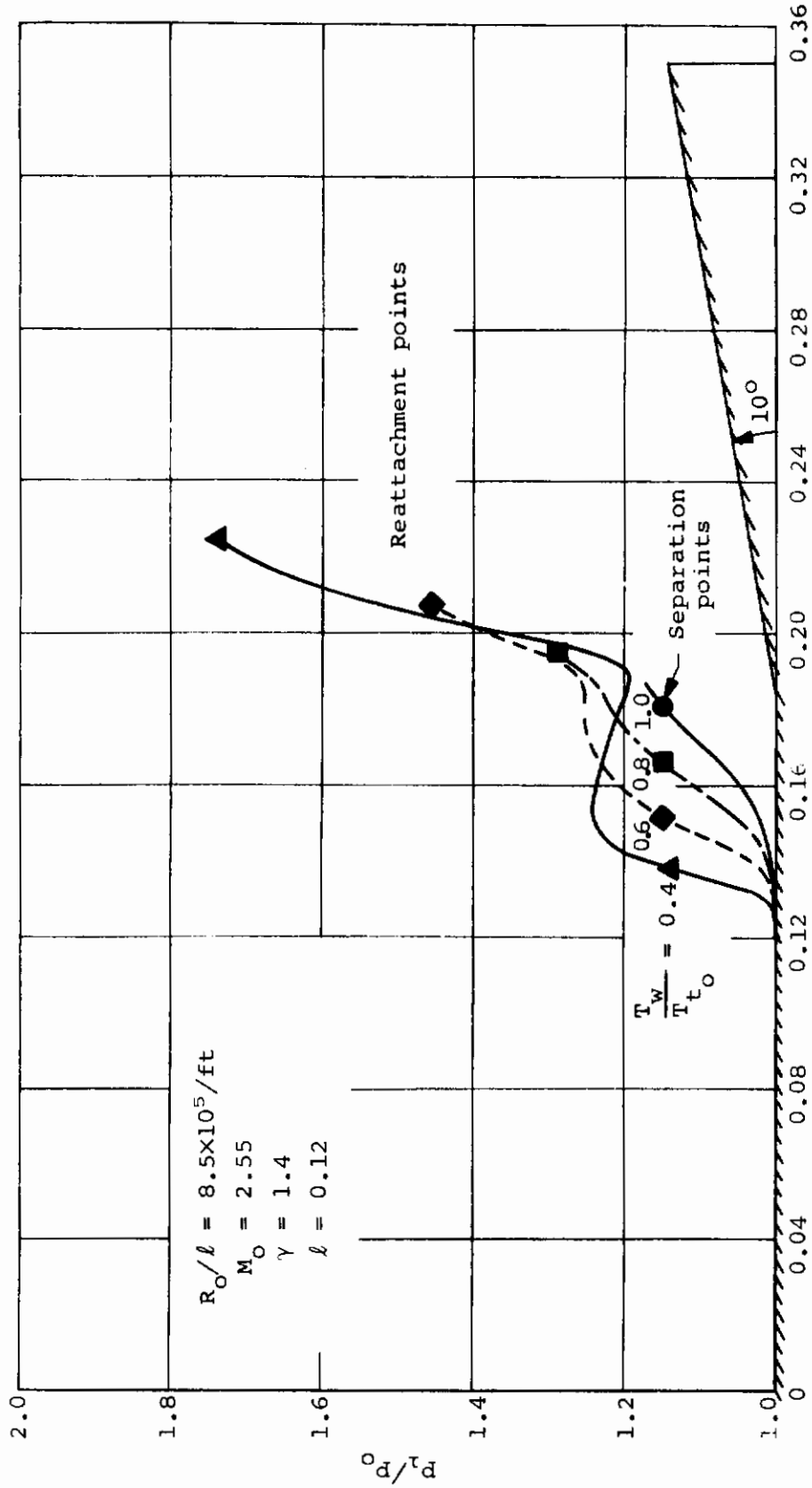

Figure 6.- Effect of cooling on separated pressure distribution for fixed position of beginning of interaction; two-dimensional flow.

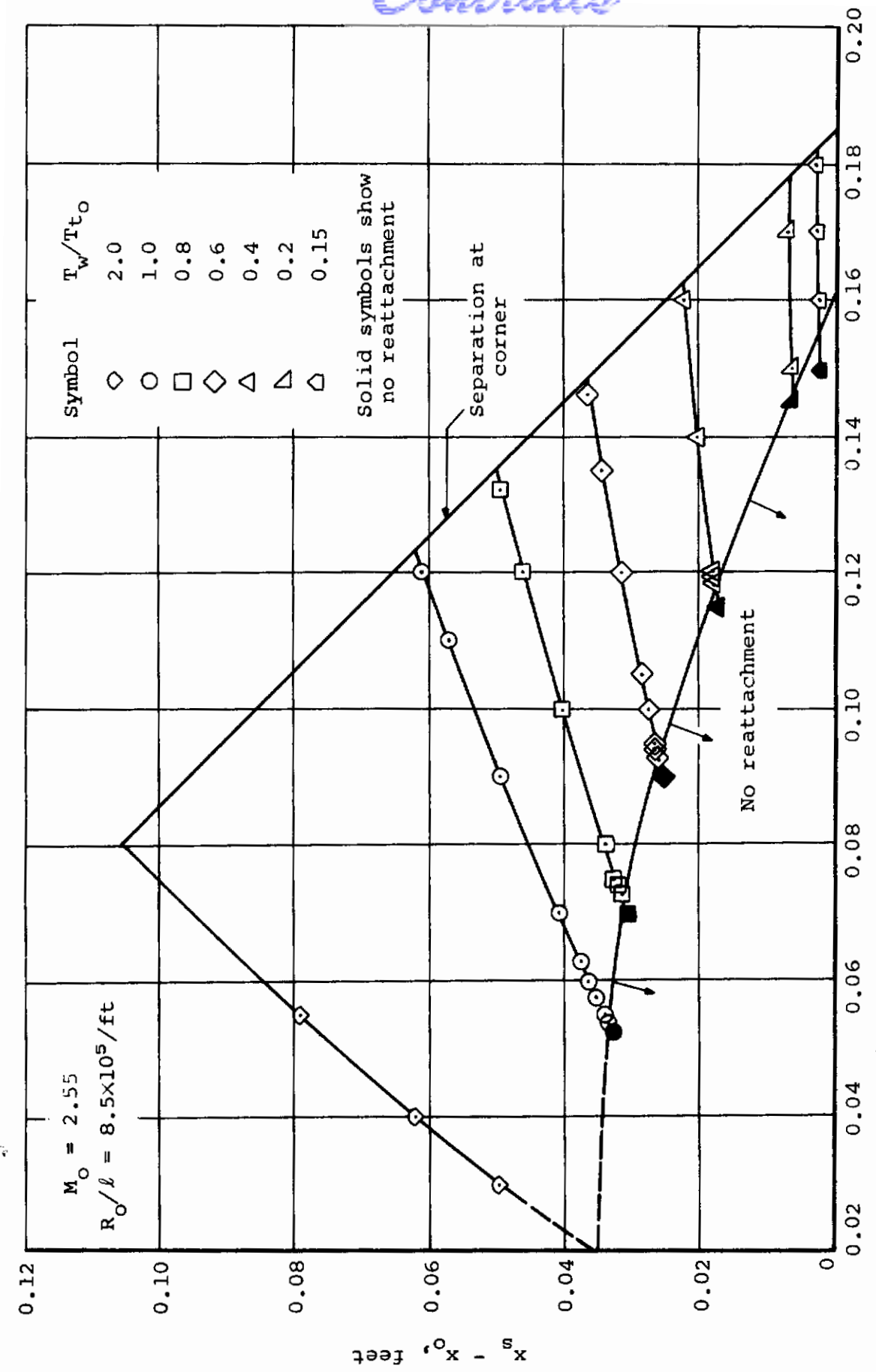

Figure 7.- Distance between beginning of interaction and location of separation as influenced by cooling.

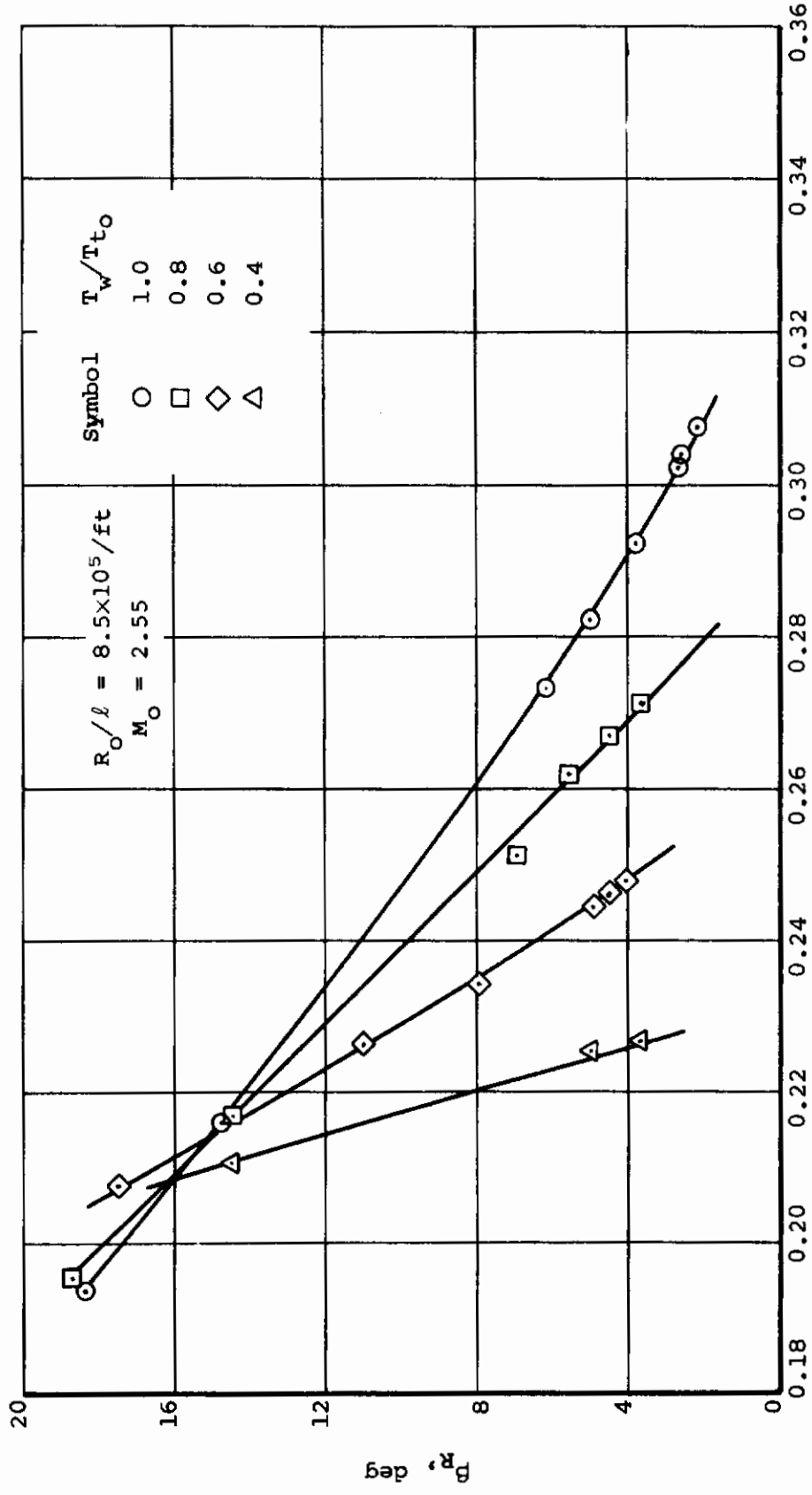

Figure 8.- Angle between dividing streamline and wedge at reattachment point as influenced by cooling from Table I.

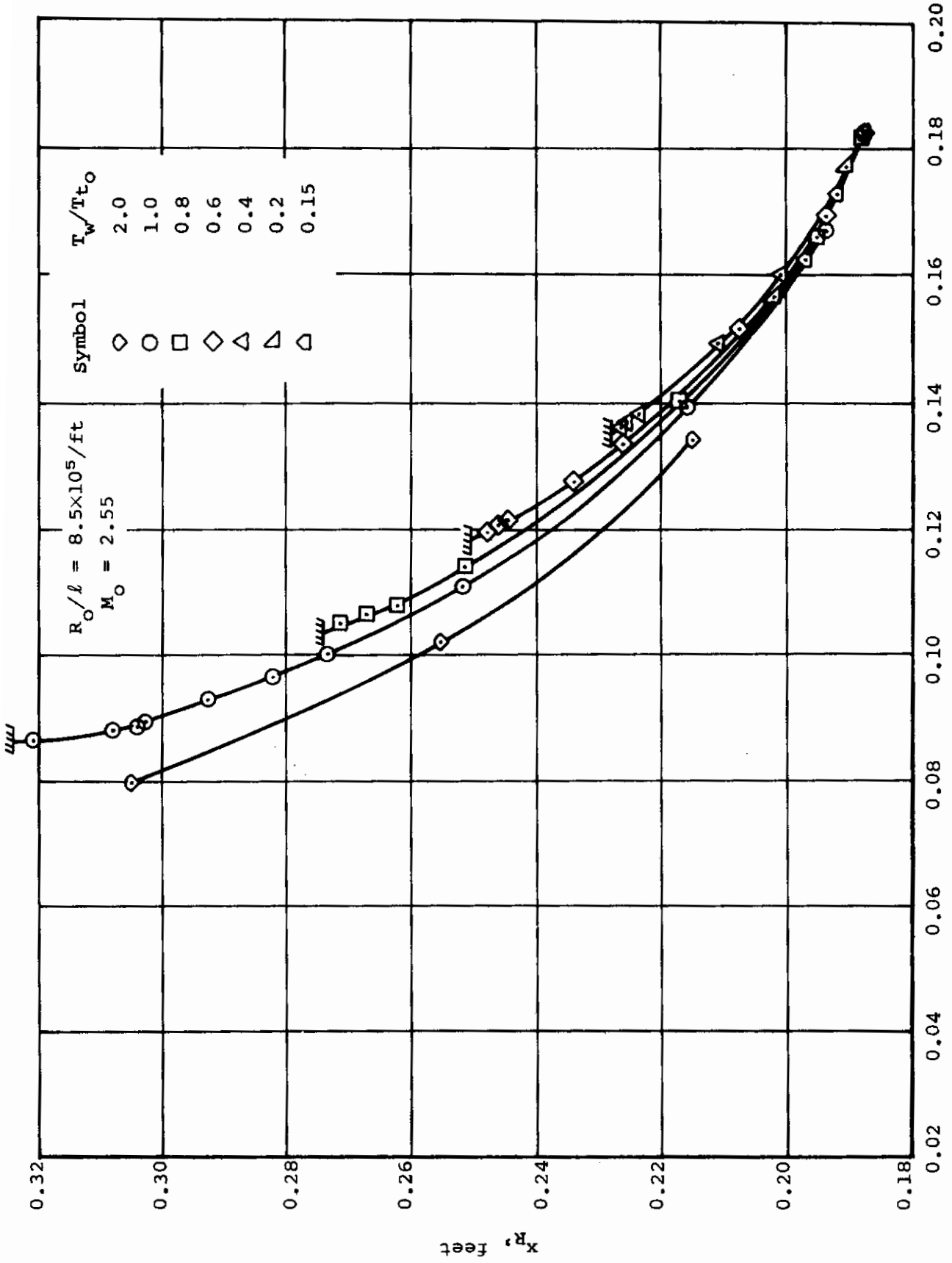

Figure 9.- Range of separation and reattachment points as influenced by cooling and heating from Table I.

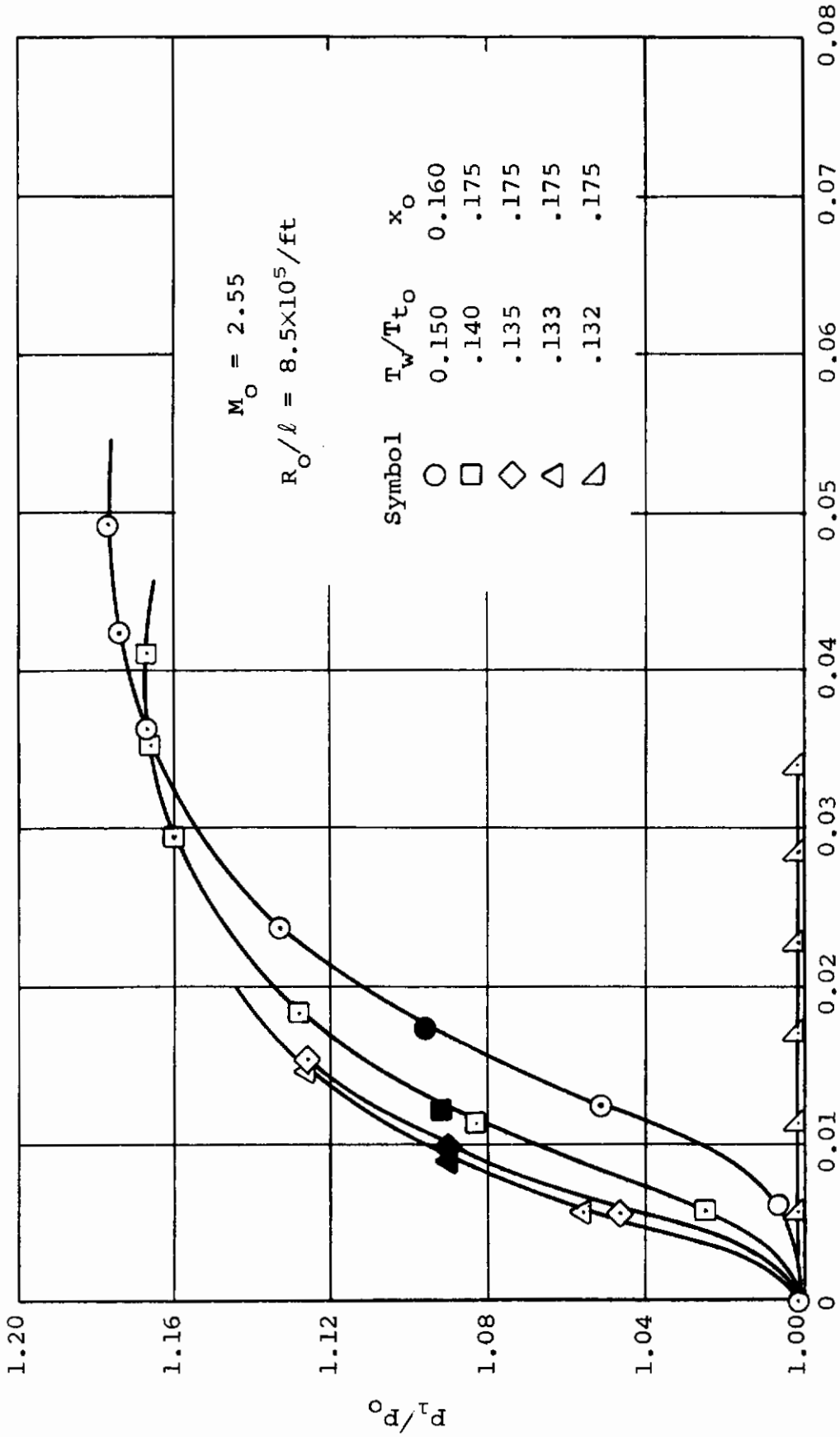

Figure 10.- Separation pressure distributions for various plate temperature near the critical cooling condition.

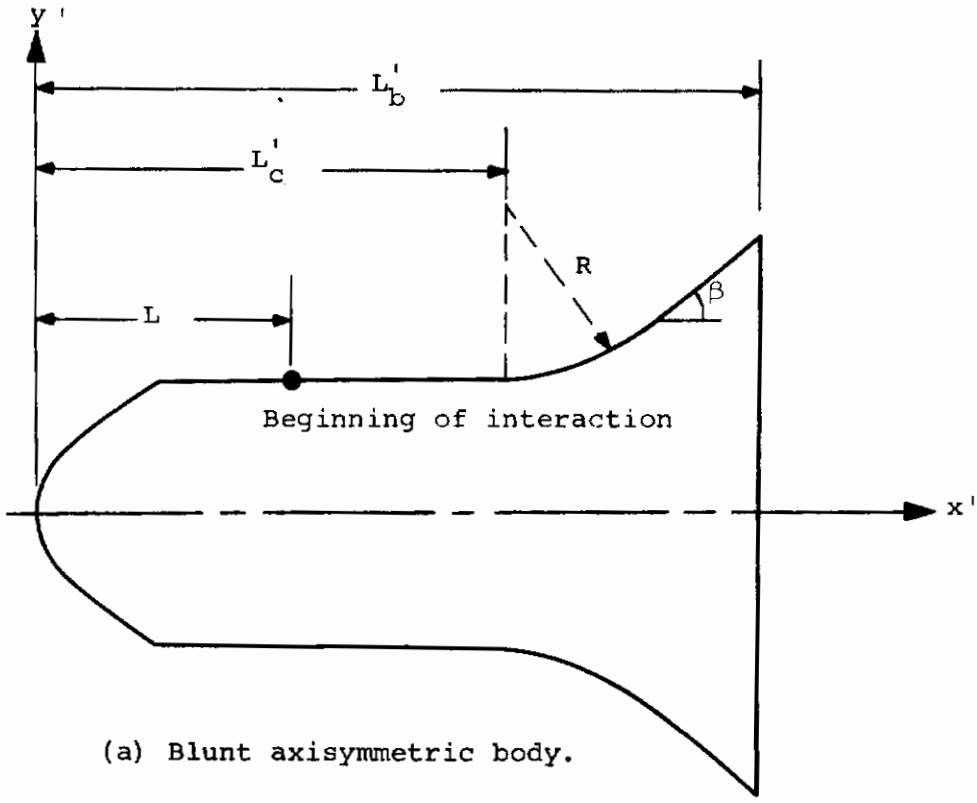

(a) Blunt axisymmetric body.

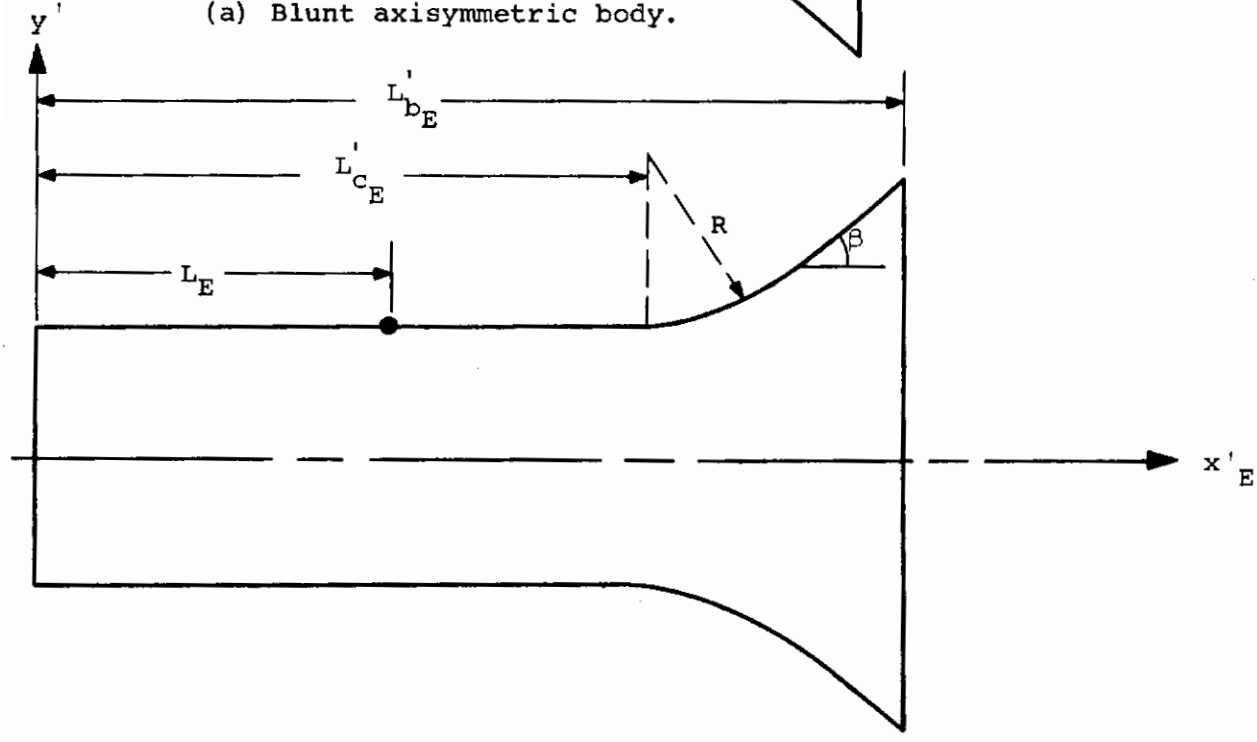

(b) Equivalent hollow axisymmetric body.

Figure 11.- Equivalent body used in computer program to replace blunt axisymmetric body.

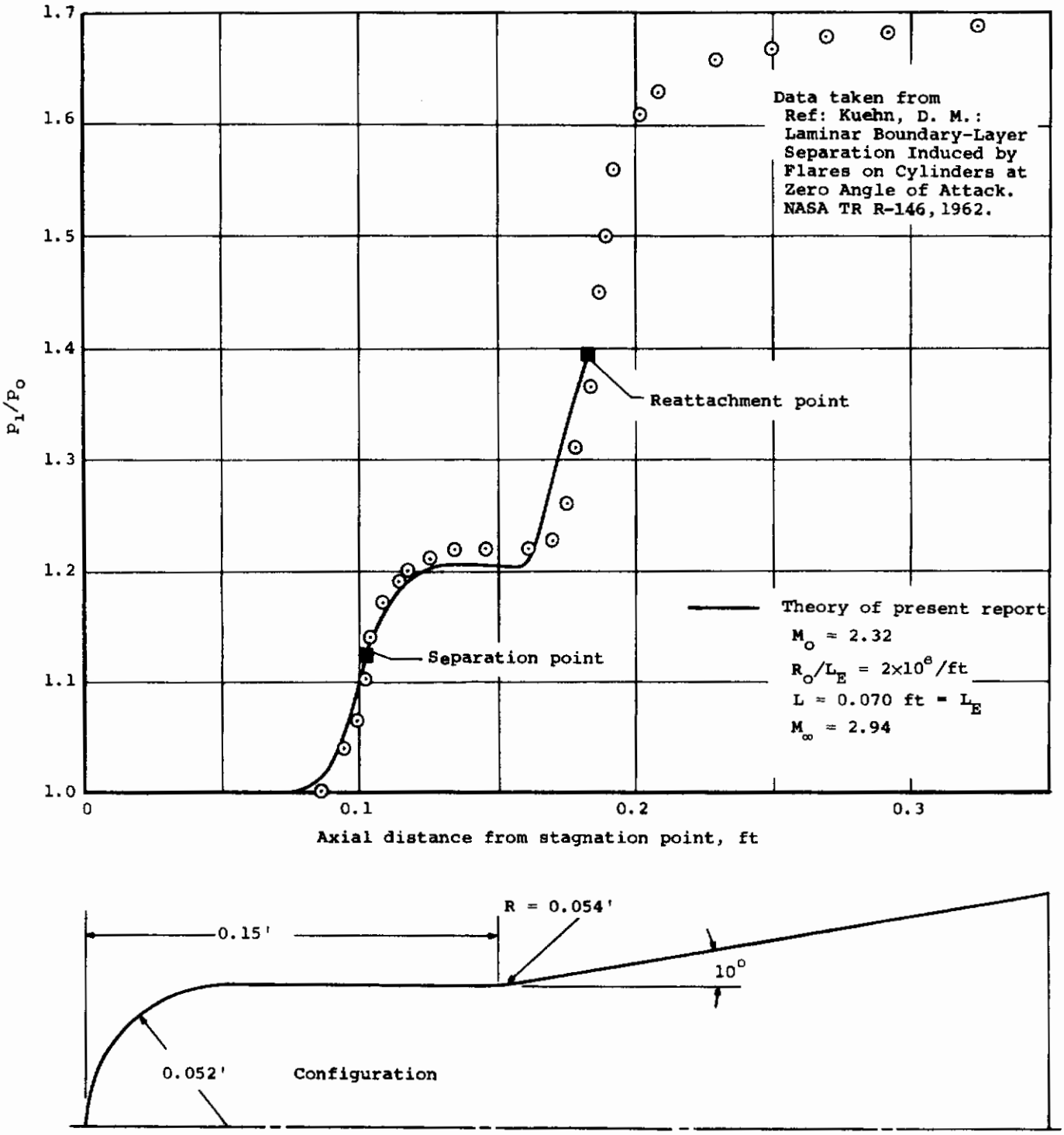

Figure 12.- Comparison between experiment and theory for axisymmetric configuration of Kuehn.

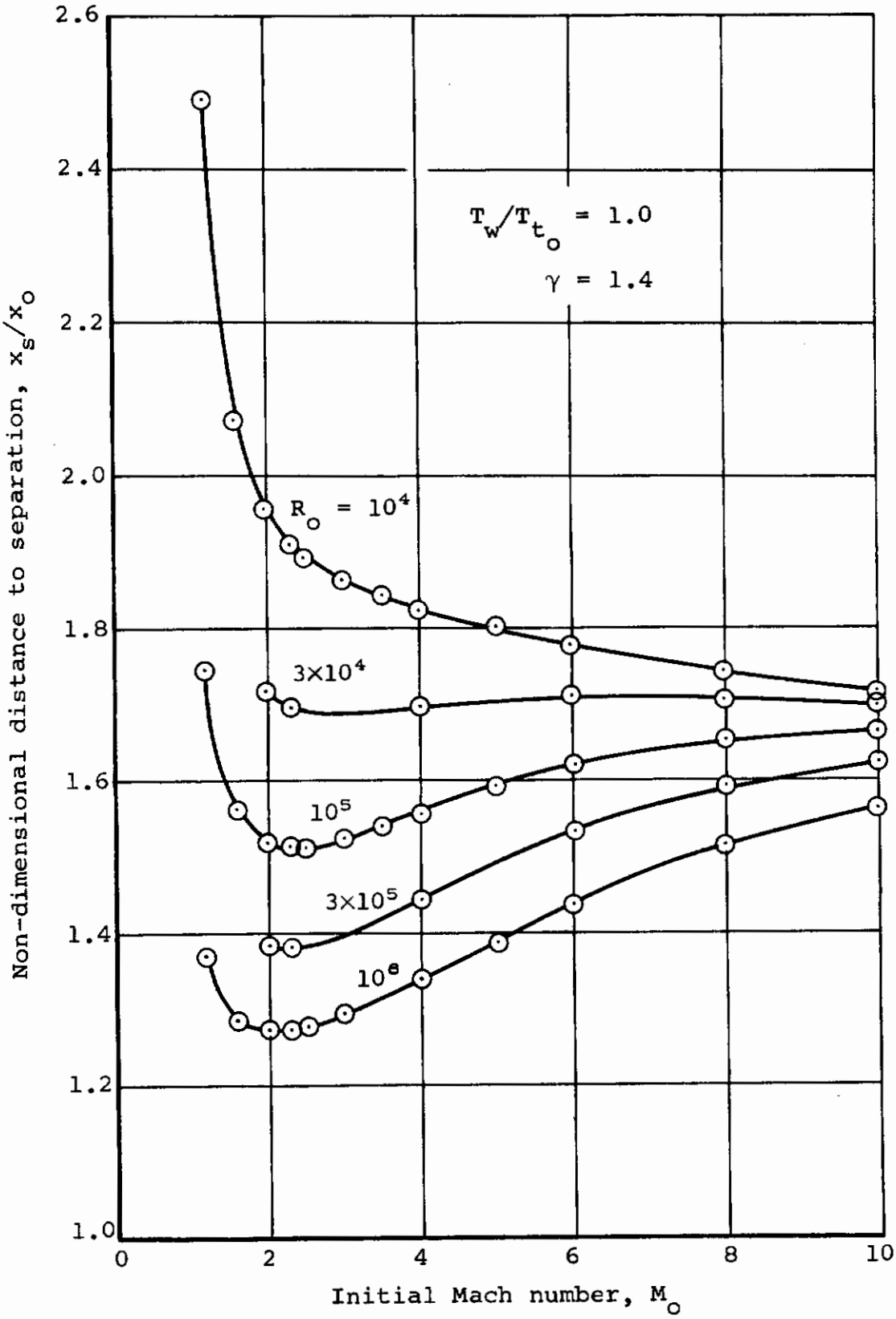

Figure 13.- Effect of Reynolds number and Mach number on non-dimensional distance to separation.

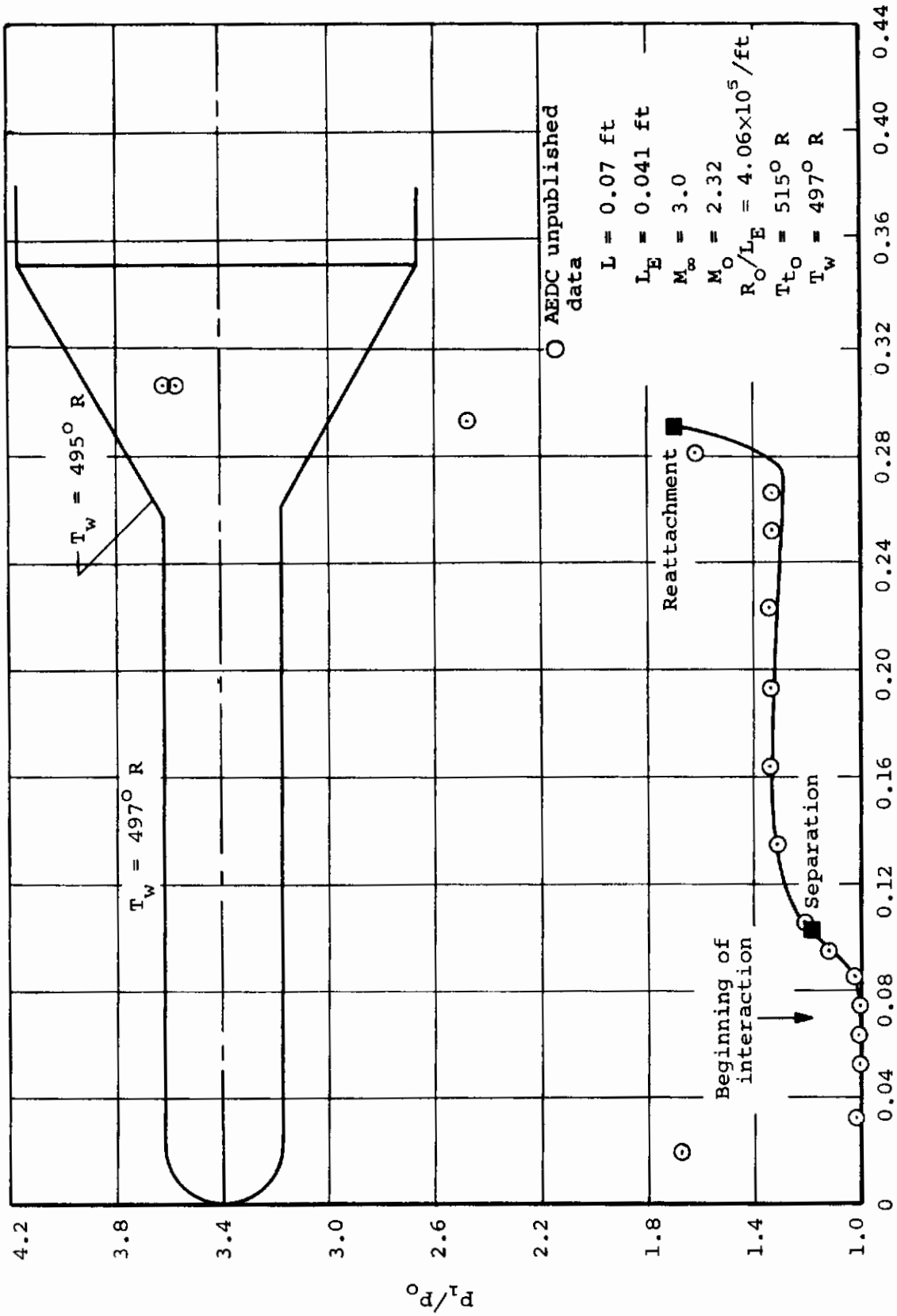

(a) M_∞ = 3.0, adiabatic.

Figure 14.- Comparison between experiment and theory for axisymmetric configuration tested at AEDC.

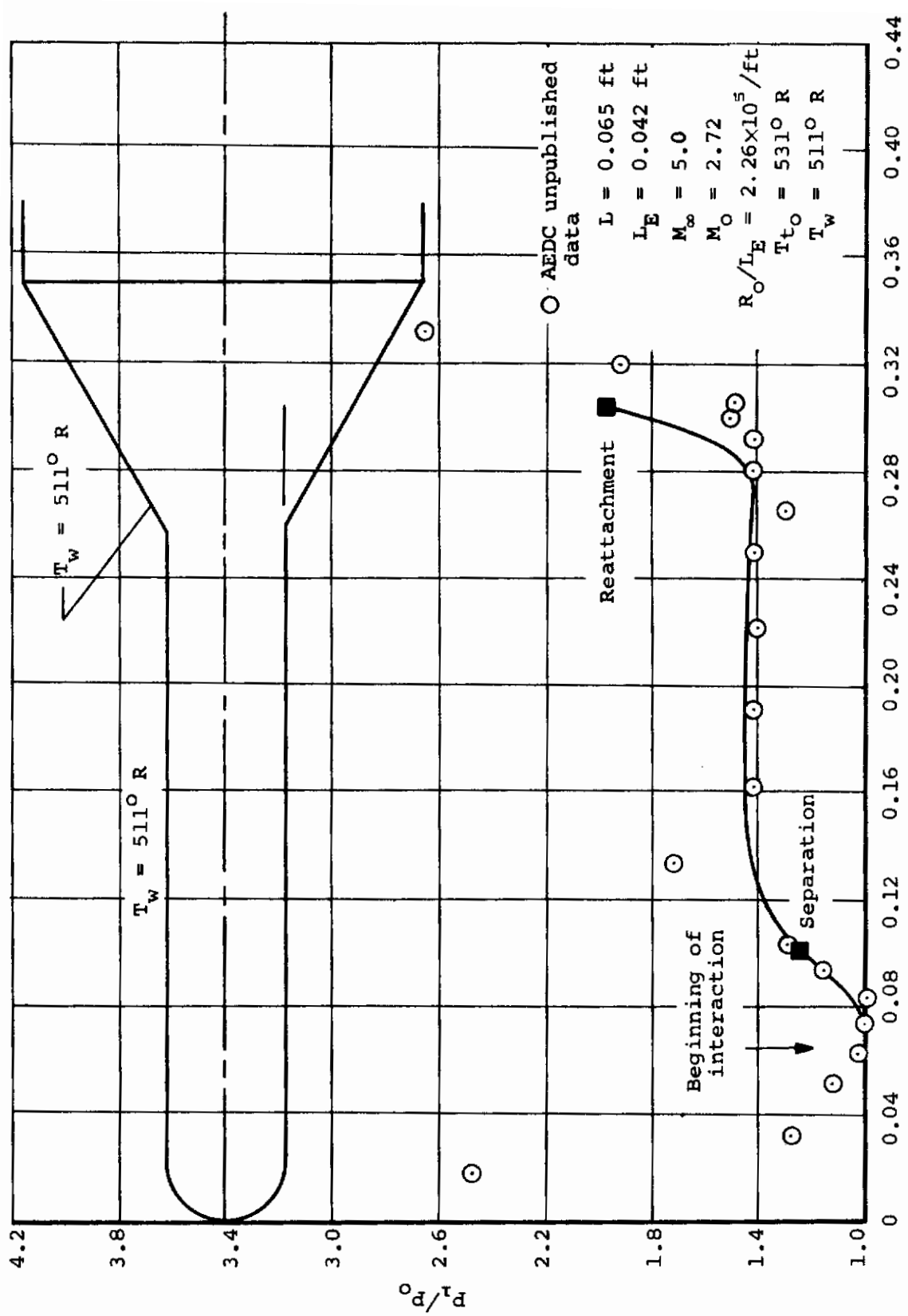

(b) M_∞ = 5.0, adiabatic.

Figure 14.- Continued.

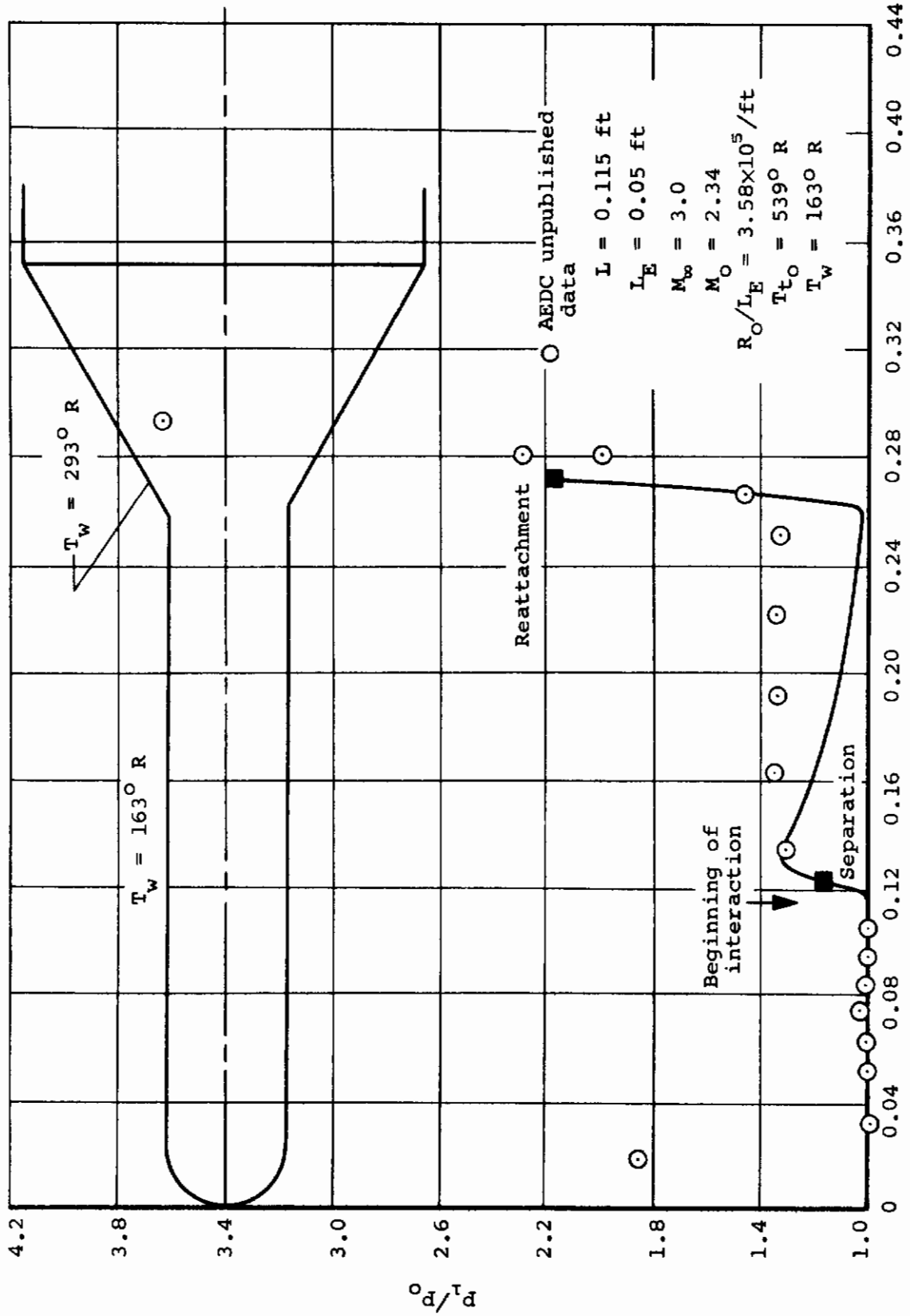

(c) M_∞ = 3.0, highly cooled.

Figure 14.- Continued.

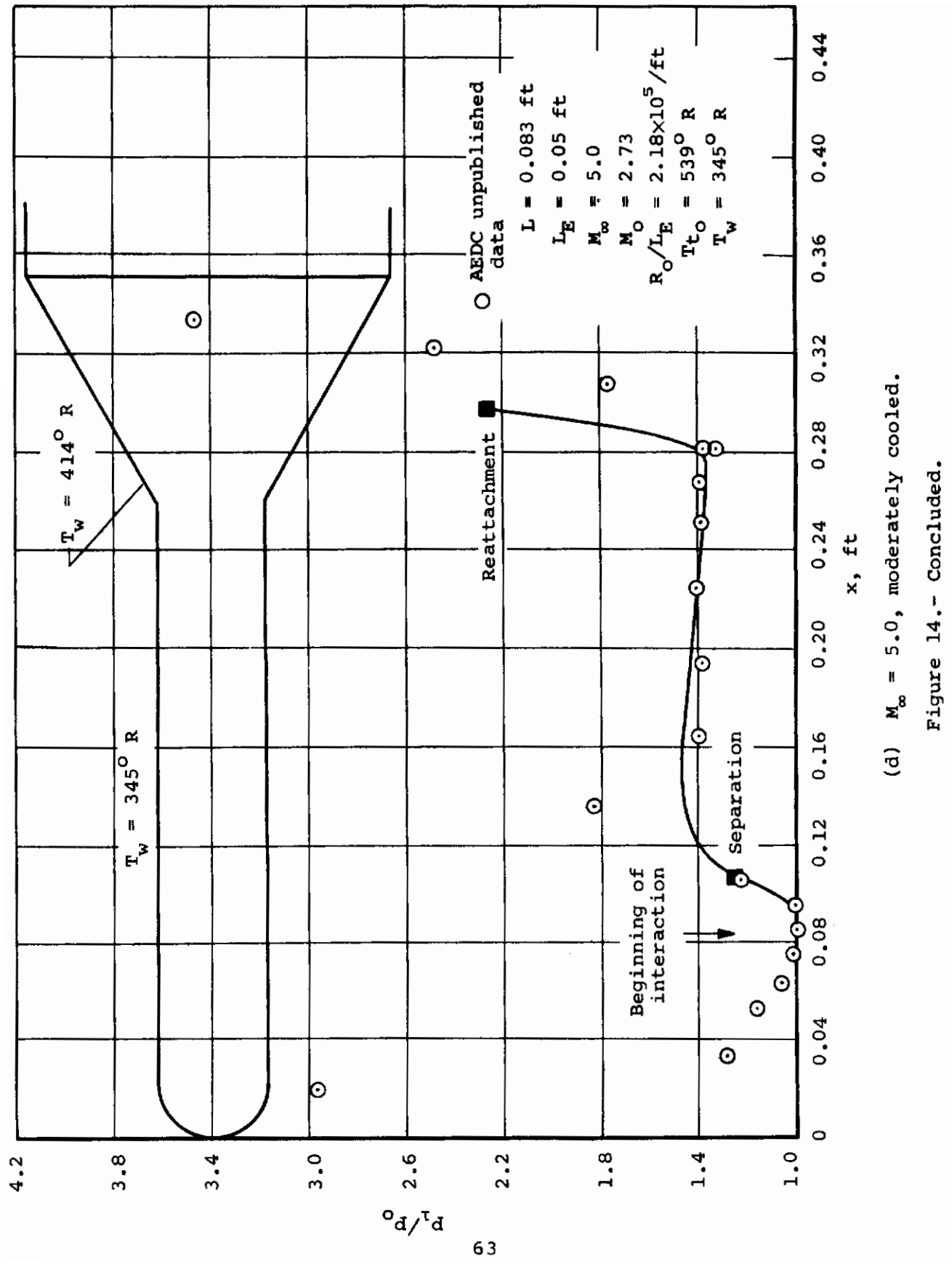

(d) M_∞ = 5.0, moderately cooled.

Figure 14.- Concluded.

APPENDIX I

DIFFERENTIAL EQUATIONS FOR FOURTH-ORDER COUPLING IN PRE-SEPARATION REGION

Following the methods outlined in Section 3, a full fourth-order derivation of the momentum and energy relations has been carried out. The expansion for the total temperature profile has been assumed to be of the form

$$S = S_w(1 - \bar{u}) + E_o(1 - \bar{u})\left(\sqrt{c_3} - \sqrt{\bar{u} + c_3}\right) + (1 - \bar{u})\left(E_1\bar{u} + E_2\bar{u}^2 + E_3\bar{u}^3\right) \qquad (I\text{-}1)$$

The final results are now given in compact form:

$$\left.\begin{aligned}
{}_1D_1\dot{c}_o + {}_1D_2\dot{c}_1 + {}_1D_3\dot{c}_2 + {}_1D_4\dot{c}_3 + {}_1D_5\dot{E}_o + {}_1D_6\dot{E}_1 + {}_1D_7\dot{E}_2 + {}_1D_8\dot{E}_3 + {}_1D_9\frac{\dot{U}_1}{U_1} &= {}_1R \\
{}_2D_1\dot{c}_o + {}_2D_2\dot{c}_1 + {}_2D_3\dot{c}_2 + {}_2D_4\dot{c}_3 + {}_2D_5\dot{E}_o + {}_2D_6\dot{E}_1 + {}_2D_7\dot{E}_2 + {}_2D_8\dot{E}_3 + {}_2D_9\frac{\dot{U}_1}{U_1} &= {}_2R \\
{}_3D_1\dot{c}_o + {}_3D_2\dot{c}_1 + {}_3D_3\dot{c}_2 + {}_3D_4\dot{c}_3 + {}_3D_5\dot{E}_o + {}_3D_6\dot{E}_1 + {}_3D_7\dot{E}_2 + {}_3D_8\dot{E}_3 + {}_3D_9\frac{\dot{U}_1}{U_1} &= {}_3R \\
{}_4D_1\dot{c}_o + {}_4D_2\dot{c}_1 + {}_4D_3\dot{c}_2 + {}_4D_4\dot{c}_3 + {}_4D_5\dot{E}_o + {}_4D_6\dot{E}_1 + {}_4D_7\dot{E}_2 + {}_4D_8\dot{E}_3 + {}_4D_9\frac{\dot{U}_1}{U_1} &= {}_4R \\
{}_5D_1\dot{c}_o + {}_5D_2\dot{c}_1 + {}_5D_3\dot{c}_2 + {}_5D_4\dot{c}_3 + {}_5D_5\dot{E}_o + {}_5D_6\dot{E}_1 + {}_5D_7\dot{E}_2 + {}_5D_8\dot{E}_3 + {}_5D_9\frac{\dot{U}_1}{U_1} &= {}_5R \\
{}_6D_1\dot{c}_o + {}_6D_2\dot{c}_1 + {}_6D_3\dot{c}_2 + {}_6D_4\dot{c}_3 + {}_6D_5\dot{E}_o + {}_6D_6\dot{E}_1 + {}_6D_7\dot{E}_2 + {}_6D_8\dot{E}_3 + {}_6D_9\frac{\dot{U}_1}{U_1} &= {}_6R \\
{}_7D_1\dot{c}_o + {}_7D_2\dot{c}_1 + {}_7D_3\dot{c}_2 + {}_7D_4\dot{c}_3 + {}_7D_5\dot{E}_o + {}_7D_6\dot{E}_1 + {}_7D_7\dot{E}_2 + {}_7D_8\dot{E}_3 + {}_7D_9\frac{\dot{U}_1}{U_1} &= {}_7R \\
{}_8D_1\dot{c}_o + {}_8D_2\dot{c}_1 + {}_8D_3\dot{c}_2 + {}_8D_4\dot{c}_3 + {}_8D_5\dot{E}_o + {}_8D_6\dot{E}_1 + {}_8D_7\dot{E}_2 + {}_8D_8\dot{E}_3 + {}_8D_9\frac{\dot{U}_1}{U_1} &= {}_8R
\end{aligned}\right\} (I\text{-}2)$$

The coefficients are given as follows:

$$
\left.
\begin{aligned}
{}_1D_1 &= g_1 \\
{}_1D_2 &= g_2 \\
{}_1D_3 &= g_3 \\
{}_1D_4 &= d_1 \\
{}_1D_5 &= {}_1D_6 = {}_1D_7 = {}_1D_8 = 0 \\
{}_1D_9 &= \bar{f}_1 + \bar{f}_2 + \bar{H}_1 - E_o\bar{N}_o \\
{}_1R &= \frac{\sqrt{c_3}}{c_o}
\end{aligned}
\right\} \quad \text{(I-3)}
$$

$$
\left.
\begin{aligned}
{}_2D_1 &= g_2 \\
{}_2D_2 &= g_3 \\
{}_2D_3 &= g_4 \\
{}_2D_4 &= d_2 \\
{}_2D_5 &= {}_2D_6 = {}_2D_7 = {}_2D_8 = 0 \\
{}_2D_9 &= -\left[\bar{f}_1 - \bar{f}_2 - 2\bar{f}_3 + \bar{H}_1 - 2\bar{H}_2 - E_o(\bar{N}_o - 2\bar{N}_1)\right] \\
{}_2R &= 2(P_o - P_1) - \frac{\sqrt{c_3}}{c_o}
\end{aligned}
\right\} \quad \text{(I-4)}
$$

$$
\left.
\begin{aligned}
{}_3D_1 &= g_3 \\
{}_3D_2 &= g_4 \\
{}_3D_3 &= g_5 \\
{}_3D_4 &= d_3 \\
{}_3D_5 &= {}_3D_6 = {}_3D_7 = {}_3D_8 = 0 \\
{}_3D_9 &= -\left[2\bar{f}_2 - \bar{f}_3 - 3\bar{f}_4 + 2\bar{H}_2 - 3\bar{H}_3 - E_o(2\bar{N}_1 - 3\bar{N}_2)\right] \\
{}_3R &= -2\left[(P_o - P_1) - 3(P_1 - P_2)\right]
\end{aligned}
\right\} \quad \text{(I-5)}
$$

$$
\left.
\begin{aligned}
{}_4D_1 &= g_4 \\
{}_4D_2 &= g_5 \\
{}_4D_3 &= g_6 \\
{}_4D_4 &= d_4 \\
{}_4D_5 &= {}_4D_6 = {}_4D_7 = {}_4D_8 = 0 \\
{}_4D_9 &= -\left[3\bar{f}_3 - \bar{f}_4 - 4\bar{f}_5 + 3\bar{H}_3 - 4\bar{H}_4 - E_o(3\bar{N}_2 - 4\bar{N}_3)\right] \\
{}_4R &= -6\left[(P_1 - P_2) - 2(P_2 - P_3)\right]
\end{aligned}
\right\} \quad (I\text{-}6)
$$

$$
\left.
\begin{aligned}
{}_5D_1 &= H_1 - \frac{E_o}{6} \\
{}_5D_2 &= H_2 - \frac{E_o}{12} \\
{}_5D_3 &= H_3 - \frac{E_o}{20} \\
{}_5D_4 &= \frac{E_o}{2\sqrt{c_3}}(\bar{f}_2 - \bar{f}_3) + \dot{d}_1 \\
{}_5D_5 &= \sqrt{c_3}(\bar{f}_2 - \bar{f}_3) - (\bar{N}_1 - \bar{N}_2) \\
{}_5D_6 &= \bar{f}_3 - \bar{f}_4 \\
{}_5D_7 &= \bar{f}_4 - \bar{f}_5 \\
{}_5D_8 &= \bar{f}_5 - \bar{f}_6 \\
{}_5D_9 &= J_1 - J_2 + E_o{}^2(\bar{f}^1 - \bar{f}^2) - 2E_o(\bar{I}_o - \bar{I}_1) + \bar{H}_1 - \bar{H}_3 - E_o(\bar{N}_o - \bar{N}_2) \\
{}_5R &= \frac{S_w\sqrt{c_3}}{c_o} + \frac{\left[\left(E_o\sqrt{c_3} + S_w\right) - E_1\right]\sqrt{c_3}}{c_o} - \frac{E_o c_3}{c_o} + \frac{E_o}{2c_o} + 2\bar{P}_o + E_o\bar{Q}_o
\end{aligned}
\right\} \quad (I\text{-}7)
$$

$$
\left.
\begin{aligned}
{}_6D_1 &= -\left(H_2 - \frac{E_o}{12}\right) \\
{}_6D_2 &= -\left(H_3 - \frac{E_o}{20}\right) \\
{}_6D_3 &= -\left(H_4 - \frac{E_o}{30}\right) \\
{}_6D_4 &= -\left[\frac{E_o}{2\sqrt{c_3}}\left(\bar{f}_3 - \bar{f}_4\right) + \dot{d}_2\right] \\
{}_6D_5 &= -\left[\sqrt{c_3}\left(\bar{f}_3 - \bar{f}_4\right) - \left(\bar{N}_2 - \bar{N}_3\right)\right] \\
{}_6D_6 &= -\left(\bar{f}_4 - \bar{f}_5\right) \\
{}_6D_7 &= -\left(\bar{f}_5 - \bar{f}_6\right) \\
{}_6D_8 &= -\left(\bar{f}_6 - \bar{f}_7\right) \\
{}_6D_9 &= J_1 - 3J_2 + 2J_3 + E_o^2\left(\bar{f}^1 - 3\bar{f}^2 + 2\bar{f}^3\right) - 2E_o\left(\bar{I}_o - 3\bar{I}_1 + 2\bar{I}_2\right) + \bar{H}_1 - 2\bar{H}_2 \\
&\quad - \bar{H}_3 + 2\bar{H}_4 - E_o\left(\bar{N}_o - 2\bar{N}_1 - \bar{N}_2 + 2\bar{N}_3\right) \\
{}_6R &= \frac{S_w\sqrt{c_3}}{c_o} + 2\left(\bar{P}_o - 2\bar{P}_1\right) + E_o\left(\bar{Q}_o - 2\bar{Q}_1\right) - 2\tilde{P}_o + 2E_o\tilde{Q}_o
\end{aligned}
\right\} \quad \text{(I-8)}
$$

$$
\left.
\begin{aligned}
{}_7D_1 &= H_3 - \frac{E_o}{20} \\
{}_7D_2 &= H_4 - \frac{E_o}{30} \\
{}_7D_3 &= H_5 - \frac{E_o}{42} \\
{}_7D_4 &= \frac{E_o}{2\sqrt{c_3}} (\bar{f}_4 - \bar{f}_5) + \dot{d}_3 \\
{}_7D_5 &= \sqrt{c_3} (\bar{f}_4 - \bar{f}_5) - (\bar{N}_3 - \bar{N}_4) \\
{}_7D_6 &= (\bar{f}_5 - \bar{f}_6) \\
{}_7D_7 &= (\bar{f}_6 - \bar{f}_7) \\
{}_7D_8 &= (\bar{f}_7 - \bar{f}_8) \\
{}_7D_9 &= - \Big[2J_2 - 5J_3 + 3J_4 + E_o^2 (2\bar{f}^2 - 5\bar{f}^3 + 3\bar{f}^4) - 2E_o (2\bar{I}_1 - 5\bar{I}_2 + 3\bar{I}_3) \\
&\quad + 2\bar{H}_2 - 3\bar{H}_3 - 2\bar{H}_4 + 3\bar{H}_5 - E_o (2\bar{N}_1 - 3\bar{N}_2 - 2\bar{N}_3 + 3N_4) \Big] \\
{}_7R &= - 2(2\bar{P}_1 - 3\bar{P}_2) - E_o (2\bar{Q}_1 - 3\bar{Q}_2) - 2(\tilde{P}_o - 3\tilde{P}_1) + 2E_o (\tilde{Q}_o - 3\tilde{Q}_1)
\end{aligned}
\right\} \quad \text{(I-9)}
$$

$$
\left.
\begin{aligned}
{}_8D_1 &= H_4 - \frac{E_o}{30} \\
{}_8D_2 &= H_5 - \frac{E_o}{42} \\
{}_8D_3 &= H_6 - \frac{E_o}{56} \\
{}_8D_4 &= \frac{E_o}{2\sqrt{c_3}} (\bar{f}_5 - \bar{f}_6) + \dot{d}_4 \\
{}_8D_5 &= \sqrt{c_3}\ (\bar{f}_5 - \bar{f}_6) - (\bar{N}_4 - \bar{N}_5) \\
{}_8D_6 &= \bar{f}_6 - \bar{f}_7 \\
{}_8D_7 &= \bar{f}_7 - \bar{f}_8 \\
{}_8D_8 &= \bar{f}_8 - \bar{f}_9 \\
{}_8D_9 &= -\Big[3J_3 - 7J_4 + 4J_5 + E_o{}^2(3\bar{f}^3 - 7\bar{f}^4 + 4\bar{f}^5) - 2E_o(3\bar{I}_2 - 7\bar{I}_3 + 4\bar{I}_4) \\
&\quad + 3\bar{H}_3 - 4\bar{H}_4 - 3\bar{H}_5 + 4\bar{H}_6 - E_o(3\bar{N}_2 - 4\bar{N}_3 - 3\bar{N}_4 + 4\bar{N}_5)\Big] \\
{}_8R &= -2(3\bar{P}_2 - 4\bar{P}_3) - E_o(3\bar{Q}_2 - 4\bar{Q}_3) - 6(\tilde{P}_1 - 2\tilde{P}_2) + 6E_o(\tilde{Q}_1 - 2\tilde{Q}_2)
\end{aligned}
\right\} \quad (I\text{-}10)
$$

The following notation has been used in specifying the coefficients:

$$
\left.
\begin{aligned}
g_n(c_3) &= \int_0^1 \frac{\bar{u}^n\, d\bar{u}}{\sqrt{\bar{u} + c_3}} && n = 0,1,\cdots,12 \\
\dot{g}_n(c_3) &= -\frac{1}{2}\int_0^1 \frac{\bar{u}^n\, d\bar{u}}{(\bar{u} + c_3)^{3/2}} && n = 1,2,\cdots,10 \\
P_n &= \int_0^1 \frac{\bar{u}^n\sqrt{\bar{u} + c_3}\, d\bar{u}}{c_o + c_1\bar{u} + c_2\bar{u}^2} && n = 0,1,\cdots,7 \\
Q_n &= \int_0^1 \frac{\bar{u}^n\, d\bar{u}}{c_o + c_1\bar{u} + c_2\bar{u}^2} && n = 0,1,\cdots,5 \\
d_n &= c_o\dot{g}_n + c_1\dot{g}_{n+1} + c_2\dot{g}_{n+2} \\
\dot{d}_n &= \left(E_o\sqrt{c_3} + S_w\right)(d_n - d_{n+1}) + E_1(d_{n+1} - d_{n+2}) + E_2(d_{n+2} - d_{n+3}) + E_3(d_{n+3} - d_{n+4}) \\
\bar{f}_n &= c_o g_{n-1} + c_1 g_n + c_2 g_{n+1} \\
\bar{f}^n &= \bar{f}_{(n+1)} + c_3\bar{f}_n \\
H_n &= \left(E_o\sqrt{c_3} + S_w\right)(g_n - g_{n+1}) + E_1(g_{n+1} - g_{n+2}) + E_2(g_{n+2} - g_{n+3}) + E_3(g_{n+3} - g_{n+4}) \\
\bar{H}_n &= \left(E_o\sqrt{c_3} + S_w\right)\bar{f}_n + E_1\bar{f}_{n+1} + E_2\bar{f}_{n+2} + E_3\bar{f}_{n+3} \\
J_n &= \left(E_o\sqrt{c_3} + S_w\right)\bar{H}_n + E_1\bar{H}_{n+1} + E_2\bar{H}_{n+2} + E_3\bar{H}_{n+3} \\
\bar{I}_n &= \left(E_o\sqrt{c_3} + S_w\right)\bar{N}_n + E_1\bar{N}_{n+1} + E_2\bar{N}_{n+2} + E_3\bar{N}_{n+3} \\
\bar{N}_n &= \frac{c_o}{n+1} + \frac{c_1}{n+2} + \frac{c_2}{n+3} \\
\bar{P}_n &= \left[E_1 - \left(E_o\sqrt{c_3} + S_w\right)\right](P_n - P_{n+1}) + 2(E_2 - E_1)(P_{n+1} - P_{n+2}) \\
&\quad + 3(E_3 - E_2)(P_{n+2} - P_{n+3}) - 4E_3(P_{n+3} - P_{n+4}) \\
\tilde{P}_n &= \left(E_o\sqrt{c_3} + S_w\right)(P_n - P_{n+1}) + \left[E_1 - \left(E_o\sqrt{c_3} + S_w\right)\right](P_{n+1} - P_{n+2}) \\
&\quad + (E_2 - E_1)(P_{n+2} - P_{n+3}) + (E_3 - E_2)(P_{n+3} - P_{n+4}) - E_3(P_{n+4} - P_{n+5}) \\
\bar{Q}_n &= (2c_3 - 1)(Q_n - Q_{n+1}) + 3(Q_{n+1} - Q_{n+2}) \\
\tilde{Q}_n &= c_3(Q_n - Q_{n+1}) + (1 - c_3)(Q_{n+1} - Q_{n+2}) - (Q_{n+2} - Q_{n+3})
\end{aligned}
\right\} \quad \text{(I-11)}
$$

APPENDIX II

FREE-INTERACTION EQUATION FOR NONADIABATIC SUPERSONIC TWO-DIMENSIONAL FLOW

The free-interaction equation will be influenced by wall cooling or heating since such cooling or heating will change the density of the fluid particularly near the wall and will thereby change the displacement thickness. We follow the general development given in Appendix II of Reference 1.

The basic assumption for calculating the pressure distribution on a body immersed in a viscous flow is that this pressure distribution is the same as that for an inviscid flow about the same body for which the solid boundary coordinates have been augmented by an amount δ^* due to the boundary layer. For supersonic two-dimensional flow we will use the Prandtl-Meyer relationship for calculating the pressure distribution

$$\frac{dp_i}{p_i} = \frac{\gamma M_i^2}{\cos\phi\sqrt{M_i^2 - \cos^2\phi}}\, d\phi \qquad \text{(II-1)}$$

The angle ϕ is the change in angle of the external flow due to changes in boundary-layer displacement thickness and to changes in slope of the surface. These quantities are related as follows:

$$\frac{d\delta_o^*}{dx} + \frac{d\delta_i^*}{dx} + \frac{dw}{dx} = \tan\phi \qquad \text{(II-2)}$$

where

δ_o^* displacement thickness of outer flow

δ_i^* displacement thickness of inner flow

dw/dx streamwise slope

In our example δ_i^* and dw/dx will be zero in front of the separation point.

Pre-Separation Region

In the pre-separation region we have

$$\tan\phi = \frac{d\delta_o^*}{dx} \qquad \text{(II-3)}$$

with

$$\delta_o^* = \int_o^\infty \left(1 - \frac{\rho u}{\rho_1 u_1}\right) dy \qquad \text{(II-4)}$$

Under the Stewartson transformation, the displacement thickness becomes

$$\delta^* = \frac{\rho_o a_o}{\rho_1 a_1} \int_o^\infty \left(\frac{\rho_1}{\rho} - \frac{U}{U_1}\right) dY \qquad \text{(II-5)}$$

The temperature profile

$$\frac{T}{T_1} = (S + 1)(1 + m_1) - \frac{m_1 U^2}{U_1^2}, \qquad m_1 = \frac{\gamma - 1}{2} M_1^2 \qquad \text{(II-6)}$$

when introduced into Equation (II-5) yields

$$\delta_o^* = \frac{\rho_o a_o}{\rho_1 a_1} \int_o^\infty \left[(S + 1)(1 + m_1) - \frac{m_1 U^2}{U_1^2} - \frac{U}{U_1}\right] dY \qquad \text{(II-7)}$$

Under the Dorodnitsyn transformation δ_o^* becomes

$$\delta_o^* = \frac{\rho_o a_o}{\rho_1 a_1} \frac{U_o \ell}{U_1} \frac{1}{\sqrt{R_o}} \left[(1 + m_1) \int_o^\infty S \, d\eta + (1 + m_1) \int_o^\infty (1 - \bar{u}) d\eta + m_1 \int_o^\infty \bar{u}(1 - \bar{u}) d\eta\right] \qquad \text{(II-8)}$$

Carrying out the integration yields

$$\delta_o^* = \frac{(1 + m_o)}{\sqrt{R_o}} \left(\frac{1 + m_1}{1 + m_o}\right)^{\frac{3\gamma - 1}{2(\gamma - 1)}} \frac{U_o \ell}{U_1} \left[\left(E_o \sqrt{c_3} + S_w\right)(c_o g_o + c_1 g_1 + c_2 g_2) - E_o\left(c_o + \frac{c_1}{2} + \frac{c_2}{3}\right) + (c_o g_o + c_1 g_1 + c_2 g_2) + \frac{m_1}{1 + m_1}(c_o g_1 + c_1 g_2 + c_2 g_3)\right] \qquad \text{(II-9)}$$

Carrying out the differentiation and substituting into Equation (II-3) yields the following free-interaction equation for the pre-separation region valid for first-order or second-order coupling:

$$\frac{R_o^{1/2}}{(1+m_o)}\tan\phi = \left[\left(E_o\sqrt{c_3}+S_w\right)g_o - E_o + g_o + \frac{m_1}{1+m_1}g_1\right]\dot{c}_o$$

$$+\left[\left(E_o\sqrt{c_3}+S_w\right)g_1 - \frac{E_o}{2} + g_1 + \frac{m_1}{1+m_1}g_2\right]\dot{c}_1$$

$$+\left[\left(E_o\sqrt{c_3}+S_w\right)g_2 - \frac{E_o}{3} + g_2 + \frac{m_1}{1+m_1}g_3\right]\dot{c}_2$$

$$+\left[\frac{E_o}{2\sqrt{c_3}}\left(c_og_o+c_1g_1+c_2g_2\right) + \left(E_o\sqrt{c_3}+S_w+1\right)\left(c_o\dot{g}_o+c_1\dot{g}_1+c_2\dot{g}_2\right)\right.$$

$$\left.+\frac{m_1}{1+m_1}\left(c_o\dot{g}_1+c_1\dot{g}_2+c_2\dot{g}_3\right)\right]\dot{c}_3 + \left[\sqrt{c_3}\left(c_og_o+c_1g_1+c_2g_2\right)\right.$$

$$\left.-\left(c_o+\frac{c_1}{2}+\frac{c_2}{3}\right)\right]\dot{E}_o$$

$$+\left(\frac{m_1}{1+m_1}\right)\left\{\left(\frac{3\gamma-1}{\gamma-1}-\frac{1+m_1}{m_1}\right)\left[\left(E_o\sqrt{c_3}+S_w+1\right)\left(c_og_o+c_1g_1+c_2g_2\right)\right.\right.$$

$$\left.-E_o\left(c_o+\frac{c_1}{2}+\frac{c_2}{3}\right)\right]$$

$$\left.+\left[\left(\frac{\gamma+1}{\gamma-1}\right)\left(\frac{m_1}{1+m_1}\right)+1\right]\left(c_og_1+c_1g_2+c_2g_3\right)\right\}\frac{\dot{U}_1}{U_1} = \frac{R_o^{1/2}}{1+m_o}\frac{d\delta_o^*}{dx} \qquad \text{(II-10)}$$

Post-Separation Region

In the post-separation region, it is necessary to take account of the displacement thickness due to the inner region in formulating the free-interaction relationship. Let us distinguish between the displacement thickness of the inner flow for the adiabatic and nonadiabatic cases

δ_{i_A} = displacement thickness of inner flow for adiabatic case

δ_{i_N} = displacement thickness of inner flow for nonadiabatic case

The free-interaction equation can then be written

$$\frac{\sqrt{R_o}}{1 + m_o}\left(\tan \phi - \frac{dw}{dx}\right) = \frac{\sqrt{R_o}}{1 + m_o}\left[\frac{d\delta_o^*}{dx} + \frac{d\delta_{i_A}^*}{dx} + \frac{d\left(\delta_{i_N}^* - \delta_{i_A}^*\right)}{dx}\right] \tag{II-11}$$

The form of the term involving δ_o^* is the same in front of separation and downstream of it and is given by Equation (II-10). This is true only for first-order coupling where the value of S along the $\bar{u} = 0$ line downstream of separation is uniform at the value of S_w. The term associated with $d\delta_{i_A}^*/dx$ is given by Equation (II-15) of Reference 1 and is not reproduced here because of its complexity. Thus, only the term associated with $(\delta_{i_N}^* - \delta_{i_A}^*)$ needs to be evaluated.

We can write the following expression for $\delta_{i_N}^*$ by analogy with reference to Equation (II-8):

$$\delta_{i_N}^* = \frac{\rho_o a_o}{\rho_1 a_1}\frac{U_o \ell}{U_1}\frac{1}{\sqrt{R_o}}\left[(1 + m_1)\int_o^{\eta_s} S\, d\eta + (1 + m_1)\int_o^{\eta_s}(1 - \bar{u})d\eta + m_1\int_o^{\eta_s}\bar{u}(1 - \bar{u})d\eta\right] \tag{II-12}$$

It is noted that the first integral is the additional term due to the assumption of nonadiabatic flow. Thus

$$\delta_{i_N}^* - \delta_{i_A}^* = \frac{\rho_o a_o}{\rho_1 a_1}\frac{U_o \ell}{U_1}\frac{1}{\sqrt{R_o}}(1 + m_1)\int_o^{\eta_s} S\, d\eta \tag{II-13}$$

In first-order coupling S is uniform at S_w in the inner region, so that

$$\delta_{i_N}^* - \delta_{i_A}^* = \frac{\rho_o a_o}{\rho_1 a_1}\frac{U_o \ell}{U_1}\frac{1}{\sqrt{R_o}}(1 + m_1)S_w\eta_s = \frac{(1 + m_o)}{\sqrt{R_o}}\left(\frac{1 + m_1}{1 + m_o}\right)^{\frac{3\gamma - 1}{2(\gamma - 1)}}\frac{U_o \ell}{U_1}S_w\eta_s \tag{II-14}$$

Finally, since

$$\frac{dx}{d\xi} = \ell \frac{U_o}{U_1} \left(\frac{1 + m_1}{1 + m_o} \right)^{\frac{3\gamma - 1}{2(\gamma - 1)}} \qquad \text{(II-15)}$$

we find

$$\frac{\sqrt{R_o}}{1 + m_o} \frac{d}{dx} \left(\delta_{i_N}{}^* - \delta_{i_A}{}^* \right) = S_w \dot{\eta}_s + S_w \eta_s \left[\left(\frac{3\gamma - 1}{\gamma - 1} \right) \left(\frac{m_1}{1 + m_1} \right) - 1 \right] \frac{\dot{U}_1}{U_1} \qquad \text{(II-16)}$$

Since we have established expressions for all terms entering into Equation (II-11) for first-order coupling, we have established the free-interaction equation for this case. The value of E_o should be set equal to zero for first-order coupling.

Unclassified
Security Classification

DOCUMENT CONTROL DATA - R&D
(Security classification of title, body of abstract and indexing annotation must be entered when the overall report is classified)

1. ORIGINATING ACTIVITY (Corporate author) Vidya Division, Itek Corporation 1450 Page Mill Road Palo Alto, California	2a. REPORT SECURITY CLASSIFICATION UNCLASSIFIED 2b. GROUP N/A

3. REPORT TITLE
CALCULATION OF LAMINAR SEPARATION WITH FREE INTERACTION BY THE METHOD OF INTEGRAL RELATIONS, Part II - Two Dimensional Supersonic Nonadiabatic Flow and Axisymmetric Supersonic Adiabatic and Nonadiabatic Flows

4. DESCRIPTIVE NOTES (Type of report and inclusive dates)
Technical Documentary Report, Part II - May 1965 to October 1965

5. AUTHOR(S) (Last name, first name, initial)
Nielsen, Jack N.
Lynes, Larry L.
Goodwin, Frederick K.

6. REPORT DATE	7a. TOTAL NO. OF PAGES	7b. NO. OF REFS
January 1966	88	4

8a. CONTRACT OR GRANT NO.	9a. ORIGINATOR'S REPORT NUMBER(S)
AF33(615)-1591 b. PROJECT NO. 8219 c. Task Nr 821902 d.	AFFDL TR 65-107, Pt II 9b. OTHER REPORT NO(S) (Any other numbers that may be assigned this report) Vidya Rpt Nr 203

10. AVAILABILITY/LIMITATION NOTICES
Distribution of this document is unlimited.

11. SUPPLEMENTARY NOTES	12. SPONSORING MILITARY ACTIVITY
None	AFFDL (FDCC) Wright-Patterson AFB, Ohio 45433

13. ABSTRACT

A calculative method is presented for determining separated, laminar, boundary-layer characteristics from in front of the separation point to the reattachment point under the influence of "free interaction" between the main flow and the boundary layer. The analysis herein covers supersonic flow over two-dimensional and axisymmetric configurations with adiabatic or nonadiabatic wall conditions. For nonadiabatic wall conditions, theories based on first-order and second-order coupling between velocity and total temperature profiles have been presented. The theory based on first-order coupling has been included in a machine calculation program with options for two-dimensional or axisymmetric flow and adiabatic or nonadiabatic wall conditions. Extensive systematic calculations have been made to determine the range of possible separated flows over a two-dimensional configuration as a function of separation point location and wall temperatures. Comparison between experiment and theory for separation pressure distributions on two-dimensional or axisymmetric adiabatic configurations shows generally good agreement. Good comparison between experiment and theory is indicated for a moderately-cooled axisymmetric configuration. For a highly-cooled axisymmetric configuration, the prediction of the machine program based on first-order coupling is inadequate, indicating the necessity for a higher-order coupling theory.

DD FORM 1 JAN 64 1473

Unclassified
Security Classification

Unclassified

Security Classification

14. KEY WORDS	LINK A		LINK B		LINK C	
	ROLE	WT	ROLE	WT	ROLE	WT
Thermal boundary layer Laminar boundary layer Separated flow Supersonic flow Aerodynamics Aerodynamic Heating						

INSTRUCTIONS

1. ORIGINATING ACTIVITY: Enter the name and address of the contractor, subcontractor, grantee, Department of Defense activity or other organization *(corporate author)* issuing the report.

2*a*. REPORT SECURITY CLASSIFICATION: Enter the overall security classification of the report. Indicate whether "Restricted Data" is included. Marking is to be in accordance with appropriate security regulations.

2*b*. GROUP: Automatic downgrading is specified in DoD Directive 5200.10 and Armed Forces Industrial Manual. Enter the group number. Also, when applicable, show that optional markings have been used for Group 3 and Group 4 as authorized.

3. REPORT TITLE: Enter the complete report title in all capital letters. Titles in all cases should be unclassified. If a meaningful title cannot be selected without classification, show title classification in all capitals in parenthesis immediately following the title.

4. DESCRIPTIVE NOTES: If appropriate, enter the type of report, e.g., interim, progress, summary, annual, or final. Give the inclusive dates when a specific reporting period is covered.

5. AUTHOR(S): Enter the name(s) of author(s) as shown on or in the report. Enter last name, first name, middle initial. If military, show rank and branch of service. The name of the principal author is an absolute minimum requirement.

6. REPORT DATE: Enter the date of the report as day, month, year; or month, year. If more than one date appears on the report, use date of publication.

7*a*. TOTAL NUMBER OF PAGES: The total page count should follow normal pagination procedures, i.e., enter the number of pages containing information.

7*b*. NUMBER OF REFERENCES: Enter the total number of references cited in the report.

8*a*. CONTRACT OR GRANT NUMBER: If appropriate, enter the applicable number of the contract or grant under which the report was written.

8*b*, 8*c*, & 8*d*. PROJECT NUMBER: Enter the appropriate military department identification, such as project number, subproject number, system numbers, task number, etc.

9*a*. ORIGINATOR'S REPORT NUMBER(S): Enter the official report number by which the document will be identified and controlled by the originating activity. This number must be unique to this report.

9*b*. OTHER REPORT NUMBER(S): If the report has been assigned any other report numbers *(either by the originator or by the sponsor)*, also enter this number(s).

10. AVAILABILITY/LIMITATION NOTICES: Enter any limitations on further dissemination of the report, other than those imposed by security classification, using standard statements such as:

(1) "Qualified requesters may obtain copies of this report from DDC."

(2) "Foreign announcement and dissemination of this report by DDC is not authorized."

(3) "U. S. Government agencies may obtain copies of this report directly from DDC. Other qualified DDC users shall request through

_____."

(4) "U. S. military agencies may obtain copies of this report directly from DDC. Other qualified users shall request through

_____."

(5) "All distribution of this report is controlled. Qualified DDC users shall request through

_____."

If the report has been furnished to the Office of Technical Services, Department of Commerce, for sale to the public, indicate this fact and enter the price, if known.

11. SUPPLEMENTARY NOTES: Use for additional explanatory notes.

12. SPONSORING MILITARY ACTIVITY: Enter the name of the departmental project office or laboratory sponsoring *(paying for)* the research and development. Include address.

13. ABSTRACT: Enter an abstract giving a brief and factual summary of the document indicative of the report, even though it may also appear elsewhere in the body of the technical report. If additional space is required, a continuation sheet shall be attached.

It is highly desirable that the abstract of classified reports be unclassified. Each paragraph of the abstract shall end with an indication of the military security classification of the information in the paragraph, represented as *(TS)*, *(S)*, *(C)*, or *(U)*.

There is no limitation on the length of the abstract. However, the suggested length is from 150 to 225 words.

14. KEY WORDS: Key words are technically meaningful terms or short phrases that characterize a report and may be used as index entries for cataloging the report. Key words must be selected so that no security classification is required. Identifiers, such as equipment model designation, trade name, military project code name, geographic location, may be used as key words but will be followed by an indication of technical context. The assignment of links, rules, and weights is optional.

Unclassified

Security Classification